



**UCAM**

UNIVERSIDAD CATÓLICA  
DE MURCIA

ESCUELA INTERNACIONAL DE DOCTORADO  
Programa de Doctorado en Tecnologías de la Computación e  
Ingeniería Ambiental

Remediation of endocrine disruptor in contaminated water  
through advanced oxidation processes

Autora:

Dña. M<sup>a</sup> Carmen Calín Mora

Directores:

Dra. Dña. Nuria Vela de Oro

Dr. D. José Fenoll Serrano

Murcia, diciembre 2020





**UCAM**

UNIVERSIDAD CATÓLICA  
DE MURCIA

ESCUELA INTERNACIONAL DE DOCTORADO  
Programa de Doctorado en Tecnologías de la Computación e  
Ingeniería Ambiental

Remediation of endocrine disruptor in contaminated water  
through advanced oxidation processes

Autora:

Dña. M<sup>a</sup> Carmen Calín Mora

Directores:

Dra. Dña. Nuria Vela de Oro

Dr. D. José Fenoll Serrano

Murcia, diciembre 2020





**UCAM**  
UNIVERSIDAD CATÓLICA  
DE MURCIA

**AUTORIZACIÓN DE LO/S DIRECTOR/ES DE LA TESIS**  
**PARA SU PRESENTACIÓN**

La Dra. Dña. Nuria Vela de Oro y el Dr. D. José Fenoll Serrano como directores de la Tesis Doctoral titulada “Remediation of endocrine disruptor in contaminated water through advanced oxidation processes” realizada por Dña. M<sup>a</sup> Carmen Calín Mora en el Programa de Doctorado en Tecnologías de la Computación e Ingeniería Ambiental, **autorizan su presentación a trámite** dado que reúne las condiciones necesarias para su defensa.

Lo que firmamos, para dar cumplimiento al Real Decreto 99/2011, 1393/2007, 56/2005 y 778/98, en Murcia a 1 de diciembre de 2020.





# UCAM

UNIVERSIDAD CATÓLICA  
DE MURCIA

## AUTHORIZATION OF THE DIRECTORS OF THE THESIS FOR SUBMISSION

Prof. Dr. Nuria Vela de Oro and Prof. Dr. José Fenoll Serrano as Directors<sup>(1)</sup> of the Doctoral Thesis “Remediation of endocrine disruptor in contaminated water through advanced oxidation processes” by in the PhD Programme in Computer Technology and Environmental Engineering, **authorizes for submission** since it has the conditions necessary for its defense.

In order to comply the Royal Decrees 99/2011, 1393/2007, 56/2005 and 778/98, we sign it in Murcia, 1<sup>th</sup> December 2020.





## AGRADECIMIENTOS / ACKNOWLEDGMENTS

En todo este largo recorrido, a veces casi interminable, son muchas las personas que me han acompañado y han hecho posible, de forma directa o indirecta, que esta tesis viera su final. Por lo tanto y, en primer lugar, quiero agradecer a la Universidad Católica de Murcia el apoyo tanto económico como institucional al desarrollo de esta tesis de investigación. En particular a mi directora Nuria, compañera de carrera, amiga de toda una vida y trabajadora incansable. Le agradezco su paciencia, su determinación a la hora de mandarme a congresos, su confianza y, sobre todo, el empujón final dónde las fuerzas ya me faltaban.

En segundo lugar, agradezco a todo el equipo del Instituto Murciano de Investigación y Desarrollo Agroalimentario (IMIDA) los medios técnicos que ha puesto a mi disposición. Pero para mí, lo más importante es el grupo de personas que me han ayudado en este camino. Les agradezco, principalmente, las veces que me han hecho reír en los momentos difíciles, el acompañamiento y sus palabras de cariño, porque no me llevo compañeros, para mí, todos ellos son mi familia y como tales los llevaré siempre en mi corazón. No puedo acabar este apartado sin dedicarle una mención especial a mi codirector José Fenoll, pues, a pesar de no conocerme, me incorporó en su equipo como un miembro más. Le agradezco su forma de trabajar conmigo: confiada y libre, es difícil no sentirse cómoda con un codirector así.

En tercer lugar, es importante para mí agradecer al Profesor Navarro, de la Universidad de Murcia, su generosidad pues compartió conmigo sus años de experiencia y conocimiento. Me ayudó en los ensayos y puso a mi disposición todos los medios requeridos, pero desde luego, su gran contribución ha sido su

ayuda inestimable en las publicaciones. Todo este trabajo, gracias a su trayectoria profesional, ha sido, sin ningún lugar a dudas, posible.

Quisiera agradecer igualmente a la Entidad de Saneamiento y Depuración de Aguas Residuales de la Región de Murcia (ESAMUR) el soporte técnico ofrecido.

Finalmente, no quiero olvidarme de todas esas personas, anónimas para vosotros, pero indispensables en mi vida que han contribuido a mantener mi ilusión y que nunca han dudado de mí. Este grupo de personas lo conforman mis amigos que con su calor han hecho de la oscuridad, la luz.

GRACIAS

To my sons,  
As I learnt what love is

A mis amigos,  
Por toda una vida junto a mí

Al mio carissimo insegnante,  
Per tutto quello condiviso con me



## RESUMEN

El problema originado por la escasez de agua en determinadas zonas del planeta se agudiza en gran manera por la contaminación de la misma debido al vertido indiscriminado de residuos generados por la actividad del hombre, lo que supone una amenaza para el medio acuático y en consecuencia para la salud humana. Entre los principales contaminantes emergentes que se pueden encontrar en el agua cabe destacar, por su importancia, debido a su amplia utilización y/o potencial ecotoxicológico sobre los ecosistemas hídricos naturales, a los Disruptores Endocrinos (DEs). DEs son sustancias químicas de diversa naturaleza (parabenes, fenoles, ftalatos, plaguicidas, etc.) que se encuentran en muchos productos de origen cotidiano, alimentos y agua, así como en otros compartimentos medioambientales, que pueden interferir la síntesis, secreción, transporte, acción y eliminación de las hormonas naturales. Por lo tanto, se hace necesario, establecer mecanismos preventivos que minimicen la presencia de estas sustancias en el Medio Ambiente, incluido, por supuesto, el medio hídrico, y, además, resulta fundamental, desarrollar técnicas de remediación, que favorezcan la eliminación total de cualquier traza de contaminantes en el agua, a fin de potenciar su reutilización posterior. Con carácter prioritario, tal y como se establece en la Directiva 2013/39/UE, es preciso identificar las causas de la contaminación y tratar las emisiones de contaminantes en la fuente misma, de la forma más eficaz en términos económicos y ambientales. Las aguas contaminadas por la actividad humana pueden, en general, ser procesadas eficientemente por plantas de tratamiento biológico o por métodos químicos convencionales en estaciones depuradoras de aguas residuales. Sin embargo, en algunos casos, estos procedimientos resultan inadecuados para eliminar compuestos orgánicos recalcitrantes y alcanzar el grado de depuración o pureza requerido por ley. En este sentido, la implementación de Procesos Avanzados de Oxidación, como la Fotocatálisis Heterogénea, ofrecen una solución eficiente y altamente innovadora para conseguir tal fin. Estas técnicas están basadas en el empleo combinado de un fotocatalizador y luz solar o UV artificial para generar especies altamente oxidantes, y, por tanto, capaces de degradar muchas moléculas orgánicas incluso hasta  $\text{CO}_2$ ,  $\text{H}_2\text{O}$  y sales minerales.

En esta Tesis se ha estudiado la degradación fotocatalítica en una planta piloto bajo condiciones de irradiación solar de doce DEs en efluentes de aguas residuales mediante el empleo de Fotocatálisis Heterogénea. Previamente se realizó la caracterización físico-química de los efluentes de depuradora utilizados en los distintos ensayos. Los DEs estudiados fueron seis plaguicidas (malatión, fenitrotión, quinalfos, vinclozolina, dimetoato y fenarimol), cuatro plastificantes (bisfenol A, bisfenol B, butil bencil ftalato, diamil ftalato) y dos conservantes (etil 4-hidroxibenzoato y metil p-hidroxibenzoato). Igualmente, se validó el método de extracción y análisis de los DEs. Las nanopartículas comerciales empleadas como fotocatalizadores fueron ZnO, TiO<sub>2</sub> P25, TiO<sub>2</sub> Alfa Aesar y TiO<sub>2</sub> vlp 7000, y el aceptor de electrones fue Na<sub>2</sub>S<sub>2</sub>O<sub>8</sub>. Del mismo modo, se procedió a la caracterización de cada uno de los semiconductores empleados.

Las variables operacionales en los distintos ensayos de fotodegradación (tipo y carga de catalizador, efecto del aceptor de electrones y pH) fueron previamente optimizados bajo condiciones de laboratorio en un fotorreactor bajo luz UVA artificial. Del mismo modo, se realizaron los correspondientes experimentos fotolíticos en ausencia de catalizador u oxidante, pero con la misma carga de contaminante.

Los ensayos realizados en condiciones de laboratorio mostraron que las condiciones óptimas operacionales a aplicar en los experimentos de fotodegradación solar en planta piloto fueron 200 mg L<sup>-1</sup> de catalizador y 250 mg L<sup>-1</sup> de oxidante a pH 7. La cantidad de catalizador afectó al proceso, aumentando la degradación de los compuestos a medida que aumentaba la carga hasta la concentración óptima (200 mg L<sup>-1</sup>). La eficiencia del proceso fue del orden: ZnO > TiO<sub>2</sub> P25 >>TiO<sub>2</sub> vlp 7000 > TiO<sub>2</sub> Alfa Aesar, para todos los compuestos estudiados. La adición del persulfato mejoró notablemente el rendimiento de la fotocatalisis. La baja eficacia mostrada por TiO<sub>2</sub> Alfa Aesar en los ensayos de laboratorio hicieron que se descartara este semiconductor para los posteriores experimentos en la planta piloto.

Los experimentos realizados bajo irradiación solar en la planta piloto pusieron de manifiesto que el uso del tandem ZnO/Na<sub>2</sub>S<sub>2</sub>O<sub>8</sub> y TiO<sub>2</sub>/Na<sub>2</sub>S<sub>2</sub>O<sub>8</sub> mejoraron enormemente el grado de fotodegradación de los compuestos. En todos los casos, las tasas de degradación fueron significativamente más bajas en la fotólisis que en los experimentos que utilizan fotocatalizadores.

El proceso de fotodegradación siguió un modelo cinético de pseudo-primer orden. La media de las constantes de velocidad del sistema calculadas a partir de los 12 compuestos puso de manifiesto que el tándem ZnO/Na<sub>2</sub>S<sub>2</sub>O<sub>8</sub> fue el que obtuvo mayor eficacia fotocatalítica. Las constantes de velocidad medias (n = 12) fueron  $0.6303 \pm 0.7342$ ,  $0.3618 \pm 0.5055$  y  $0.1475 \pm 0.1620 \text{ min}^{-1}$  para el ZnO, TiO<sub>2</sub> P25 y TiO<sub>2</sub> vlp 7000, respectivamente. Esto significó que la constante de velocidad (como valor medio para todos los DEs) para el sistema de ZnO fue aproximadamente un factor de 1.7 y 4.3 más alta que la calculada para los sistemas de TiO<sub>2</sub> P25 y TiO<sub>2</sub> vlp 7000, respectivamente. Los experimentos realizados con TiO<sub>2</sub> vlp 7000 revelaron que, la estrategia de dopar las partículas de TiO<sub>2</sub> con carbono para aumentar el rendimiento del fotocatalizador bajo el espectro visible, no ofreció los resultados que se esperaban. Por consiguiente, la tasa de degradación de los DEs en las aguas residuales tratadas se pudo establecer en el orden: ZnO > TiO<sub>2</sub> P25 > TiO<sub>2</sub> vlp 7000.

El uso de la fotocatálisis solar heterogénea puede considerarse como una tecnología adecuada para eliminar muchos DEs de los efluentes de aguas residuales, especialmente en zonas como el sudeste de España, donde la escasez de agua de riego es un problema importante, y hay más de 3.000 h de luz solar por año. Además, el tratamiento puede considerarse económicamente sostenible aunque el coste depende en gran medida de la naturaleza del contaminante presente en el efluente y del tratamiento fotocatalítico empleado.

**Palabras clave:** Disruptores endocrinos, bisfenoles, ftalatos, parabenes, plaguicidas, fotocatálisis solar, ZnO, TiO<sub>2</sub>, aguas residuales.





## ABSTRACT

The problem caused by water shortages in certain areas of the planet is greatly exacerbated by the pollution of water due to the indiscriminate dumping of waste generated by human activity, which involves a threat to the aquatic environment and consequently to human health. Among the main emerging pollutants that can be found in water, it is important to highlight, due to their extensive use and/or ecotoxicological potential on natural water ecosystems, Endocrine Disruptors (EDs). EDs are chemical substances of diverse nature (parabens, phenols, phthalates, pesticides, etc.) found in many products of daily origin, food and water, as well as in other environmental compartments, which can interfere with the synthesis, secretion, transport, action and elimination of natural hormones. It is therefore necessary to establish preventive mechanisms that minimise the presence of these substances in the environment, including, of course, the water environment, and it is also essential to develop remediation techniques that promote the total elimination of any trace of pollutants in the water, in order to enhance its subsequent reuse. As a priority, as set out in Directive 2013/39/EU, the causes of pollution must be identified and emissions of pollutants at source must be dealt with in the most economically and environmentally effective way. Water polluted by human activity can generally be processed efficiently by biological treatment plants or by conventional chemical methods in wastewater treatment plants. However, in some cases, these procedures are inadequate to remove recalcitrant organic compounds and to achieve the degree of purity required by law. In this sense, the implementation of Advanced Oxidation Processes, such as Heterogeneous Photocatalysis, offers an efficient and highly innovative solution to achieve this end. These techniques are based on the combined use of a photocatalyst and sunlight or artificial UV light to generate highly oxidising species, and therefore capable of degrading many organic molecules even to CO<sub>2</sub>, H<sub>2</sub>O and mineral salts.

In this Thesis, photocatalytic degradation has been studied in a pilot plant under conditions of solar irradiation of twelve EDs in wastewater effluents through the use of Heterogeneous Photocatalysis. Previously, the physical-chemical characterisation of the wastewater treatment plant effluents used in the different tests was carried out. The EDs studied were six pesticides (malathion,

phenitrothion, quinalphos, vinclozolin, dimethoate and fenarimol), four plasticisers (bisphenol A, bisphenol B, butyl benzyl phthalate, diamyl phthalate) and two preservatives (ethyl 4-hydroxybenzoate and methyl p-hydroxybenzoate). The method of extraction and analysis of the EDs was also validated. The commercial nanoparticles used as photocatalysts were ZnO, TiO<sub>2</sub> P25, TiO<sub>2</sub> Alpha Aesar and TiO<sub>2</sub> vlp 7000, and the electron acceptor was Na<sub>2</sub>S<sub>2</sub>O<sub>8</sub>. Similarly, the characterisation of each of the semiconductors used was carried out.

The operational variables in the various photodegradation tests (type and charge of catalyst, effect of the electron acceptor and pH) were previously optimized under laboratory conditions in a photoreactor under artificial UVA light. Similarly, the corresponding photolytic experiments were carried out in the absence of a catalyst or oxidant, but with the same pollutant load.

Tests carried out under laboratory conditions showed that the optimum operational conditions to be applied in the pilot plant solar photodegradation experiments were 200 mg L<sup>-1</sup> of catalyst and 250 mg L<sup>-1</sup> of oxidant at pH 7. The amount of catalyst affected the process, increasing the degradation of the compounds as the load increased to the optimum concentration (200 mg L<sup>-1</sup>). The efficiency of the process was of the order: ZnO > TiO<sub>2</sub> P25 >> TiO<sub>2</sub> vlp 7000 > TiO<sub>2</sub> Alpha Aesar, for all the compounds studied. The addition of persulphate significantly improved the performance of photocatalysis. The low efficiency shown by TiO<sub>2</sub> Alpha Aesar in the laboratory tests led to the discarding of this semiconductor for the subsequent experiments in the pilot plant.

The experiments carried out with low solar radiation in the pilot plant showed that the use of the tandem ZnO/Na<sub>2</sub>S<sub>2</sub>O<sub>8</sub> and TiO<sub>2</sub>/Na<sub>2</sub>S<sub>2</sub>O<sub>8</sub> greatly improved the degree of photodegradation of the compounds. In all cases, degradation rates were significantly lower in photolysis than in experiments using photocatalysts.

The photodegradation process followed a pseudo-first order kinetic model. The average of the system speed constants calculated from the 12 compounds showed that the ZnO/Na<sub>2</sub>S<sub>2</sub>O<sub>8</sub> tandem had the highest photocatalytic efficiency. The mean rate constants (n = 12) were  $0.6303 \pm 0.7342$ ,  $0.3618 \pm 0.5055$  and  $0.1475 \pm 0.1620$  min<sup>-1</sup> for ZnO, TiO<sub>2</sub> P25 and TiO<sub>2</sub> vlp 7000, respectively. This meant that the rate constant (as an average value for all the EDs) for the ZnO system was approximately a factor of 1.7 and 4.3 higher than that calculated for the TiO<sub>2</sub> P25

and TiO<sub>2</sub> vlp 7000 systems, respectively. Experiments with TiO<sub>2</sub> vlp 7000 revealed that the strategy of doping TiO<sub>2</sub> particles with carbon to increase the performance of the photocatalyst under the visible spectrum did not give the expected results. Consequently, the rate of degradation of EDs in treated wastewater could be established in the order: ZnO > TiO<sub>2</sub> P25 > TiO<sub>2</sub> vlp 7000.

The use of heterogeneous solar photocatalysis can be considered as a suitable technology to remove many EDs from wastewater effluents, especially in areas such as south-eastern Spain, where the availability of irrigation water is a major problem, and there are more than 3,000 h of sunlight per year. In addition, the treatment can be considered economically sustainable although the cost depends largely on the nature of the pollutant present in the effluent and the photocatalytic treatment used.

**Keywords:** Endocrine disruptors, bisphenols, phthalates, parabens, pesticides, solar photocatalysis, ZnO, TiO<sub>2</sub>, wastewater.



## INDEX

AUTORIZACIÓN DE LOS DIRECTORES	
AUTHORIZATION FOR THE DIRECTORS	
AGRADECIMIENTOS / ACKNOWLEDGMENTS	
RESUMEN	
ABSTRACT	
INDEX	
ACRONYMS AND ABBREVIATIONS	
INDEX OF FIGURES	
INDEX OF TABLES	
I - INTRODUCTION .....	31
1.1. WATER POLLUTION: THE STATE OF THE ART .....	33
1.2. ENDOCRINE DISRUPTORS .....	36
1.2.1. Definition.....	36
1.2.2. The state of the art.....	37
1.2.3. Mechanism of action .....	39
1.2.4. Effects on health .....	40
1.3 LEGAL FRAMEWORK .....	41
1.4 ADVANCED OXIDATION PROCESS: HETEROGENEOUS PHOTOCATALYSIS .....	47
II - JUSTIFICATION AND OBJECTIVES.....	53
III – MATERIAL AND METHODS.....	57
3.1. EXPERIMENTAL DESIGN .....	59
3.2. INVESTIGATED COMPOUNDS.....	61
3.3. REAGENTS AND CATALYSTS .....	64
3.4. WASTEWATER EFFLUENT .....	64
3.3. EXTRACTION AND ANALYSIS OF EDS.....	65
3.5. CHARACTERIZATION OF CATALYSTS .....	67
3.6. PHOTOCATALYTIC EXPERIMENTS AT LAB SCALE.....	68
3.7. EXPERIMENTAL SETUP OF SOLAR PHOTOCATALYTIC TRIAL .....	70
3.8. SOLAR PHOTOCATALYTIC KINETICS.....	72
3.9. STATISTICAL ANALYSIS.....	74
IV – RESULTS AND DISCUSSION .....	75

4.1. ANALYTIC METHODOLOGY VALIDATION FOR EDS DETERMINATION .....	77
4.2. CATALYST CHARACTERIZATION .....	79
4.3. OPTIMIZATION OF HETEROGENEOUS PHOTOCATALYSIS PROCESSES IN LABORATORY CONDITIONS .....	82
4.3.1. Photocatalytic experiments with ZnO at lab scale.....	83
4.3.2. Photocatalytic experiments with TiO <sub>2</sub> at lab scale.....	92
4.4. PHOTOCATALYSIS EXPERIMENTS IN A PILOT PLANT UNDER SOLAR RADIATION .....	100
4.4.1. Solar photocatalytic experiments with ZnO.....	100
4.4.2. Solar photocatalytic experiments with TiO <sub>2</sub> .....	111
4.4.3. Comparative analysis between the solar photocatalytic assays with ZnO y TiO <sub>2</sub> .....	123
4.4.5. Economic assessment for water treatment .....	126
V - CONCLUSIONS.....	129
VI - REFERENCES.....	133
VII - APPENDIX.....	149

## ACRONYMS AND ABBREVIATIONS

AOP: Advance Oxidation Process  
BA: Bisphenol A  
BB: Bisphenol B  
BET: Brunauer-Emmet Teller  
BOD<sub>5</sub>: Biological oxygen demand  
BP: Butyl benzylphthalate  
DOC: Dissolved organic carbon  
DOM: Dissolved organic materia  
DP: Diamyl phthalate  
DT: Dimethoate  
EC: Electric conductivity  
EC Emerging Contaminant  
ED: Endocrine Disruptor  
EP: Ethyl 4- hydroxybenzoate  
FR: Fenarimol  
FT: Fenitrothion  
GC-MS: Gas chromatography and mass spectrometric detection  
ICP: Inductively coupled plasma  
LL: Liquid-liquid  
MP: Methyl p-hydroxybenzoato  
MT: Malathion  
ORP: Oxidation-reduction potential  
POP: Persistent Organic Pollutant  
PZC: Point zero charge  
QOD: Chemical oxygen demand  
QP: Quinalphos  
SEM: Scanning electron microscopy  
SIM: Selected ion monitoring  
TOC: Total organic carbon  
UV-DR: Diffuse reflectance spectroscopy over UV-VIS  
VZ: Vinclozoline  
WFD: Water Framework Directive  
WWTP: Wastewater treatment plant  
XRD: X-Ray Diffractometry





## INDEX OF FIGURES

Figure 1.1. ECs classification present in the environment.....	34
Figure 1.2. Schematic pathway of some emerging contaminants from source to receptors .....	35
Figure 1.3. Legal framework schematic diagram .....	46
Figure 1.4. Schematic illustration of heterogeneous photocatalysis using solid semiconductors.....	50
Figure 3.1. Representative scheme of the experimental work developed.....	60
Figure 3.2. Analytical process scheme.....	66
Figure 3.3. Simplified drawing of the photochemical reactor and operational process followed.....	69
Figure 3.4. Schematic drawing of the solar pilot plant used.....	70
Figure 3.5. Solar photocatalytic design scheme at pilot plant scale .....	71
Figure 4.1. XRD patterns of (A) TiO <sub>2</sub> vlp 7000, (B) TiO <sub>2</sub> P25, (C) TiO <sub>2</sub> Alfa Aesar and (D) ZnO.....	80
Figure 4.2. SEM image and elemental microanalysis of (A) TiO <sub>2</sub> vlp 7000, (B) TiO <sub>2</sub> P25, TiO <sub>2</sub> Alfa Aesar and (D) ZnO.....	82
Figure 4.3. Effect of Zn concentration on the photodegradation of the plasticizers and preservatives under laboratory conditions.....	84
Figure 4.4. Effect of Zn concentration on the photodegradation of the pesticides under laboratory conditions .....	85
Figure 4.5. Effect of electron acceptor on the photodegradation of the plasticizers and preservatives using different concentrations of Na <sub>2</sub> S <sub>2</sub> O <sub>8</sub> at fixed ZnO loading (200 mg L <sup>-1</sup> ) under laboratory conditions .....	86
Figure 4.6. Effect of electron acceptor on the photodegradation of the pesticides using different concentrations of Na <sub>2</sub> S <sub>2</sub> O <sub>8</sub> at fixed ZnO loading (200 mg L <sup>-1</sup> ) under laboratory conditions.....	87
Figure 4.7. pH effect on the plasticizers and preservatives photodegradation at fixed ZnO (200 mg L <sup>-1</sup> ) and Na <sub>2</sub> S <sub>2</sub> O <sub>8</sub> (250 mg L <sup>-1</sup> ) concentrations under laboratory conditions .....	90

Figure 4.8. pH effect on the pesticides photodegradation at fixed ZnO (200 mg L <sup>-1</sup> ) and Na <sub>2</sub> S <sub>2</sub> O <sub>8</sub> (250 mg L <sup>-1</sup> ) concentrations under laboratory conditions.....	91
Figure 4.9. Effect of TiO <sub>2</sub> concentration on the photodegradation of the plasticizers and the preservatives under laboratory conditions .....	93
Figure 4.10. Effect of TiO <sub>2</sub> concentration on the photodegradation of the pesticides under laboratory conditions .....	94
Figure 4.11. Effect of electron acceptor on the photodegradation of plasticizers and preservatives using different concentrations of Na <sub>2</sub> S <sub>2</sub> O <sub>8</sub> at fixed TiO <sub>2</sub> loading (200 mg L <sup>-1</sup> ) under laboratory conditions .....	95
Figure 4.12. Effect of electron acceptor on the photodegradation of pesticides using different concentrations of Na <sub>2</sub> S <sub>2</sub> O <sub>8</sub> at fixed TiO <sub>2</sub> loading (200 mg L <sup>-1</sup> ) under laboratory conditions.....	96
Figure 4.13. Effect of pH on the photodegradation of plasticizers and preservatives at fixed TiO <sub>2</sub> (200 mg L <sup>-1</sup> ) and Na <sub>2</sub> S <sub>2</sub> O <sub>8</sub> (250 mg L <sup>-1</sup> ) concentrations under laboratory conditions .....	98
Figure 4.14. Effect of pH on the photodegradation of pesticides at fixed TiO <sub>2</sub> (200 mg L <sup>-1</sup> ) and Na <sub>2</sub> S <sub>2</sub> O <sub>8</sub> (250 mg L <sup>-1</sup> ) concentrations under laboratory conditions .....	99
Figure 4.15. Evolution of the plasticizer and preservative residues as a function of natural sunlight irradiation time using the tandem ZnO (200 mg L <sup>-1</sup> )/Na <sub>2</sub> S <sub>2</sub> O <sub>8</sub> (250 mg L <sup>-1</sup> ) at pilot plant scale .....	101
Figure 4.16. Evolution of dissolved organic carbon (DOC) during the photolytic and photocatalytic experiments with ZnO and the plasticizer and preservative under natural sunlight irradiation.....	103
Figure 4.17. Evolution of toxicity to <i>Vibrio fischeri</i> during the photolytic and photocatalytic experiments with ZnO and plasticizer and preservative under solar irradiation.....	104
Figure 4.18. Evolution of the pesticide residues as a function of sunlight irradiation using the tandem ZnO (200 mg L <sup>-1</sup> )/Na <sub>2</sub> S <sub>2</sub> O <sub>8</sub> (250 mg L <sup>-1</sup> ) at pilot plant scale .....	105
Figure 4.19. Evolution of dissolved organic carbon (DOC) during the photolytic and photocatalytic experiments with ZnO and pesticides under natural sunlight irradiation.....	106
Figure 4.20. Evolution of toxicity to <i>Vibrio fischeri</i> during the photolytic and photocatalytic experiments with ZnO and pesticides under solar irradiation ....	107

Figure 4.21. Evolution of plasticizer and preservative residues as a function of natural sunlight irradiation time using the tandem TiO <sub>2</sub> (200 mg L <sup>-1</sup> )/Na <sub>2</sub> S <sub>2</sub> O <sub>8</sub> (250 mg L <sup>-1</sup> ) at pilot plant scale.....	112
Figure 4.22. Evolution of dissolved organic carbon (DOC) during the photolytic and photocatalytic experiments with TiO <sub>2</sub> and plasticizer and preservative under natural sunlight irradiation .....	113
Figure 4.23. Evolution of toxicity to <i>Vibrio fischeri</i> during the photolytic and photocatalytic experiments with TiO <sub>2</sub> and plasticizer and preservative under solar irradiation.....	114
Figure 4.24. Evolution of pesticides residues as a function of natural sunlight irradiation time using the tandem TiO <sub>2</sub> (200 mg L <sup>-1</sup> )/Na <sub>2</sub> S <sub>2</sub> O <sub>8</sub> (250 mg L <sup>-1</sup> ) at pilot plant scale.....	116
Figure 4.25. Evolution of dissolved organic carbon (DOC) during the photolytic and photocatalytic experiments with TiO <sub>2</sub> and pesticides under natural sunlight irradiation.....	117
Figure 4.26. Evolution of toxicity to <i>Vibrio fischeri</i> during the photolytic and photocatalytic experiments with TiO <sub>2</sub> and pesticides under solar irradiation.....	118



## INDEX OF TABLES

Table 1.1. Endocrine disruptor action mechanisms and responses .....	40
Table 1.2. Toxicological features' EDs .....	40
Table 1.3. AOPs advantages .....	48
Table 3.1. Physical-chemical characteristics, structures and uses of the compounds studied .....	62
Table 3.2. Composition of sewage wastewater effluent used in this study .....	65
Table 4.1: Validation parameters and analytical conditions of EDs by GC-MS .....	78
Table 4.2. Physico-chemical properties of photocatalysts .....	79
Table 4.3. First order kinetic parameters (n=3) and normalized illumination time for 50% and 90% degradation calculated for the photolytic degradation of the plasticizers and preservatives under natural sunlight irradiation without photocatalyzer/oxidant.....	108
Table 4.4. First order kinetic parameters (n=3) and normalized illumination time for 50% and 90% degradation calculated for the photocatalytic degradation of the plasticizers and preservatives under natural sunlight irradiation using ZnO/Na <sub>2</sub> S <sub>2</sub> O <sub>8</sub> .....	109
Table 4.5. First order kinetic parameters (n=3) and normalized illumination time for 50% and 90% degradation calculated for the photolytic degradation of the pesticides under natural sunlight irradiation without photocatalyzer/oxidant ..	110
Table 4.6. First order kinetic parameters (n=3) and normalized illumination time for 50% and 90% degradation calculated for the photocatalytic degradation of the pesticides under natural sunlight irradiation using ZnO/Na <sub>2</sub> S <sub>2</sub> O <sub>8</sub> .....	110
Table 4.7. First order kinetic parameters (n=3) and normalized illumination time for 50% and 90% degradation calculated for the photocatalytic degradation of the plasticizers and preservatives under natural sunlight irradiation using TiO <sub>2</sub> vlp 7000.....	120
Table 4.8. First order kinetic parameters (n=3) and normalized illumination time for 90% degradation calculated for the photocatalytic degradation of the plasticizers & preservatives under natural sunlight irradiation using TiO <sub>2</sub> P25.	121
Table 4.9. First order kinetic parameters (n=3) and normalized illumination time for 50% and 90% degradation calculated for the photocatalytic degradation of the pesticides under natural sunlight irradiation using TiO <sub>2</sub> vlp 7000.....	121

Table 4.10. First order kinetic parameters (n=3) and normalized illumination time for 50% and 90% degradation calculated for the photocatalytic degradation of the pesticides under natural sunlight irradiation using TiO <sub>2</sub> P25 .....	122
Table 4.11. EDs rate constants obtained in the photocatalytic treatment under solar irradiation .....	123
Table 4.12: Economic assessment for water photocatalytic treatment with ZnO and TiO <sub>2</sub> (P25 and vlp 7000) .....	127

# **I - INTRODUCTION**





## I - INTRODUCTION

### 1.1. WATER POLLUTION: THE STATE OF THE ART

Water is an essential resource for life and a crucial factor for economic and social development. In our planet, the 75 percent of the Earth land surface is covered by water however, not all the water is suitable for human consumption. Approximately, the 97.5 percent is marine water, therefore a small proportion is freshwater consisted in lakes, rivers and reservoirs. This minimum quantity of water is available for population and used in agriculture, industry and household purposes.

Although water is a renewable resource and it has a high-effective self-cleaning ability from pollution, the problem arises when the pollutants concentration level is higher than its own absorption ability what makes water harmful for humans and the environment. This natural purification ability is precisely for which water has been the main waste receiver of human activities.

The water contamination caused by anthropogenic activity has its origin during The Second Industrial Revolution, in the middle 19<sup>th</sup> century. The increase in consumer goods and the rapid advances in manufacturing required huge quantities of water to transform unprocessed materials into finished products. The wastes generated were released directly into the aquatic environment with a total lack of control, initiating the present problem of water pollution.

It is important to remark, the Mediterranean basin is a sensitive area because of its arid features as the period of dryness lasts between three and five months in which evapotranspiration ratio is higher than precipitations. This special circumstance, the increase of different pollutants, the demographic growth due to tourism and the population demands, have become the Mediterranean basin as the centre of the residues collected from anthropogenic activities during the last three decades.

Although the measures taken during the last century to control the environmental pollution has reduce drastically the presence of several contaminants, for instance the well-known Persistent Organic Pollutants (POPs),

the number of new contaminants consider as potentially threats for the environment and human health has increased and, for this reason, they have given scientist attention, initiating a network of research. These new pollutants are known as Emerging Contaminants (ECs) [Sauve and Desrosiers 2014].

ECs are a group of natural and synthetic chemicals whose existence in the different ecosystems is not new. Due to the development of sophisticated detection technologies and analytical methods, it has been possible to identify them in several ecosystems, what has intensified the concern about the possible damages to human health and environment [Geissen et al., 2015].

ECs occur in many kinds of daily chemicals including pharmaceuticals, cosmetics and personal care or household products. Others are pesticides, nanoparticles, preservatives, synthetic hormones or perfluorinated compounds, among others. According to [Lei et al., 2015], ECs can be classified in different categories shown on **Figure 1.1**.

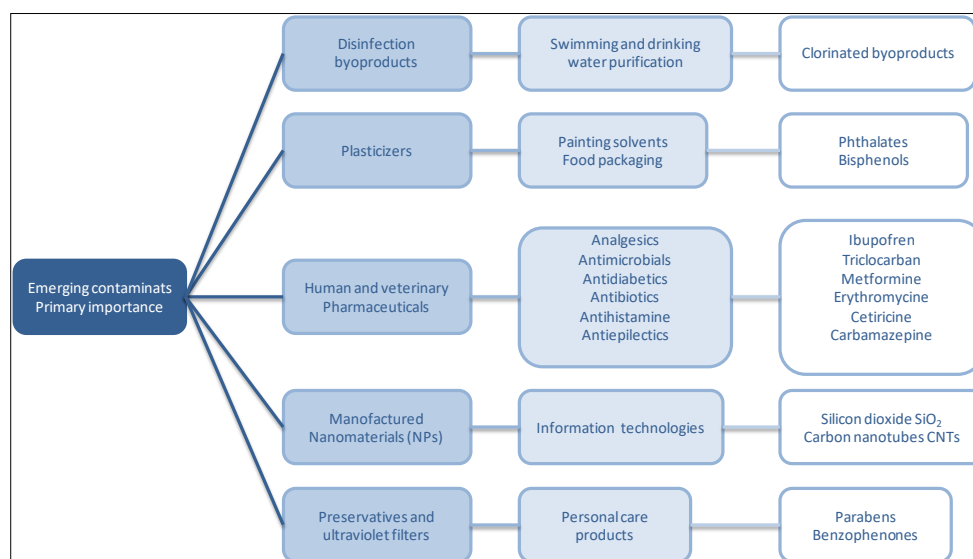


**Figure 1.1.** ECs classification present in the environment [Lei et al., 2015].

The high risk lies in the fact that environmental and human toxicological information for the majority of the ECs have not been studied yet, therefore is almost impossible to predict the health effects on living creatures [Petrie et al.,

2015]. In addition, the suspected effects could even be intensified on vulnerable groups such as infants and pregnant women as the damage in the very early development stages is significant [Mangalgi et al., 2015].

Another important consideration is the fact that ECs are unsafe for humans not only because they could persist but also because they enter the environment daily and these contaminants may transform into metabolites which interact with the different ecosystems [Barceló, 2003]. **Figure 1.2** shows the sources and fate of some emerging contaminants.

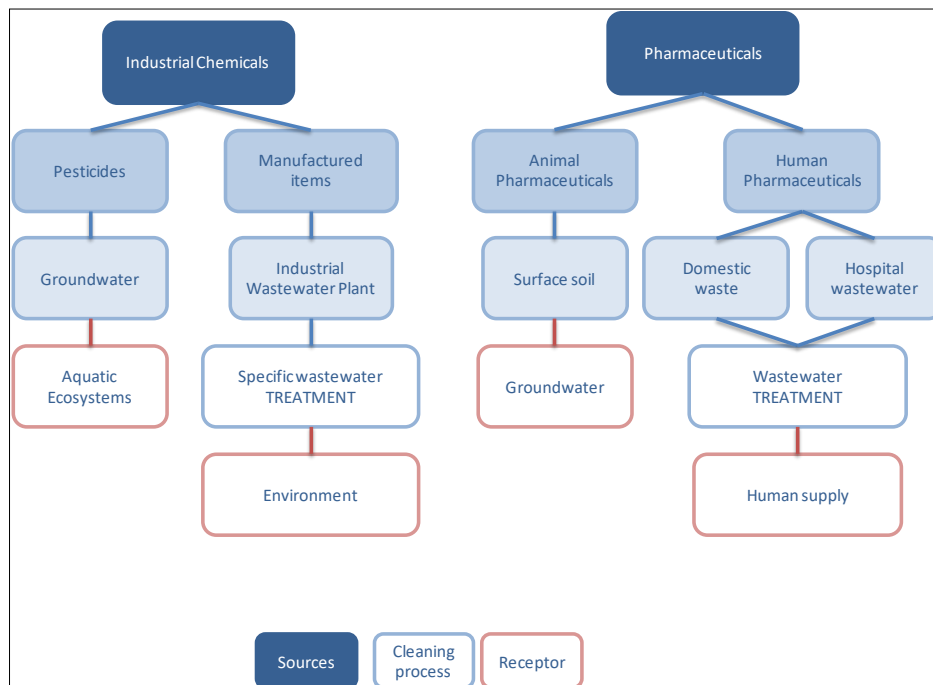


**Figure 1.2.** Schematic pathway of some emerging contaminants from source to receptors [Lapworth et al., 2012].

It is only required to pay attention to our lifestyle to understand where they come from. People use personal care products on regular basis, and they remain in wastewater. Industrial processes generate residues in water and their own treatments are not effective in removing them. As a result, humans are exposed to these pollutants from their manufactured moment to last degradation as the water treatment processes were not designed to remove the ECs.

Most ECs are not regulated either in environmental water quality or wastewater discharge regulations and there are not enough monitoring studies of these chemicals. Therefore, there is a need to research these pollutants as the main Organizations, such as European Commission, Environmental Protection Agency or The Health World Organization, demand [Daughton, 2004].

Previous studies have shown an increase in the ECs concentration levels in wastewater [Fawell and Ong 2012; Petrie et al., 2015; Lopez-Pacheco et al., 2019], groundwater [Jurado et al., 2012; Kurwadkar, 2017] and seawater [Nilsen et al., 2019]. As a result, there is a worldwide concern about the consequences of such global exposure and the impacts on the environment and human health. Hence, new technologies are required to be developed in order to tackle this issue to guarantee water quality standards [Batt et al., 2017].

Due to it is complicated to tackle water pollution, it is essential to develop strategies to managing water resources. Effective management must design strategies to guarantee use of water without damaging the resource or the environment, but they must ensure available supplies for the normal life development.

One difficulty to cope with this challenge it is the uncertainty about the climate change as it reduces hydro resources because of the global warming. Global increase of temperature changes precipitations patterns and intensify adverse weather conditions.

As water pollution is a global concern, it is important to understand the contaminants present in water and their role in reducing its quality what makes possible to anticipate water contamination and the expected effects on environment.

## **1.2. ENDOCRINE DISRUPTORS**

### **1.2.1. Definition**

Among the principal ECs present in water, an important group is the Endocrine Disruptors (EDs) because of their wide use and potential toxicology. EDs are natural chemicals but most of them are man-made or artificial ones [Monneret 2017]. Some common EDs include parabens, phthalates, phenols or

polycyclic aromatic hydrocarbons, among others. Found in baby products [Berger et al., 2015], fragrances, cleaning chemicals, lining of canned-food, dental sealants, pesticides [Mnif et al., 2011], pharmaceuticals [Dodge et al., 2015] personal care products [Philippat et al., 2015], consumer goods or toys, for which it is thought the exposure is extensive [Gonzalez et al., 2012; Banjac et al., 2015; Booij et al., 2016; Archer et al., 2017].

### 1.2.2. The state of the art

The awareness of the environment degradation and wildlife conservation is due to Rachel Carson, an American marine biologist whose last book “Silent Spring” [Carson et al., 1962] is a worldwide environmental reference.

Carson and her college Clarens Cottam, having the knowledge of the risky use of DDT since 1944, started their research on the effects of these chemical and other pesticides in a Bird Sanctuary in Massachusetts. DDT was considered an ideal insecticide and very effective against a great number of insect species, some of them malaria and typhus transmitters. So successful was this discovery that Hermann Müller received a Nobel Prize in 1948 for this work.

Carson was collecting information on the consequences of pesticide overuse. She warned about the property of these chemicals to unbalance trophic levels and how this situation could affect not only bird populations but also fish, mammals and even humans. She explained the adverse effects of long-term exposure to DDT as they are accumulated and stored in adipose tissue, affecting population group health. In fact, the main feature of these chemicals is the factor they interfere with hormone signaling, causing even irreversible changes in the cells.

The pesticide indiscriminatory use was due to the chemical industry development after the Second World War. During this his period there was a huge agriculture growth, and the excesses were export abroad generating important economic benefits. Under this situation, a fierce campaign was launched against Rachel Carson by the Manufacturing Chemists. She was accused by alarmist and her research generated the opposition among farmers and she was sued by the Chemical Companies. However, Carson did not promote the use ending but the responsible use of them.

Despite the difficulties, her book was published in 1962 and it was a real success. Unfortunately, her early death did not allow her to know the impact of her book on the American social awareness. A year later, John F. Kennedy constituted a Scientific Committee to deep in this issue and DDT, she led the creation of Environmental Protection Agency and DDT was finally banned in 1972.

However, "Endocrine Disruptor" term was applied by the American zoologist Theodora Colborn [Colborn et al., 1993]. Working for the World Wild Fund (WWF) in 1988, she reviewed literature about research on Great Lakes ecosystem. She noticed 16 bird species suffered from reproduction problems and their offspring were weak, deformed or simply infertile. Therefore, she hypothesized the chemicals affected hormone system.

As Rachel Carson, Theodora Colborn spent seven years studying water quality on freshwater and the harmful effects of water pollution on living creatures. She was convinced there were chemicals in the water causing problems by modifying hormone system.

As there were many studies concerning harmful chemicals in the water but quite disperse, Colborn organized The *Wingspread Conference* in Wisconsin in July 1991. She met a group of 21 scientists from different disciplines including endocrinologists, pharmacists, toxicologists, anthropologists and ecologists. After several days sharing their research, the participants confirmed the presence of pollutants in water that alter the endocrine system normal function, especially reproductive system and sexual development.

Colborn and her colleges gathered information about endocrine disruption and published "*Our stolen future*" in 1996 [Colburn 1997]. This book completed the information of "*Silent Spring*", as it exposures the reasons for which Rachel Carson was alarmed about pesticides overuse. The book compiled the field research information, laboratory studies, and surveys that show birth defects, sexual malfunctions and reproductive faults in wild species. In addition, the book stated these compounds had become a component in our economy and, as a result, they are widespread around the Biosfera.

Dr. Colborn was founder of Endocrine Disruption Exchange, in 2003, a non-profit organization which aim was to share scientific information of endocrine

disruption. Her team cataloged around 500 possible EDs but, at that time, the suspected chemicals were 8 million whose real effects were unknown.

She cooperated with the Ecosystem Health Committee of the International Joint Commission of the United States and Canada to produce a strategy on endocrine disruption in 2009, what it was her last work.

### 1.2.3. Mechanism of action

Endocrine disruption is a dysfunction in endocrine system due to the presence of exogenous chemicals and, as it was mention previously, these chemicals are mainly organic macromolecules labeled as endocrine disruptors.

Research has confirm EDs show many mechanisms of action [Swedenborg et al., 2009] however, direct binding to hormone receptors is by far the most studied mechanism of endocrine disruption [Olea and Fernandez, 2007; Diamanti-Kandarakis et al., 2009; Kiyama and Wada-Kiyama, 2015]. Direct binding implies these compounds interfere hormonal signals, what means the normal signal is not received and the organism does not respond properly because of the interaction between the hormonal receptor and the exogenous molecule [Zoeller et al. 2014]. Therefore, the interference is caused by mimicking endogenous hormones.

EDs can be fixed on the receptors, activate them and generate natural hormone action. On the other hand, EDs can be fixed on receptors but blocking them and inhibiting their action and the last mechanism of action is modifying the hormone concentration levels because the presence of EDs can increase or decrease the hormone levels as they are confused with endogenous hormones.

Hence, organism responses confirm endocrine disruption is an important physiological change that could end in adverse consequences on health. The following **Table 1.1** summarizes the mechanisms of action and physiological responses.

**Table 1.1.** Endocrine disruptor action mechanisms and responses.

ACTION MECHANISMS	FUNCTIONAL RESPONSES
Mimicking hormones Inhibiting receptors Modifying hormonal metabolism	Triggering hormonal action Blocking hormonal release Blocking hormonal synthesis Blocking hormonal elimination

EDs presence is not only an emerging issue but also a complex toxicological situation due to the following factors:

**Table 1.2.** Toxicological features' EDs.

TOXICOLOGICAL CHARACTERISTICS
They work at very low-level concentrations The relationship between cause effect is not lineal Synergistic effects Latency period from exposure Effects can last for the following generations Ubiquitous exposure

#### 1.2.4. Effects on health

Exposure to EDs, even at low levels, can affect human health. As they can mimic, block hormones or modify their level concentrations, biological actions happened [Frye et al. 2012]. The endocrine system is a balance system organized by glands, organs and hormones that regulates functions such as sexual reproduction, homeostasis, blood pressure, etc.

Negative outcomes because of exposure to EDs can be even worst during critical developmental stages and can cause long-lasting effects on health [Prusinski et al., 2016]. Children, infants and early embryonic stages are more vulnerable than adults because growth and tissue differentiation is under continuous and precise cellular events. As a result, embryonic stages are periods in which organogenesis plays an important role therefore, any alteration could



cause irreversible damages. Living creature sensitiveness is variable according to life stage and the consequences are different, affecting more seriously embryonic phases than adult ones.

Evidence has shown in several mammals, included humans, the adverse effects of EDs. Disruptions to hormonal balance creates the right environment for cancer development [Deb et al., 2016; Sakkiah et al., 2017; Rodgers et al., 2018].

The beginning of puberty is a complex interaction among genetics, hormones and environmental factor. The role of EDs disruptors in sexual development has been controversial topic since 1990. However, evidences support the role of these chemicals in disturbing puberty [Greenspan and Lee 2018; Harley et al., 2019]. Furthermore, the effects of EDs are primary concern for male reproductive system, as some aspects of masculinization depend on normal testicular hormone production. Hormonal disturbances has been associated to masculinization abnormalities and research shows exposure to EDs has negative effects on reproductive function and decline semen quality [Rehman et al., 2018].

Another group of diseases such as obesity, diabetes type 2 or metabolic syndrome has been considered to be caused due to genetic background, diet, activity levels and ageing but there is enough scientific evidence that EDs contribute to the rapid increase of these metabolic diseases [Edwards and Myers 2008; Heindel et al., 2017; Lauretta et al., 2019].

As it can be seen, EDs are a worldwide issue for which, it is important to establish mechanisms to prevent the presence of these chemicals in Environment. Furthermore, it is required to develop new technologies to remove these compounds from water to guarantee the water quality not also in Environment but also in domestic water, as its re-use is more and more required nowadays.

### **1.3 LEGAL FRAMEWORK**

Most of the laws concerning water are trying to find answers to the problems this limited resource currently poses. Water is a fundamental element for economic development and to achieve its rational use is necessary not only through the implementation of regulatory frameworks but also through actions aimed at recycling, reusing or recovering this resource.

The use of this resource must guarantee all the necessary water and it is important to protect through the technical possibilities offered by the present development. However, its use should be not only considered from a quantitative perspective but also it is necessary considering water quality regulation.

Nowadays, the fact that most determine the legal water management is the defence and maintenance of water quality against any use industrial, household, recreational, agricultural or environmental activities. Our society is facing a new culture of water under the target of conservation and an adequate management. Water is not only a productive factor for our society but also it has an important environmental function. Thus, water environmental demands have to be present in its management and planning.

Having the main objective of improving water quality at a European level, the Water Framework Directive (WFD) [EC, 2000] was implemented in 2000. The purpose of this Directive was to establish a framework for the protection of surface waters, transitional waters, coastal waters and groundwater which:

1. Prevents further deterioration, protects and enhances the status of aquatic ecosystems.
2. Promotes sustainable water use based on a long-term protection of available water resources.
3. Aims at enhanced protection and improvement of the aquatic environment.
4. Ensures the progressive reduction of pollution of groundwater and prevents its further pollution.

And consequently, contributes to:

- a. The provision of the sufficient supply of good quality surface water and groundwater as needed for sustainable, balanced and equitable water use
- b. A significant reduction in pollution of groundwater
- c. The protection of territorial and marine waters
- d. Achieving the objectives of relevant international agreements, including those which aim to prevent and eliminate pollution of the marine environment, by Community action under Article 16(3) to cease or phase out discharges, emissions and losses of priority hazardous substances, with the ultimate aim of achieving concentrations in the marine environment

near background values for naturally occurring substances and close to zero for man-made synthetic substances.

Regarding the chemical quality of water, the WFD established a provision list of Priority Substances (Annex X of the Directive). Decision 2455/2001/EC established the First list [EC, 2001] and Directive 2008/105/EC, the Environmental Quality Standards Directive – EQSD, set the quality standards for water [EC, 2008].

The WFD also includes groundwater in its river basin management planning and sets clear milestones for groundwater bodies in terms of delineation, economic analysis, characterization (analysis of pressures and impacts), monitoring and the design of action programs to ensure that, by the end of 2015, there is a sufficient quantity of groundwater with a good chemical status.

The WFD was then complemented by the adoption on 12 December 2006 of a Development Directive laying down additional technical specifications, Directive 2006/118/EC on the protection of groundwater against pollution and deterioration [EC, 2006].

Finally, Directive 2013/39/EU was published in 2013, modifying Directives 2000/60/EC and 2008/105/EC as regards priority substances in the field of water policy [EC, 2013]. This directive promotes the development of innovative wastewater treatment technologies, avoiding expensive solutions.

In addition, to tackle global water contamination, European countries were concerned about hormone disruption issue which arose after Theodora Colborn published, “Our Stolen Future” in 1996.

Having known Colborn research, members of European Parliament stated their concern about the substances suspected of interfering with the hormone system and claimed queries to the European Commission. As a result, European Parliament decided to draw up a report and the Strategy for Endocrine Disruptors were approved in 1999 COM (1999) 706 [CEC, 1999]. The strategy was implemented through three stages, the two first ones were merely technical phases and the last one was to define a legislative framework.

Therefore, the first stage was dedicated to define a list of substances to assess their role in disrupting hormone system. The second phase was addressed to develop and valid methods, due to the technical limitations and the last step

were in charge of implementing legislation to guarantee human health and environment protection.

The report to prepare the list of substances to study was developed by an independent consulting, BKH Consulting Engineering, and it lasted one year. 533 chemicals were included, all of them used in agriculture, industry and consumer goods. Only 118 were selected, as all of them met the requirements of persistence, levels of production ( $\geq 10$  T/year), as exposition level for humans and environment were considered high level.

Despite the lack of knowledge about these pollutants, it was demonstrated 118 chemicals could disrupt hormone system and 109 of them were under legislation restrictions. The 9 remaining pollutants escaped to any type of control and there was no information regarding the other 435 substances. The results were registered in the Commission Document COM (2001) 262 [CEC, 2001] and it was the set up to establish the priority chemicals to study concerning Endocrine Disruption. The information was referred to the Scientific Committee for Toxicity Ecotoxicity and Environment (SCTEE) and two new studies were defined. The first one to evaluate these 9 chemicals and 3 extra hormones which presence in environment was relevant. The second research was focus on the 435 remaining pollutants.

Once the report came into light, the last step was to achieve sustainable development in chemicals industry. The goal of this strategy consisted in establishing a single system to revise the current and new substances in order to assess their impact on human health and environment. The document was known as White Paper, Strategy for a Future Chemicals Policy.

As previously stated, having regard to Directive 2000/60/CE, the Decision 2455/2001/EC of the European Parliament established the list of priority substances to reduce their level concentrations in water to combat water pollution. It is important to remark, the list included 33 chemicals which 11 appeared in the previous study published by BKH Consulting Engineering.

The following research carried out by BKH on the 435 remaining pollutants showed 204 chemicals met the requirements to study their role in endocrine disruption therefore, 231 substances were excluded for different reasons: 172 chemicals were not marketed in high volumes, 40 pollutants were catalogued as undefined mixtures and 9 of them were excluded for lack of information.

The research demonstrated that 147 out of 204 chemicals were potential endocrine disruptors but only 129 of them were under legal restrictions. The list of the suspected substances of interfering the endocrine system was published in SEC (2004) 1372 [CEC, 2004].

The last purpose to review was the 172 chemicals excluded previously and another new 22 substances but only 107 remained as candidates to study. The results concluded that only 34 chemicals were classified as suspected of interfering hormone system and there was not enough information for 52 of them. The results were published in SEC (2007) 1635 [CEC, 2007].

Currently, there is increasingly concern in the European Union about environmental and human health impacts derived from the use of EDs. Thus, the EU members have been recently established innovative obligations related to water management driven to remove EDs from water [Slama et al., 2016].

**Figure 1.3** summarizes the Legal Framework in the field of EDs for the European countries and the different reports to develop the European Legislation since Dr Colborn's studies came into light in 1996.

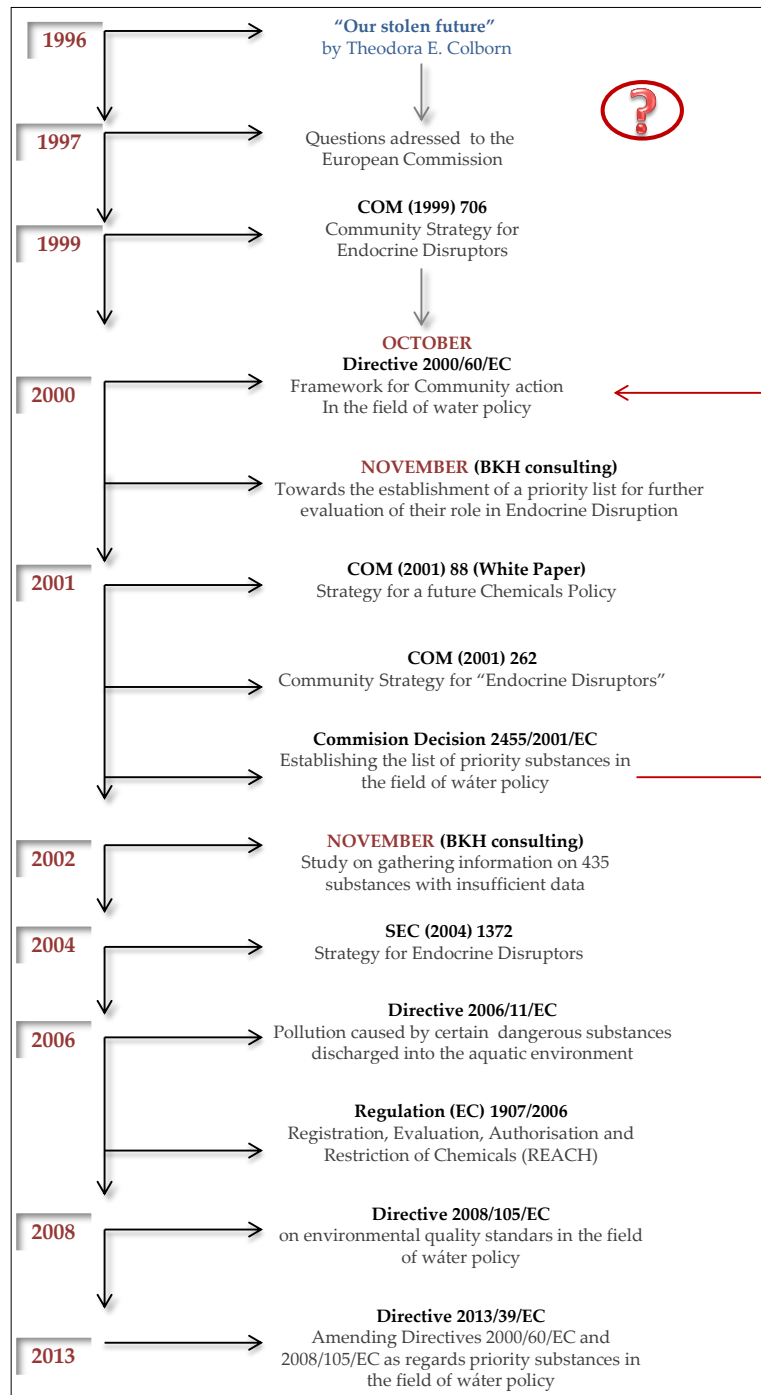


Figure 1.3. Legal framework schematic diagram.

Much progress has been made in water protection in Europe, in individual Member States, but also in tackling significant problems at European level. Yet, Europe's waters are still in need of increasing efforts to get them clean or to keep them clean. After 30 years of European water legislation, this demand is expressed not only by the scientific community and other experts but also to an ever-increasing extent by citizens and environmental organizations. We should take up the challenge of water protection, one of the great challenges for the European Union in the new millennium.

The control of pollution by Governments, Official Agencies or Environmental Agencies implies following the appropriate guidelines for an effective solution to the problem through:

- Recognition of the problem.
- Monitoring and controlling to determine the extent of the problem.
- Monitoring to ensure that the problem has been controlled.
- Implementation of control procedures.
- Legislation to ensure the control of the implemented procedures.

Therefore, it is necessary to establish preventive mechanisms that minimize the presence of ECs, among them EDs, in the environment, through the optimization of wastewater purification techniques, so that they do not become a source of discharge to the natural aquatic ecosystems [Desbiolles et al., 2018].

#### **1.4 ADVANCED OXIDATION PROCESS: HETEROGENEOUS PHOTOCATALYSIS**

European Union gave a step forward in controlling and preventing water pollution through Directive 2013/39/EU [EC, 2013], which amended Directive 2000/60/EC [EC, 2000] and 2008/105/EC [EC, 2008]. The innovative action was the fact of reducing contamination by identifying the causes of pollution and treating them from its source but in the most economically and environmentally effective mode [EC, 2013]. This new perspective implied the development of new technologies to eliminate these chemicals as the traditional methods were not efficient enough and, quite often, costly [Tran et al., 2018; Leusch et al., 2018].

Contaminated water by anthropogenic causes could be efficiently treated in wastewater plants using the traditional methods. However, these treatments are not efficient enough to remove persistent pollutants, included the ones with endocrine disruption properties, and treated water is not as clean as is required according to legal framework. Reverse osmosis systems or absorption by carbons are inefficient at removing persistent pollutants as it has been demonstrated in different assays [Postigo et al., 2010; López-Serna et al., 2012; Frias Chicharro et al., 2014]. Therefore, it is necessary other mechanisms to achieve this target.

Further research on processes related to water purification has shown that Advance Oxidation Processes (AOPs) are suitable for aqueous pollutants degradation, since in the early 1980s they were first proposed for water treatment [Stevens 1982; Glaze 1986]. The main objective of AOPs is the production of radicals with high oxidation potential such as hydroxyl radicals (OH<sup>•</sup>) ( $E^0=2.8$  V), which are able to reduce organic pollutants up to mineralization, as they react rapidly and in a non-selectively way [Domènech et al., 2004].

AOPs have a high application potential in water treatments as hydroxyl radicals interact with persistent pollutants and, as a result, they are an important source to release these contaminants from environment [Salimi et al., 2017]. The implementation of these technologies in water treatments constitute an efficient method plenty of advantages, all of them summarized in **Table 1.3**.

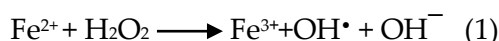
**Table 1.3.** AOPs advantages [Malato et al., 2009].

<b>AOPs ADVANTAGES</b>
The process is based on chemical changes into the pollutants
Complete mineralization in most of the contaminants
Degradation of chemicals without formation of harmful intermediates
Suitable for refractory organic pollutants
Effective for low contaminant concentration levels
Organoleptic water properties improvement
Low energy consumption
The effects on human health and wildlife are minimum

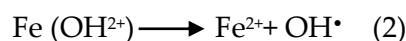
AOPs are classified in homogeneous and heterogeneous processes. The most common homogeneous photocatalytic processes include Fenton (Fe<sup>2+</sup>/H<sub>2</sub>O<sub>2</sub>)



and Photo-Fenton ( $\text{Fe}^{3+}/\text{H}_2\text{O}_2/\text{UV}$ ) oxidation. The classic reaction consists of an aqueous combination of hydrogen peroxide ( $\text{H}_2\text{O}_2$ ) and ferrous ions in acid medium [Wink et al., 1994]. Ferrous ions lead the decomposition of  $\text{H}_2\text{O}_2$  into hydroxyl radicals and hydroxyl anions and de oxidation of  $\text{Fe}^{2+}$  into  $\text{Fe}^{3+}$ , as it is represented by Equation 1.



In the Photo-Fenton reaction, the ferric complex is the main source of hydroxyl radicals [Zepp et al., 1992] and the main reaction is shown in Equation 2.



The principle of heterogeneous photocatalysis is based on the activation of a semiconductor material by irradiation with the appropriate wavelength. This material acts as a catalyst and it is involved in the chemical transformation of the organic pollutants into substances less toxic [Fenoll et al., 2013].

Heterogeneous photocatalysis efficiency is maximized using the appropriate catalysts. The most suitable materials are metal oxides because they are semiconductors, and the surface of these materials provides the right place where oxidation–reduction reactions are started by irradiation. Therefore, catalyst irradiation generates hydroxyl radicals promoting pollutants oxidation and this happens because electrons in solid semiconductors occupy fully valence band (VB) and they are separated from empty higher energy conduction band by a band gap (BG) that it is characteristic of the material.

Upon irradiation of energy equal to or greater than the band gap, electrons are moved from valence band to band gap leaving a deficient hole ( $\text{h}^+$ ) in the VB. Therefore, electrons ( $\text{e}^-$ ) and holes ( $\text{h}^+$ ) drive reduction and oxidation reactions of chemicals adsorbed on the surface of the catalyst [Ohtani 2013].

Electrons ( $\text{e}^-$ ) react with molecular oxygen forming superoxide anion radicals ( $\text{O}_2^{\bullet-}$ ) and the holes ( $\text{h}^+$ ) are able to form hydroxyl radicals ( $\text{OH}^\bullet$ ) and hydrogen peroxide ( $\text{H}_2\text{O}_2$ ) produced by the interaction of water [Kmetykó et al., 2014]. These reactive species are powerful oxidants, and they show little

selectivity to attack substances. Superoxide radicals ( $O_2^{\bullet-}$ ) and hydrogen peroxide ( $H_2O_2$ ) provide an additional pathway to oxidize a wide range of organic compounds. [Frontistis et al., 2017; Vela et al., 2017; Reddy et al., 2018].

The overall scheme of photocatalysis mediated by solid semiconductors is shown in the Figure 1.4.

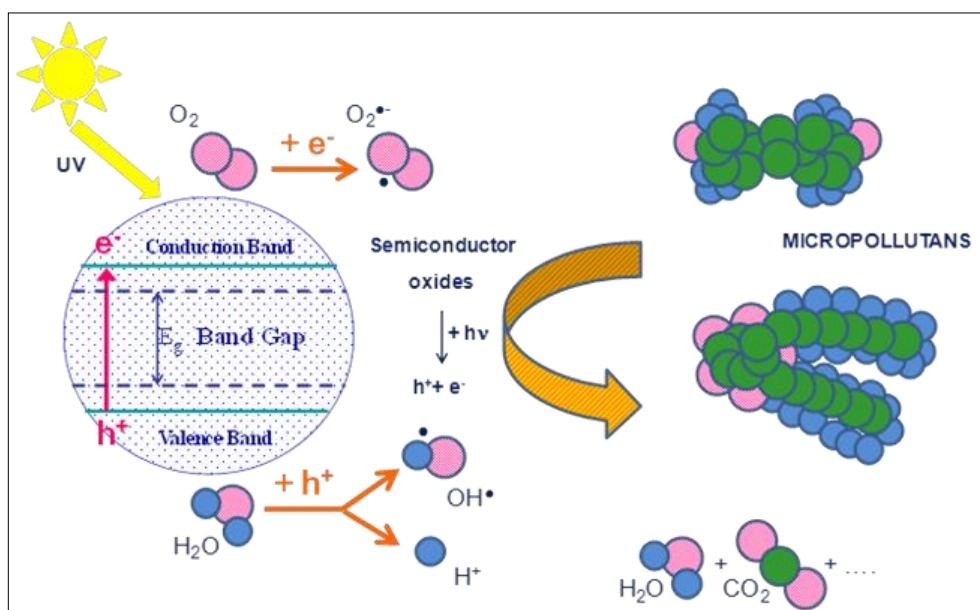


Figure 1.4. Schematic illustration of heterogeneous photocatalysis using solid semiconductors.

Considering the redox potential needed to oxidize organic pollutants is determined by the position of valence band, Titanium dioxide ( $TiO_2$ ) is one of the most popular materials studied and used in photocatalytic processes [Gaya and Abdullah 2008]. In addition, its high chemical stability, low toxicity, relative low cost and its highly oxidizing power make it suitable for decomposition of organic compounds at a very low concentrations, for which it is a competitive candidate for photocatalytic processes [Ibhadon and Fitzpatrick, 2013].

$TiO_2$  exists in three crystalline structures: anatase, brookite and rutile but the mostly investigated phases are rutile followed by anatase because they respond under UV irradiation and sunlight.  $TiO_2$  has a wide band gap energy: 3.2 eV for anatase, 3.0 eV for rutile and  $\sim 3.2$  eV for brookite [Amtout and Leonelli

1995; Asahi et al., 2000], band gaps that correspond to photons with a wave length  $< 400$  nm. This excellent optical transmittance in the UV and near the visible region is the reason for which  $\text{TiO}_2$  has caught much attention and has been widely studied.

The efficient visible light absorption is a task to develop, as photocatalytic process based on  $\text{TiO}_2$  is mainly restricted by the UV region of the light spectrum.  $\text{TiO}_2$  properties can be modified by incorporating Carbon into the lattice of  $\text{TiO}_2$  to extend optical absorption to visible light. Kronos vlp 7000 is an ultra-fine powder carbon-doped that responds under visible light and UV.

Although  $\text{TiO}_2$  has been considered the most important catalyst in photocatalysis processes,  $\text{ZnO}$  has become another attractive material because its high photostability and similar band gap. (3.37 eV).  $\text{ZnO}$ , under the right irradiation, produces  $\text{H}_2\text{O}_2$  in aqueous solution and in presence of  $\text{O}_2$  and it has been recognized as an excellent material because its low cost for large scale water treatment and high efficiency at removing pollutants from water.  $\text{ZnO}$  crystallizes in two main forms cubic zincblende and hexagonal wurtzite, being the last one, the most common and stable in nature.

One important aspect in photocatalysis is the fact that both  $\text{ZnO}$  and  $\text{TiO}_2$  are affordable materials, as they are relatively inexpensive for which they have become top trending in water purification processes.

However, the efficiency of the photocatalytic process is dependent on different parameters [Ahmed et al., 2011; Yasmina et al., 2014] and they are:

1. pH of the solution. Changes in the pH solution affect the condition of the catalyst surface and depending on the acidic or alkaline conditions the surface of the catalyst can be protonated or deprotonated. According to the essays, the photodegradation shows its maximum adsorption at low pH or under acidic conditions.
2. Catalyst type. Titanium dioxide has been widely studied as a photocatalyst and its mixed-form (anatase-rutile), commercially available as P25 Degussa, has been found to show the best photocatalytic properties.
3. Light intensity. The degradation rate is dependent on light as the reaction involves the electron-hole pair formation. When light intensity is increased the separation competes with recombination causing lower effect on the reaction rate.

4. Catalyst structure. Catalyst surface morphology plays an important role in the photocatalytic process as there is a direct relationship between organic compounds absorbed and the surface.
5. Pollutant concentration and nature. The degradation rate of pollutants depends on their chemical structure, concentration and the presence of other chemicals in the matrix. The degradation of stable chemical groups is not as efficient as chemical groups with less stability.

Heterogeneous photocatalysis based on the use of solar energy offers an added value to the process and makes it a clear example of sustainable energy. The combination of renewable energy and photocatalysis technology is an excellent alternative to water treatment sector [Rani and Singaram 2016]. In fact, many studies have confirmed the efficiency of this technology at removing not only persistent pollutants but also the ones with endocrine disruption properties [Pardeshi and Patil 2009; Zhang et al., 2012; Kanakaraju et al., 2014; Reddy et al., 2018]. However, it is important to continue the investigations in order to gain further information [Spasiano et al., 2015]. More advances should be done to improve the photocatalyst efficiency [Djurišić et al., 2014], it is necessary to make visible light more accessible and the possible environment applications is a goal to achieve.

## **II - JUSTIFICATION AND OBJECTIVES**



## II – JUSTIFICATION AND OBJECTIVES

The presence of toxic non-biodegradable organic compounds is one of the biggest problems in wastewater and puts ecosystems and human health at risk. These contaminants must be eliminated but conventional treatments do not normally achieve this purpose. Moreover, they generate extra waste during the purification/purification process, increasing costs and time. Consequently, it is necessary to study alternative treatments, such as AOPs, concretely Heterogeneous Photocatalysis using semiconductor materials, to develop economically and environmentally effective techniques. Therefore, the main objective of this study is the elimination of EDs in wastewater by means of heterogeneous photocatalysis using semiconductor oxides. The secondary objectives derived from the research are the following:

1. Evaluate the quality of the water by characterising the main physical-chemical parameters required by current legislation.
2. Characterise the semiconductor materials used in heterogeneous photocatalysis experiments.
3. Optimise the processes of heterogeneous photocatalysis by using different types of semiconductor oxides to eliminate the EDs under study on a laboratory scale using a photoreactor with artificial light.
4. Evaluate the photodegradation tests at pilot plant level under solar irradiation in optimal conditions for all the selected compounds.
5. Provide an economic assessment of the technology applied.





# **III – MATERIAL AND METHODS**



### III – MATERIAL AND METHODS

#### 3.1. EXPERIMENTAL DESIGN

In accordance with the objectives established in the previous section, the developed experimental work is shown in **Figure 3.1**.

First, the EDs were selected after reviewing the scientific literature. The emerging organic contaminants selected in this thesis (pesticides, plasticizers and preservatives) are classified in category 1 according to the review carried out by the European Commission in 2007 [Petersen et al., 2007], *Study on enhancing the Endocrine Disrupter priority list with a focus on low production volume chemicals*. This report indicates that there is, for all of them, proven scientific evidence of endocrine disruption in intact organisms. It also indicates that there is enormous concern about their high exposure, given the use that is made of them. Similarly, it was considered that they have been detected in different aquatic ecosystems [Jurado et al., 2012].

The analytical method for the extraction and analysis of the compounds in water was validated (limit of detection, limit of quantification, linearity and accuracy). The extraction of the EDs has been carried out by a liquid-liquid (LL) procedure with subsequent determination by gas chromatography and mass spectrometric detection (GC-MS).

Then, the characterization of catalysts (ZnO, TiO<sub>2</sub> P25, TiO<sub>2</sub> Alfa Aesar, TiO<sub>2</sub> vlp 7000) was carried out through scanning electron microscopy, x-ray diffraction, Brunauer-Emmet Teller-analyzer and diffuse reflectance spectroscopy.

Subsequently, the optimization of heterogeneous photocatalysis processes in laboratory conditions was developed. For this purpose, the different tests of photodegradation of the EDs in pure water, through a photoreactor, were carried out in order to select the optimal working conditions of the heterogeneous photocatalysis process. Plasticizers and preservatives were studied on the one hand, and pesticides were analyzed on the other. The selected catalysts were ZnO, TiO<sub>2</sub> P25, TiO<sub>2</sub> Alfa Aesar and TiO<sub>2</sub> vlp 7000. The variables studied were the load and type of catalyst, the amount of oxidant (Na<sub>2</sub>S<sub>2</sub>O<sub>8</sub>) and the pH level (5.5,

7.0 and 8.5). Similarly, the corresponding photolysis tests were carried out with pollutant load, in the presence of UV light but without catalyst or oxidant. The remaining percentage of each EDs was calculated in order to know the influence of the photocatalytic process in the elimination of EDs. The experimental test is shown in Figure 3.1.

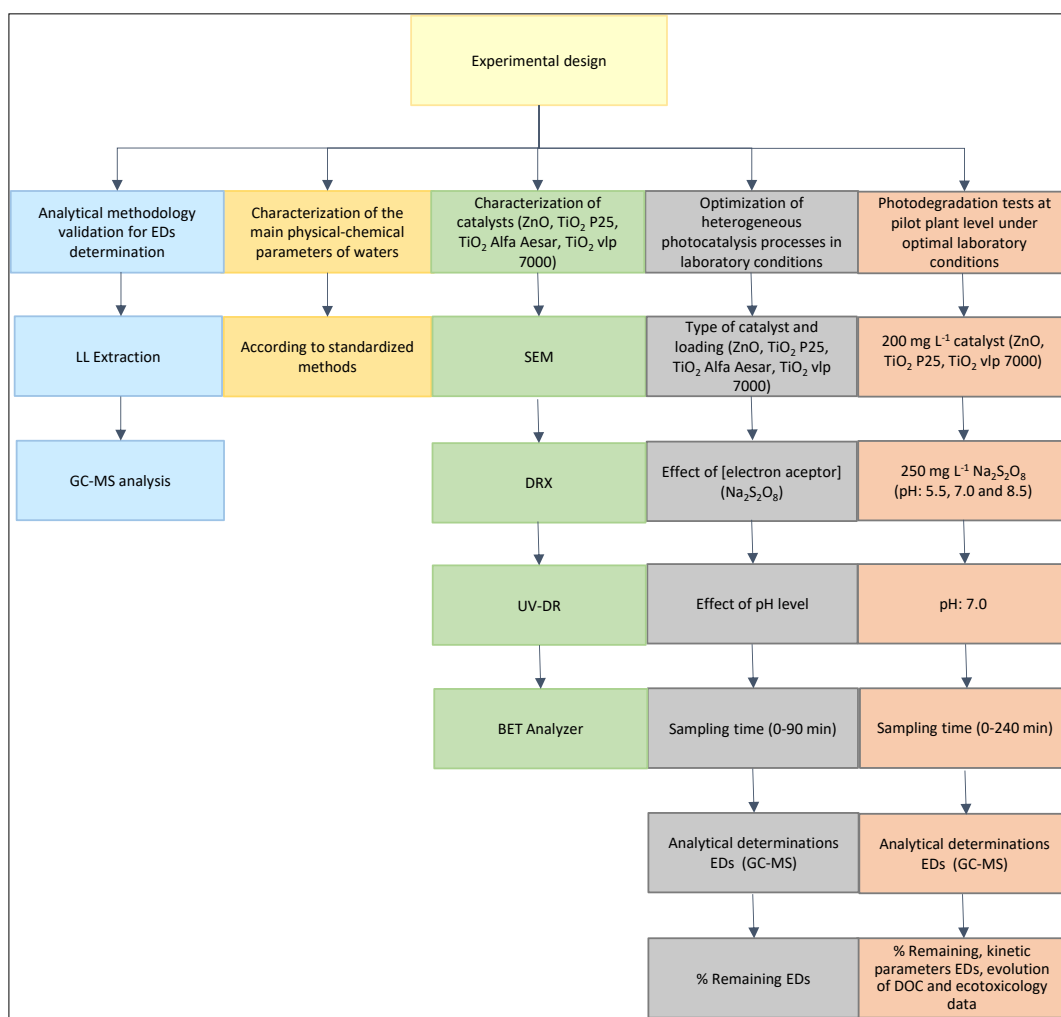


**Figure 3.1.** Representative scheme of the experimental work developed.

In a final stage, photodegradation tests at pilot plant level under sunlight and optimal laboratory conditions were developed. The experiments have been carried out with three semiconductors (ZnO, TiO<sub>2</sub> P25 and TiO<sub>2</sub> vlp 7000) in

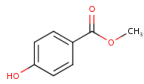
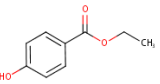
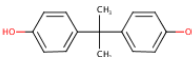
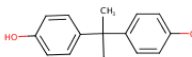
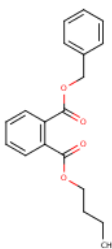
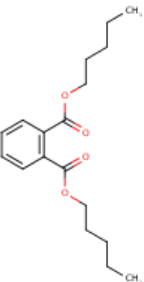
combination with an electron acceptor ( $\text{Na}_2\text{S}_2\text{O}_8$  as oxidant) in wastewater effluent from wastewater treatment plant (WWTP) Las Torres de Cotillas (Murcia, SE of Spain). At the same time, the characterization of the waters under study was made. The main physical-chemical parameters were analyzed according to standardized methods. The water contaminated with EDs was subjected to the action of sunlight for photoperiods of 4 hours, and the residual content of the different xenobiotics was analyzed from time to time (0, 30, 60, 90, 120, 240 min). After the analysis of the EDs residues in the laboratory, dissipation curves were obtained for each of the analytes studied. From these data, the rates constants of the photodegradation process and the half-life times of each compound and in each test were calculated. At the same time, the evolution of the amount of DOC and the values of ecotoxicity in water throughout the process were studied. These parameters were used to draw conclusions about the effectiveness of the technique employed.

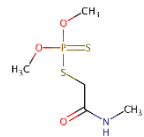
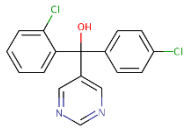
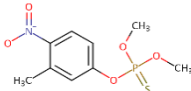
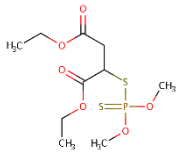
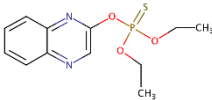
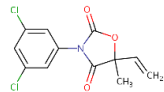
### 3.2. INVESTIGATED COMPOUNDS

The ECs selected in this Thesis (pesticides, plasticizers and preservatives) are showed in Table 3.1 [AERU, 2018; Toxnet, 2017]. Their structures use and main physical-chemical characteristics also are shown.

The analytical standards of bisphenol A (BA), bisphenol B (BB), butyl benzylphthalate (BP), diamyl phthalate (DP), ethyl 4- hydroxybenzoate (EP) and methyl p-hydroxybenzoate (MP) with a purity >98% were purchased from ChemService Inc (West Chester, PA, USA). The analytical standards of malathion (MT), fenitrothion (FT), quinalphos (QP), vinclozoline (VZ), dimethoate (DT) and fenarimol (FR) of >98% purity were purchased from Dr. Ehrenstorfer Co (Augsburg, Germany).

**Table 3.1.** Physical-chemical characteristics, structures and uses of the compounds studied.

Compound CAS	Use	Group Molecular formula Chemical structure	Molecular weight	Log K <sub>ow</sub> <sup>a</sup>	Sw <sup>b</sup>
Methyl p-hydroxybenzoate 99-76-3	Preservative: Used as a preservative in foods, cosmetics and pharmaceuticals	Parabens C <sub>8</sub> H <sub>8</sub> O <sub>3</sub> 	152.5	1.96	2,500
Ethyl 4-hydroxybenzoate 120-47-8	Preservative: Used as a preservative in pharmaceuticals, adhesives, and various cosmetic preparations (inhibits fungal and bacterial growth)	Parabens C <sub>9</sub> H <sub>10</sub> O <sub>3</sub> 	166.2	2.47	885
2,2-Bis(4-hydroxyphenyl)propan (Bisphenol A) 80-05-7	Plasticizer: Used as a chemical intermediate, mainly for epoxy resins and polycarbonate resins	Bisphenols C <sub>15</sub> H <sub>16</sub> O <sub>2</sub> 	228.3	3.32	120
2,2-Bis(4-hydroxyphenyl)-n-butan (Bisphenol B) 77-40-7	Plasticizer: Used as a chemical intermediate, mainly for epoxy resins and polycarbonate resins	Bisphenols C <sub>16</sub> H <sub>18</sub> O <sub>2</sub> 	242.3	4.13	ND
Butyl benzylphthalate 85-68-7	Plasticizer: additives in polyvinyl chloride (PVC) products	Phthalate Esters C <sub>19</sub> H <sub>20</sub> O <sub>4</sub> 	312.4	4.73	0.30
Diamyl phthalate 131-18-0	Plasticizer: additives in polyvinyl chloride (PVC) products	Phthalate Esters C <sub>18</sub> H <sub>26</sub> O <sub>4</sub> 	306.4	5.62	100

Compound CAS	Use	Group Molecular formula Chemical structure	Molecular weight	Log K <sub>ow</sub> <sup>a</sup>	Sw <sup>b</sup>
Dimethoate 60-51-5	Pesticide: Insecticide	Organophosphate C <sub>5</sub> H <sub>12</sub> NO <sub>3</sub> PS <sub>2</sub> 	229	1.0	39,800
Fenarimol 60168-88-9	Pesticide: Fungicide	Pyrimidine C <sub>17</sub> H <sub>12</sub> Cl <sub>2</sub> N <sub>2</sub> O 	331	4.1	13.7
Fenitrothion 122-14-5	Pesticide: Insecticide	Organophosphate C <sub>9</sub> H <sub>12</sub> NO <sub>5</sub> PS 	277	2.8	38.0
Malathion 121-75-5	Pesticide: Insecticide	Organophosphate C <sub>10</sub> H <sub>19</sub> O <sub>6</sub> PS <sub>2</sub> 	330	2.1	148
Quinalphos 13593-03-8	Pesticide: Insecticide	Organophosphate C <sub>12</sub> H <sub>15</sub> N <sub>2</sub> O <sub>3</sub> PS 	298	3.3	17.8
Vinclozoline 50471-44-8	Pesticide: Fungicide	Oxazole C <sub>12</sub> H <sub>9</sub> Cl <sub>2</sub> NO <sub>3</sub> 	286	3.4	3.4

<sup>a</sup> n-octanol-water partition coefficient; <sup>b</sup>Water solubility (mg L<sup>-1</sup>)

### 3.3. REAGENTS AND CATALYSTS

Dichloromethane and acetone used for residue analysis, sodium chloride and anhydrous sodium sulphate were purchased from Scharlab (Barcelona, Spain). Sodium persulfate (98%) was supplied by Panreac Química (Barcelona, Spain). Pure water was obtained from a Milli-RX purification system from Millipore. TiO<sub>2</sub> P25 Degussa (99.5%, 32 nm) was supplied from Nippon Aerosil Co Ltd (Osaka, Japan) and TiO<sub>2</sub> Kronos vlp 7000 (carbon doped Anatase, 87.5%, 15 nm) was obtain from Kronos Titan GmbH (Leverkusen, Germany). Finally, TiO<sub>2</sub> Alfa Aesar (99.9%) and Zinc oxide (99.9%) was supplied by Alfa Aesar (Karlsruhe, Germany).

### 3.4. WASTEWATER EFFLUENT

The sewage wastewater effluent was obtained from a wastewater treatment plant (WWTP) with an average capacity of 5,000 m<sup>3</sup> day<sup>-1</sup>, located in Las Torres de Cotillas (Murcia, SE of Spain). The WWTP included the following steps:

1. Filtration water treatment
2. Secondary biological aerobic process
3. Disinfection process with Ultraviolet radiation

The main physical-chemical parameters were analyzed according to standardized methods. An Agilent 7900 inductively coupled plasma (ICP-MS) with standard nickel cones, MicroMist glass concentric nebulizer, and Ultra High Matrix Introduction (UHMI) system was used for Zn<sup>2+</sup> and Ti<sup>4+</sup> measurements.

A Thermo Scientific Dionex ICS-2100 ion chromatograph (IC) with an Ionpac AS19 column (250 mm, 4 mm ID) and KOH as eluent (10 mM from 0 to 10 min, 10–45 mM KOH from 10 to 40 min) at a flow rate of 1 mL min<sup>-1</sup> (30 °C) was used for anion analysis (Cl<sup>-</sup>, NO<sub>3</sub><sup>-</sup>, SO<sub>4</sub><sup>2-</sup>, PO<sub>4</sub><sup>3-</sup>). Instrument control and data acquisition were performed using Chromeleon<sup>®</sup> software. An Optima 2000 DV ICP-OES (PerkinElmer) equipped with an AS-93 autosampler was used for the analysis of cations (Na<sup>+</sup>, Mg<sup>2+</sup>, Ca<sup>2+</sup> and K<sup>+</sup>). The measured data were sampled and processed using the WinLab32TM ICP computer program.

Total organic carbon (TOC) content was measured using a Multi N/C 3100 TOC Analyzer (Analytic Jena AG, Jena, Germany) equipped with an NDIR



detector. The dissolved organic carbon (DOC) procedure requires the sample be passed through a 0.45 mm filter prior to analysis to remove particulate organic carbon from the sample.

Toxicity was assessed following the method of bioluminescence inhibition (UNE-EN-ISO 11348-3) of *Vibrio fischeri* bacteria. The luminescence was determined by means of a MICROTOX M500 analyzer (Orbit Technologies Pvt. Ltd., India).

The main physical-chemical properties of the wastewater effluent used in this study are shown in **Table 3.2**.

**Table 3.2.** Composition of sewage wastewater effluent used in this study.

Parameters			
pH	7.2	CN <sup>-</sup> (mg L <sup>-1</sup> )	<0.02
EC (dS m <sup>-1</sup> )	3.8	Ca <sup>2+</sup> (mg L <sup>-1</sup> )	263
DOC (mg L <sup>-1</sup> )	10.8	Mg <sup>2+</sup> (mg L <sup>-1</sup> )	106
Oils and fats (mg L <sup>-1</sup> )	<0.5	Na <sup>+</sup> (mg L <sup>-1</sup> )	694
Total phenols (mg L <sup>-1</sup> )	<0.1	K <sup>+</sup> (mg L <sup>-1</sup> )	45.4
Aldehydes (mg L <sup>-1</sup> )	<0.1	Zn <sup>2+</sup> (mg L <sup>-1</sup> )	0.07
Anionic surfactants (mg L <sup>-1</sup> )	0.4	Al (mg L <sup>-1</sup> )	<0.5
Total phosphorus (mg P L <sup>-1</sup> )	4.1	As (mg L <sup>-1</sup> )	<0.5
Total nitrogen (mg N L <sup>-1</sup> )	11.0	Ba (mg L <sup>-1</sup> )	<0.5
BOD <sub>5</sub> (mg L <sup>-1</sup> )	5	B (mg L <sup>-1</sup> )	0.61
COD (mg L <sup>-1</sup> )	33.1	Cu (mg L <sup>-1</sup> )	<0.10
SS (mg L <sup>-1</sup> )	3.6	Fe (mg L <sup>-1</sup> )	<0.5
Turbidity (UNT)	1.1	Cr (mg L <sup>-1</sup> )	<0.5
NO <sub>3</sub> <sup>-</sup> (mg L <sup>-1</sup> )	8.6	Pb (mg L <sup>-1</sup> )	<0.5
NO <sub>2</sub> <sup>-</sup> (mg L <sup>-1</sup> )	<0.015	Se (mg L <sup>-1</sup> )	<0.5
Cl <sup>-</sup> (mg L <sup>-1</sup> )	464	Sn (mg L <sup>-1</sup> )	<0.5
SO <sub>3</sub> <sup>2-</sup> (mg L <sup>-1</sup> )	0.3	Hg (mg L <sup>-1</sup> )	0.002
SO <sub>4</sub> <sup>2-</sup> (mg L <sup>-1</sup> )	485	Ni (mg L <sup>-1</sup> )	<0.1
S <sup>2-</sup> (mg L <sup>-1</sup> )	<0.05	Mn (mg L <sup>-1</sup> )	<0.1
F <sup>-</sup> (mg L <sup>-1</sup> )	0.2	Ti (µg L <sup>-1</sup> )	<0.001

### 3.3. EXTRACTION AND ANALYSIS OF EDS

The LL extraction employed, and GC-MS conditions used for the identification, EDS quantitation according to their retention times, the identification of target and qualifier ions are summarized in **Figure 3.2**.

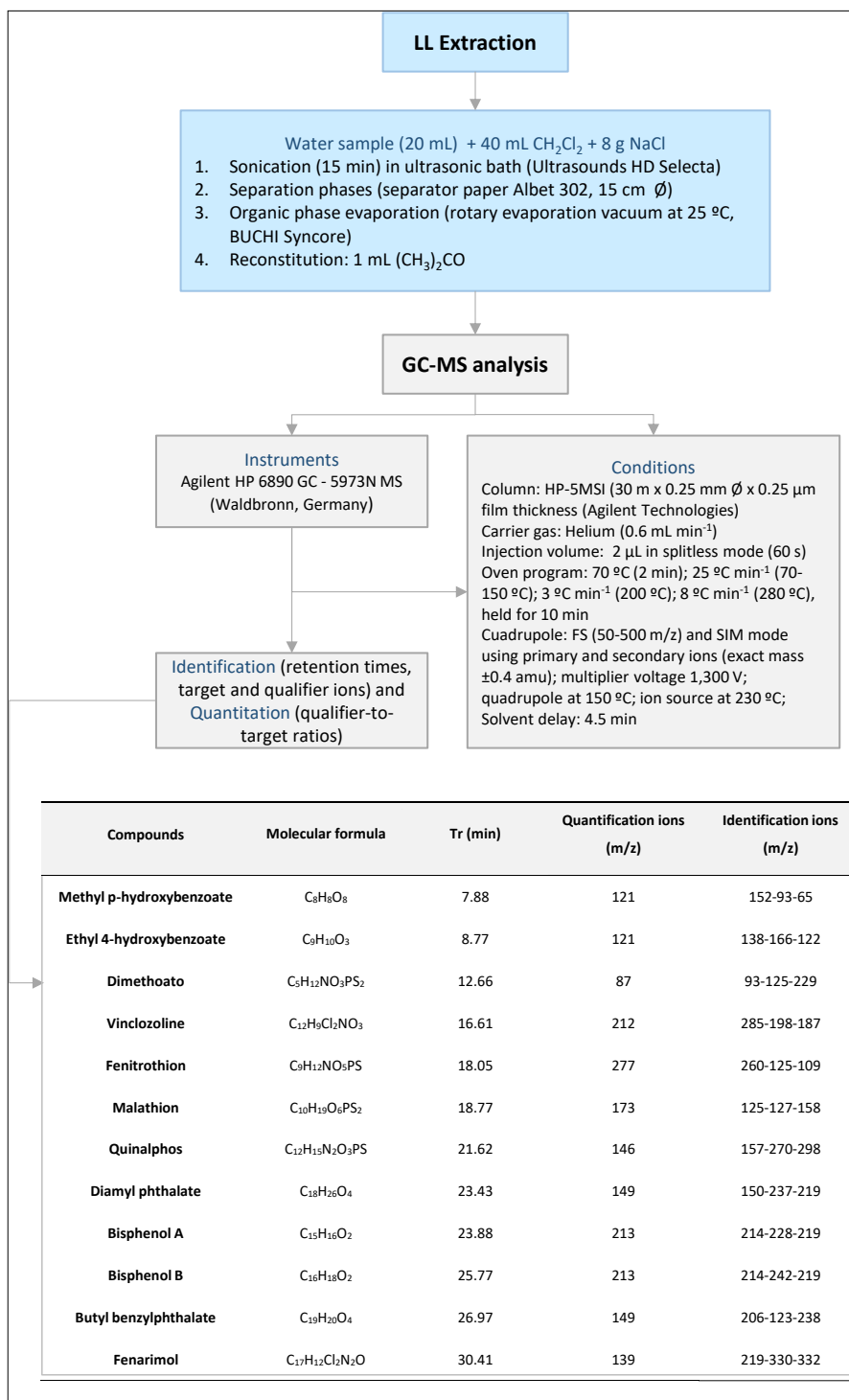


Figure 3.2. Analytical process scheme.

After filtering the water samples, ED residues were isolated by LL extraction method with dichloromethane, supported by sonication. After concentration and reconstitution, the extracts were injected into the GC-MS system composed of an Agilent (Waldbronn, Germany) HP 6890 GC coupled by transfer line to a 5973N mass spectrometer. Analysis was performed with selected ion monitoring (SIM) mode using primary and secondary ions. The target and qualifier abundances were determined by injection of individual standards under the same chromatographic conditions using full scan with the mass/charge ratio ranging from  $m/z$  50 to 500.

### 3.5. CHARACTERIZATION OF CATALYSTS

The optical properties were analysed by diffuse reflectance spectroscopy over UV-VIS (UV-DR). The photocatalysts were characterized by a PerkinElmer Lambda 750S UV/VIS spectrophotometer equipped with a PerkinElmer 60 mm integrating sphere accessory for diffuse reflectance spectra (UV-DR). Software: UV WinLab DPV 1.0 (Shelton, USA). A  $\text{BaSO}_4$  standard was used as the reference spectrum. The direct band gaps energy was calculated by plotting  $[F(R)hv]^{1/2}$  vs  $[hv-E_g]$ , where  $F(R) = (1R)/(2R)$ ,  $h$  is Plank's constant,  $E_g$  is the band gap energy,  $v$  is the frequency of light and  $R$  is diffuse reflectance based on the Kubelka–Monk theory of diffuse reflectance. The indirect band gap estimated from the intercept of the tangents to the plots.

The crystalline structure of the photocatalysts was characterized by means of powder X-Ray Diffractometry (XRD), on a Philips PW 1700. The samples were measured at 40 kV and 24 mA using  $\text{Cu-K}\alpha$  radiation at a scanning speed of  $1^\circ$  ( $2\theta$ ).

The morphology of the solids was examined by field emission scanning electron microscopy (FE-SEM) using a Carl Zeiss MERLIN VP Compact microscope (Oberkochem, Germany) with high resolution imaging up to 0.8 nm @15 KV, acceleration voltage of 0.02-30 kV and energy dispersive X-ray (EDX) attached to SEM.

The surface area ( $S_{\text{BET}}$ ) of the semiconductors was measured according to the BET method by nitrogen adsorption-desorption isotherms at 77 K on a Micromeritics Tristar 3000 instrument (Micromeritics Instruments Co., USA).

### 3.6. PHOTOCATALYTIC EXPERIMENTS AT LAB SCALE

The experimental design target was to identify the operating conditions to maximize the EDs mineralization according to the Langmuire Hinshelwood (L-H) model. For this purpose, catalyst loading at three different levels (100, 200 and 300 mg L<sup>-1</sup>) for each catalyst (ZnO, TiO<sub>2</sub> P25, TiO<sub>2</sub> Alfa Aesar, and TiO<sub>2</sub> vlp 7000), the oxidant concentration (100, 250 and 400 mg L<sup>-1</sup>) and pH effect (5.5, 7 and 8.5) were evaluated. The previous photocatalytic processes, under laboratory conditions, were developed in distilled water using a 2 L photochemical reactor (SBS, Barcelona, Spain) with double cylindrical wall glass (250 mm long, 100 mm diameter), equipped with a magnetic stirring bar, and a set of two low pressure Philips mercury lamps with a nominal output power of 8 W each as photon source. The intensity of each lamp was approximately 10 mW cm<sup>-2</sup> with major emission output at 366 nm (based on the manufacturer's data). Air was injected into the photoreactor every 15 min to maintain the O<sub>2</sub> concentration in the slurry at around 8-10 mg L<sup>-1</sup> [Vela et al., 2015].

The assay started spiking 2 L of Milli-RX water with the EDs mixture at 0.30 mg L<sup>-1</sup> of each one and the solution was homogenized in the dark for 15 min. Afterwards, photocatalyst was added to the solution at the three different concentrations (100, 200 and 300 mg L<sup>-1</sup>) and the mixture was maintained in the dark for 15 minutes, prior irradiation, to achieve the maximum compounds adsorption on the semiconductor surface. Afterwards, the system was illuminated, and samples were taken during the photoperiod every 0-5-15-30-45-60 and 90 minutes.

Once the optimal catalyst concentration was established, Na<sub>2</sub>S<sub>2</sub>O<sub>8</sub> was added at 100, 250 and 400 mg to study its effect as electron acceptor and the system was illuminated (photoperiod = 60 min). Finally, the appropriate concentration of catalyst/Na<sub>2</sub>S<sub>2</sub>O<sub>8</sub> was assessed at three pH levels (5.5, 7.0 and 8.5) to obtain the optimal operational conditions. In each case, the pH was adjusted using 1 M NaOH and 1 M HCl solutions and the photocatalytic process was performed one more time. The photolytic test in absence of semiconductor and oxidant was performed, in all the cases. Each experiment was repeated three times. Plasticizers and preservatives were studied in one assay and pesticides in another one. The operational conditions are shown in **Figure 3.3**.

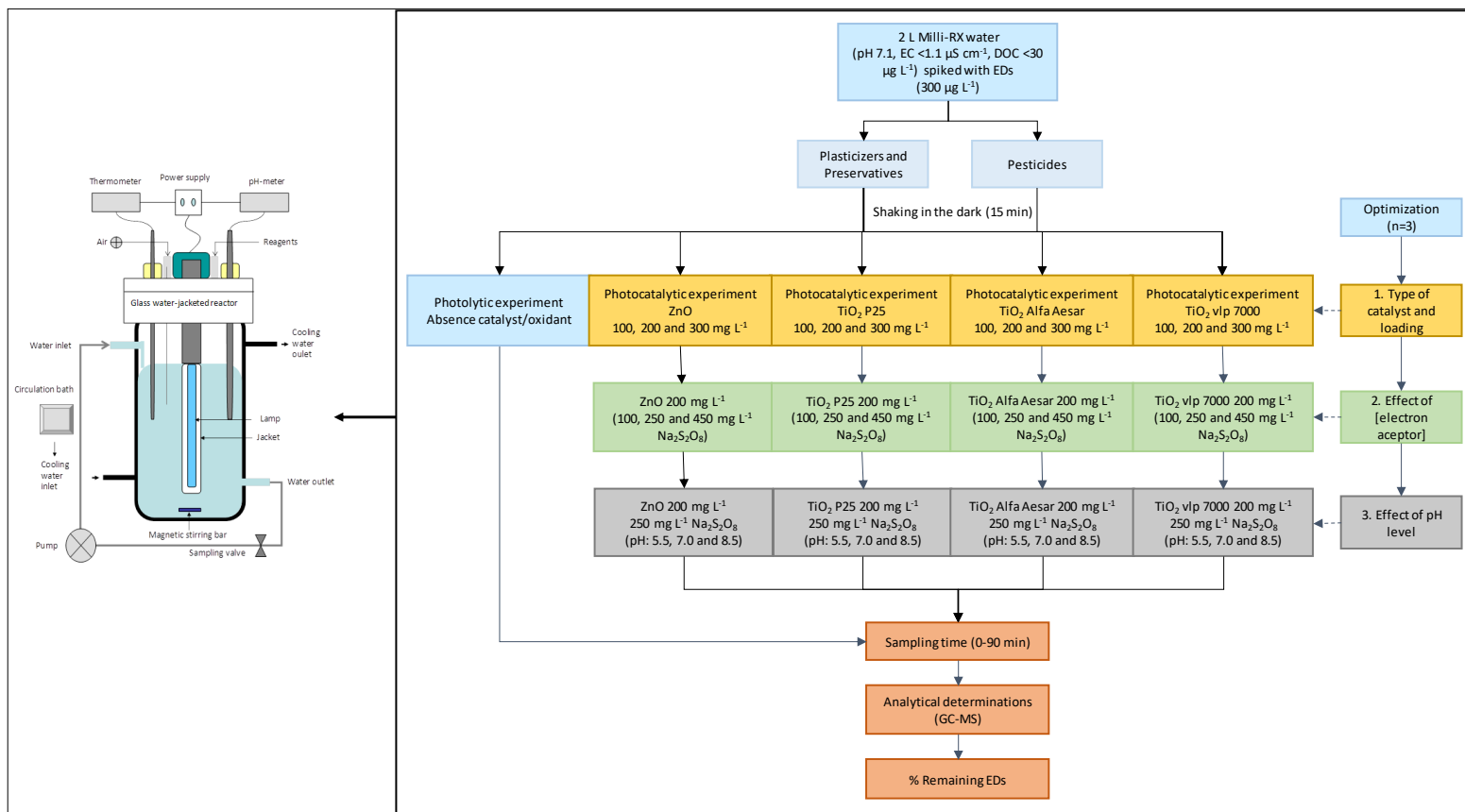
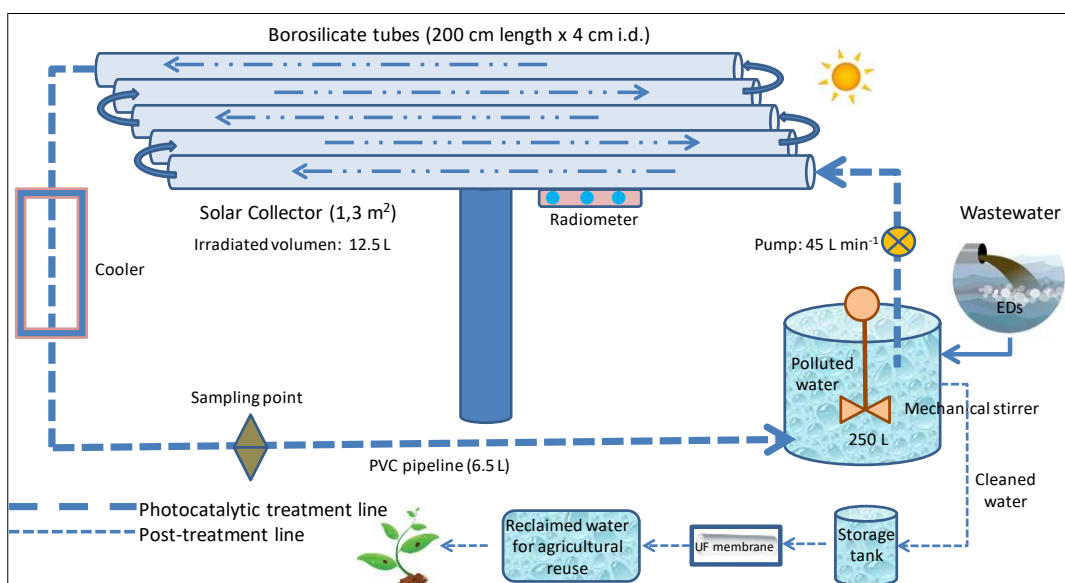


Figure 3.3. Simplified drawing of the photochemical reactor and operational process followed.

### 3.7. EXPERIMENTAL SETUP OF SOLAR PHOTOCATALYTIC TRIAL

The trial was performed under natural sunlight irradiation during June and July 2016 in a pilot plant (CPC technology) in Murcia (SE Spain, latitude 37°59'N, longitude 1°08'W).

The prototype consists in a photoreactor module with five borosilicate curved tubes set on polished aluminum reflectors (0.9 cm radius of curvature) running east-west, **Figure 3.4**. The water flows using a centrifugal pump (0.55 kW) in a closed circuit, but the system was continuously stirred to achieve a uniform suspension and thermo-stated. A 2,000 L storage tank, a flowmeter, three sensors (pH, O<sub>2</sub> and T<sup>o</sup>), pipes and fittings completed the installation. Finally, an ultrafiltration membrane enclosed in a Mann + Hummel U860 cartridge (165 cm long, 23 cm diameter) was incorporated to recover catalysts. An integrated photoradiometer Delta Ohm HD 2102.2 (Caselle di Selvazzano, Italy) was used to record values (Wm<sup>-2</sup>) of visible plus near-infrared (400–1100 nm), UVA (315–400 nm), UVB (280–315 nm) and UVC (200–280 nm) radiation.



**Figure 3.4.** Schematic drawing of the solar pilot plant used.

Figure 3.5 shows a schematic drawing and the operational parameters of photodegradation tests under natural sunlight at pilot plant.

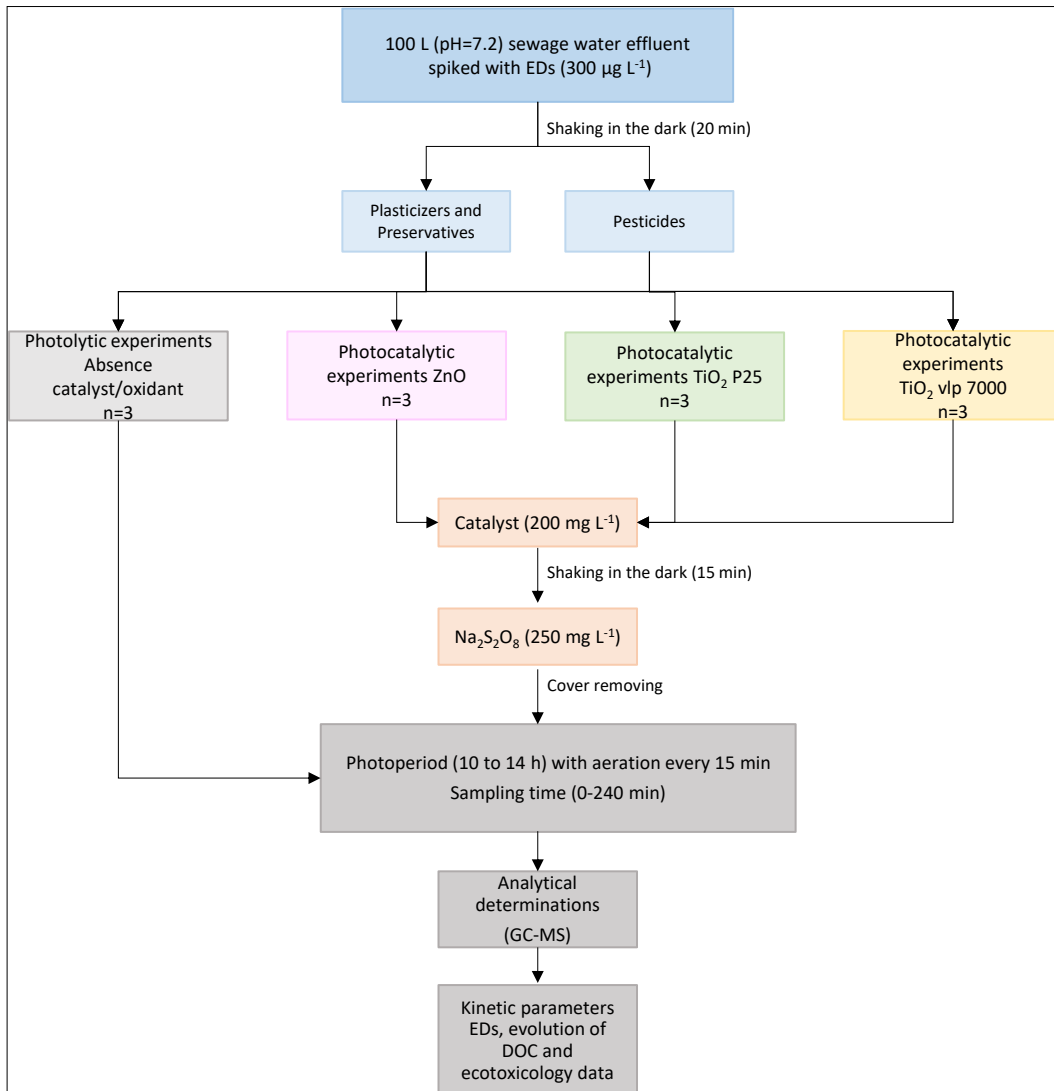


Figure 3.5. Solar photocatalytic design scheme at pilot plant scale.

At the beginning of the photocatalytic test, 100 L of sewage water effluent (pH 7.2) were spiked in the feed tank with the EDs ( $0.30 \text{ mg L}^{-1}$  of each one). As it was said previously, plasticizers and preservatives were studied in one essay and pesticides in another one.

The mixture was homogenized by shaking during 20 min in the dark. Afterwards, the optimal semiconductor concentration (200 mg L<sup>-1</sup>) was added, and the mixture was homogenized for another 15 min in the dark. Finally, 250 mg L<sup>-1</sup> of Na<sub>2</sub>S<sub>2</sub>O<sub>8</sub> were added to the tank and the cover was removed. The solution was continuously circulated to maintain the catalyst sufficiently stirred. An air compressor with a plastic tube introduced at the bottom of the tank supplied oxygen every 15 min because dissolved oxygen acts as electron sink, forming the superoxide radical (O<sub>2</sub><sup>-</sup>).

Several samples from 0 to 240 min were taken during the 4 hours that the illumination period lasted, from 10.00 to 14.00 h. A photolytic test in the same conditions, but without semiconductor and oxidant, was carried out and all the assays were replicated three times.

### 3.8. SOLAR PHOTOCATALYTIC KINETICS

Chemical kinetic plays an important role in heterogeneous photocatalysis as concentration decrease is a function of time. So, the disappearance of substances depends on the kinetics. Photocatalytic processes have been described by different models, but the most common decay model observed in photocatalysis experiments is explained in terms of the Langmuir-Hinselwood (L-H) model [Liu et al., 2014]. The equation to describe the rate for disappearance of any compounds is given below (Eq. 1):

$$r = - \frac{dc}{dt} = \frac{K_{LH} \times K_L \times C}{1 + K_L \times C} \quad (1)$$

where  $r$  is the rate of reaction,  $C$  is the concentration of the target compound,  $k_{LH}$  is the apparent L-H rate constant for the reaction and  $K_L$  ( $K_{ads/des}$ ) is the photon-flux-independent Langmuir equilibrium adsorption/desorption constant. However, considering that " $k_{LH} \times C$ " product can be a value quite low ( $\ll 1$ ) for photooxidation processes, most of researchers approximated Eq. 1 to first order kinetics (Eq. 2):



$$-\frac{dC}{dt} = k_{app} \times C \quad (2)$$

in which  $C$  is the concentration of the pesticide and  $K_{app}$  (in units of  $\text{time}^{-1}$ ) is the apparent first-order rate constant, expression that once integrated is equivalent to Eq. 3:

$$C = C_0 \times e^{-k_{app} \times t} \quad (3)$$

or as a logarithmic form to Eq. 4:

$$\ln C = \ln C_0 - k_{app} \times t \quad (4)$$

Thus, the time required for “ $x$ ” percent of pesticide to disappear ( $DT_x$ ) from the water due to degradation processes can be calculated according to the Eq. 5:

$$DT_x = \frac{\ln(100|100 - X)}{k_{app}} \quad (5)$$

In order to compare our results with other photocatalytic experiments due to differences in photocatalytic devices and/or irradiation fluctuations, the  $t_{30W}$  (normalized illumination time) was used in addition of exposure time ( $t$ ). The  $t_{30W}$  was calculated according to the Eq. 6 [Malato et al., 2009]:

$$t_{30W,n} = t_{30W,n-1} + \Delta t_n \times (UV|30) \times (V_I|V_T) \quad (6)$$

in which  $t_n$  is the exposure time for each sample,  $\Delta t_n = t_n - t_{n-1}$ ,  $UV$  ( $\lambda < 400$  nm) the average solar ultraviolet (A + B) radiation measured during  $\Delta t$ ,  $V_I$  the illuminated volume and  $V_T$  the total volume of the reactor (illuminated and unilluminated). In this expression, time refers to a constant solar UV power of  $30 \text{ W m}^{-2}$ , which is the typical solar UV power on a sunny day at noon.

### 3.9. STATISTICAL ANALYSIS

The curve fitting was obtained using the SigmaPlot version 13.0 statistical software (Systat, Software Inc., San José, CA). In order to determine significant differences between the means of the treatments, data were subjected to one-way ANOVA using the IBM-SPSS Statistics version 22 software (Armonk, NY). When the  $F$  statistic of ANOVA was significant at  $p < 0.05$ , analysis was followed by Tukey's significant difference post-hoc test.

## **IV – RESULTS AND DISCUSSION**



## IV – RESULTS AND DISCUSSION

### 4.1. ANALYTIC METHODOLOGY VALIDATION FOR EDS DETERMINATION

The analytical method for EDS determination was validated according to the conditions describe in Section 3.3 Extraction and analysis of EDS. The extraction of the EDS was carried out by LL procedure with subsequent determination by GC-MS. Table 4.1 shows the main parameters to validate the method and the analytical conditions for GC-MS.

Limits of detention (LD) values varied from 0,007 to 0,019  $\mu\text{g L}^{-1}$  and the limits of quantification (LQ) determined with a signal to noise ratio of 10:1 oscillated from 0.07 to 0.14  $\mu\text{g L}^{-1}$ .

The results for the linearity of the calibration curve for each compound (25 – 250  $\mu\text{g L}^{-1}$ ) were successful with a coefficient of determination ( $r^2$ )  $\geq 0.9889$ .

The accuracy of the method evaluated through recovery assays using a spiked solution at 25 and 100  $\mu\text{g L}^{-1}$  of each chemical, has demonstrated the extraction method by acetonitrile show recovery results from 72.4% to 113.8% for 25  $\mu\text{g L}^{-1}$  and 72.6% to 109.2% for 100  $\mu\text{g L}^{-1}$ .

EDs were confirmed by their retention times, the identification of target and qualifier ions and the determination of qualifier-to-target ratios. The concentration of each compound was determined by comparing the peak areas in the sample to those found for mixtures of ED standards of known concentration. Retention times had to be within 0.1 min of the expected time, and qualifier-to-target ratios had to be within a 10% range for positive confirmation.

**Table 4.1:** Validation parameters and analytical conditions of EDs by GC-MS.

Compound CAS	Chemical structure	LD <sup>a</sup>	LQ <sup>b</sup>	Linearity (r <sup>2</sup> )	Accuracy (25 – 100 µg L <sup>-1</sup> )	Tr <sup>c</sup>	Quantification Ions, T (m/z)	Identification Ions, Q <sub>1</sub> - Q <sub>2</sub> - Q <sub>3</sub> (m/z)	Abundances <sup>d</sup> , Q <sub>1</sub> /T - Q <sub>2</sub> /T - Q <sub>3</sub> /T (%)
Methyl p-hydroxybenzoate 99-76-3	C <sub>8</sub> H <sub>8</sub> O <sub>3</sub>	0.007	0.07	0.9889	94.8-90.5	7.83	121	152-93-65	39.2-16.9-11.0
Ethyl 4-hydroxybenzoate 120-47-8	C <sub>9</sub> H <sub>10</sub> O <sub>3</sub>	0.012	0.12	0.9993	95.7-96.0	8.77	121	138-166-122	19.2-13.4-9.6
Bisphenol A 80-05-7	C <sub>15</sub> H <sub>16</sub> O <sub>2</sub>	0.013	0.13	0.9894	72.4-91.5	23.88	213	214-228-219	19.6-15.0-12.4
Bisphenol B 77-40-7	C <sub>16</sub> H <sub>18</sub> O <sub>2</sub>	0.012	0.12	0.9962	75.3-79.1	25.77	213	214-242-219	16.2-10.2-2.1
Butyl benzylphthalate 85-68-7	C <sub>19</sub> H <sub>20</sub> O <sub>4</sub>	0.011	0.11	0.9993	103.7-72.6	26.97	149	206-123-238	19.7-6.4-2.7
Diamyl phthalate 131-18-0	C <sub>18</sub> H <sub>26</sub> O <sub>4</sub>	0.012	0.12	0.9994	109.8-85.5	23.43	149	150-237-219	9.6-6.4-2.7
Dimethoate 60-51-5	C <sub>5</sub> H <sub>12</sub> NO <sub>3</sub> PS <sub>2</sub>	0.019	0.13	0.9969	92.5-74.1	12.66	87	93-125-229	63.0-50.1-4.9
Fenarimol 60168-88-9	C <sub>17</sub> H <sub>12</sub> Cl <sub>2</sub> N <sub>2</sub> O	0.013	0.13	0.9995	105.3-80.2	30.41	139	219-330-332	66.2-25.0-15.6
Fenitrothion 122-14-5	C <sub>9</sub> H <sub>12</sub> NO <sub>5</sub> PS	0.016	0.11	0.9903	113.8-91.1	18.05	277	260-125-109	86.1-67.2-57.2
Malathion 121-75-5	C <sub>10</sub> H <sub>19</sub> O <sub>6</sub> PS <sub>2</sub>	0.017	0.12	0.9944	107.1-97.3	18.77	173	125-127-158	94.3-86.5-47.1
Quinalphos 13593-03-8	C <sub>12</sub> H <sub>15</sub> N <sub>2</sub> O <sub>3</sub> PS	0.014	0.14	0.9972	106.6-81.1	21.62	146	157-270-298	65.8-18.9-11.4
Vinclozoline 50471-44-8	C <sub>12</sub> H <sub>9</sub> Cl <sub>2</sub> NO <sub>3</sub>	0.019	0.13	0.9911	100.2-109.2	16.61	212	285-198-187	88.7-76.9-74.1

<sup>a</sup> Limit of detection (µg L<sup>-1</sup>); <sup>b</sup> Limit of quantification (µg L<sup>-1</sup>); <sup>c</sup> Time of retention (min); <sup>d</sup> Relative abundances (%) resulting from the division of identification ions abundances (Q<sub>1</sub>, Q<sub>2</sub>, Q<sub>3</sub>) by quantification ion abundance (T) × 100.

## 4.2. CATALYST CHARACTERIZATION

The decomposition of pollutants on the surface of the catalysts and the photocatalysis efficiency depends on their properties. Therefore, crystallinity, composition compounds, surface area and particle size for the four catalysts used in this study (TiO<sub>2</sub> vlp 7000, TiO<sub>2</sub> P25 Degussa, TiO<sub>2</sub> Alfa Aesar y ZnO) were characterized according the methodology describe in Section 3.5 Characterization of catalysts. The Table 4.2 shows the main physical and chemical properties of the four semiconductors.

**Table 4.2.** Physico-chemical properties of photocatalysts.

	Photocatalysts			
	TiO <sub>2</sub> Kronos vlp 7000	TiO <sub>2</sub> P25 Degussa	TiO <sub>2</sub> Alfa- Aesar	ZnO
Purity (%)	87.5	99.5	99.9	99.9
Composition compounds				
TiO <sub>2</sub> Anatase (%)	99.4	69.4	87.7	-
TiO <sub>2</sub> Rutile (%)	0.6	30.6	12.3	-
ZnO (%)	-	-	-	100
Particle size (nm)	<15	<32	<32	<194
BET surface (m <sup>2</sup> g <sup>-1</sup> )	250	55	45	7
Band-gap energy (eV)	2.4	3.1	3.2	3.1

The Figure 4.1 presents the X-ray diffractograms of the used catalysts and their crystalline forms. The quantity of Anatase (A) and Rutile phase (R) in TiO<sub>2</sub> P25 Degussa was 69.4A:30.6R, TiO<sub>2</sub> Alfa Aesar was 87.7A:12.3R while TiO<sub>2</sub> vlp 7000 crystallised in Anatase phase mainly (99.4A:0.6R). El ZnO presented hexagonal wurtzite crystal form.

The semiconductor morphologies seen by FE-SEM are shown in Figure 4.2. The results indicate ZnO nanoparticles have mainly diameters < 200 nm with hexagonal shape (Figure 4.2.D). Smaller particles were observed in TiO<sub>2</sub> vlp 7000 (Figure 4.2.A) and agglomeration of nanoparticles were seen in TiO<sub>2</sub> P25 Degussa (Figure 4.2.B) and TiO<sub>2</sub> Alfa Aesar (Figure 4.2.C).

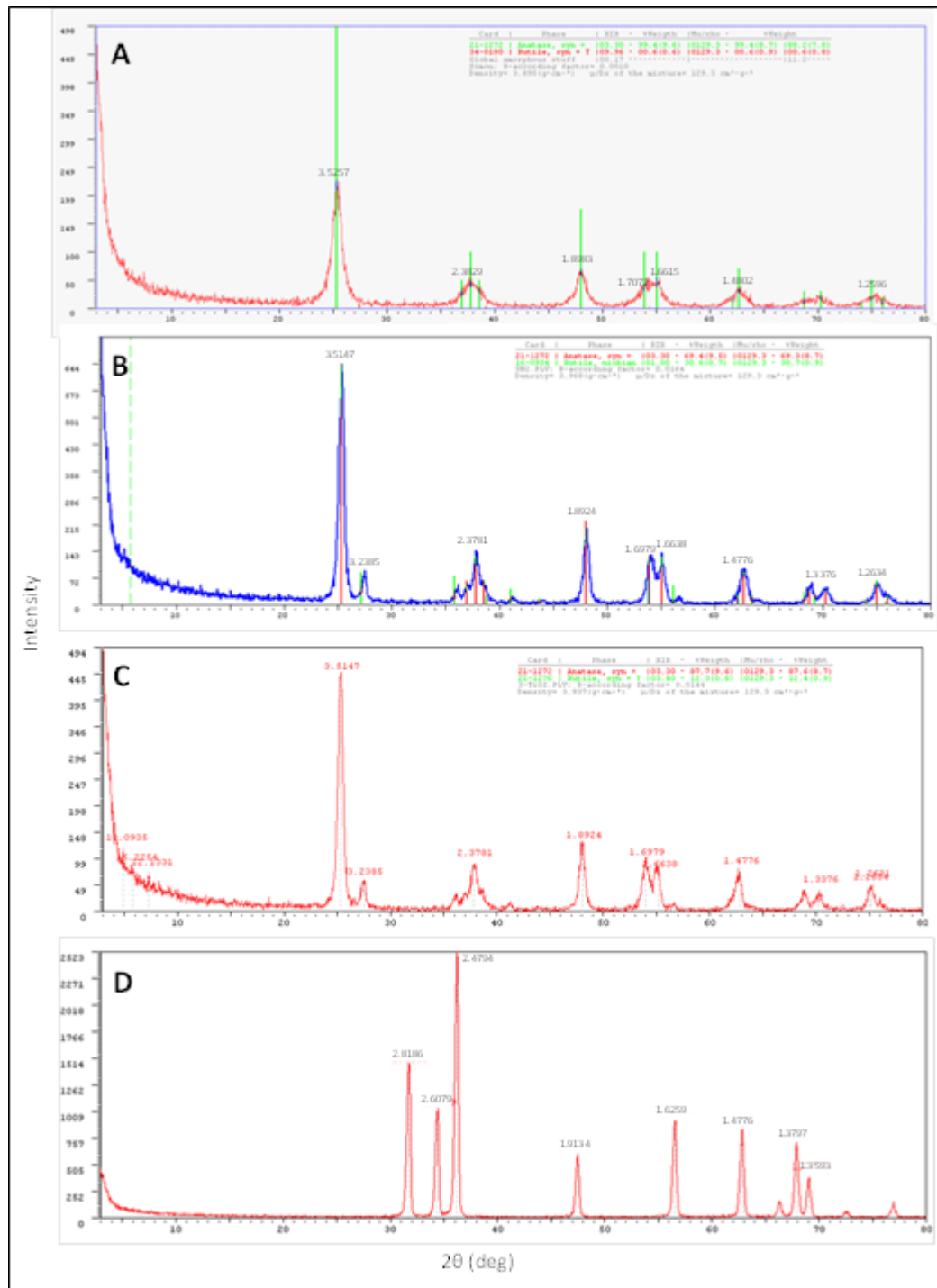


Figure 4.1. XRD patterns of (A) TiO<sub>2</sub> vlp 7000, (B) TiO<sub>2</sub> P25, (C) TiO<sub>2</sub> Alfa Aesar and (D) ZnO.



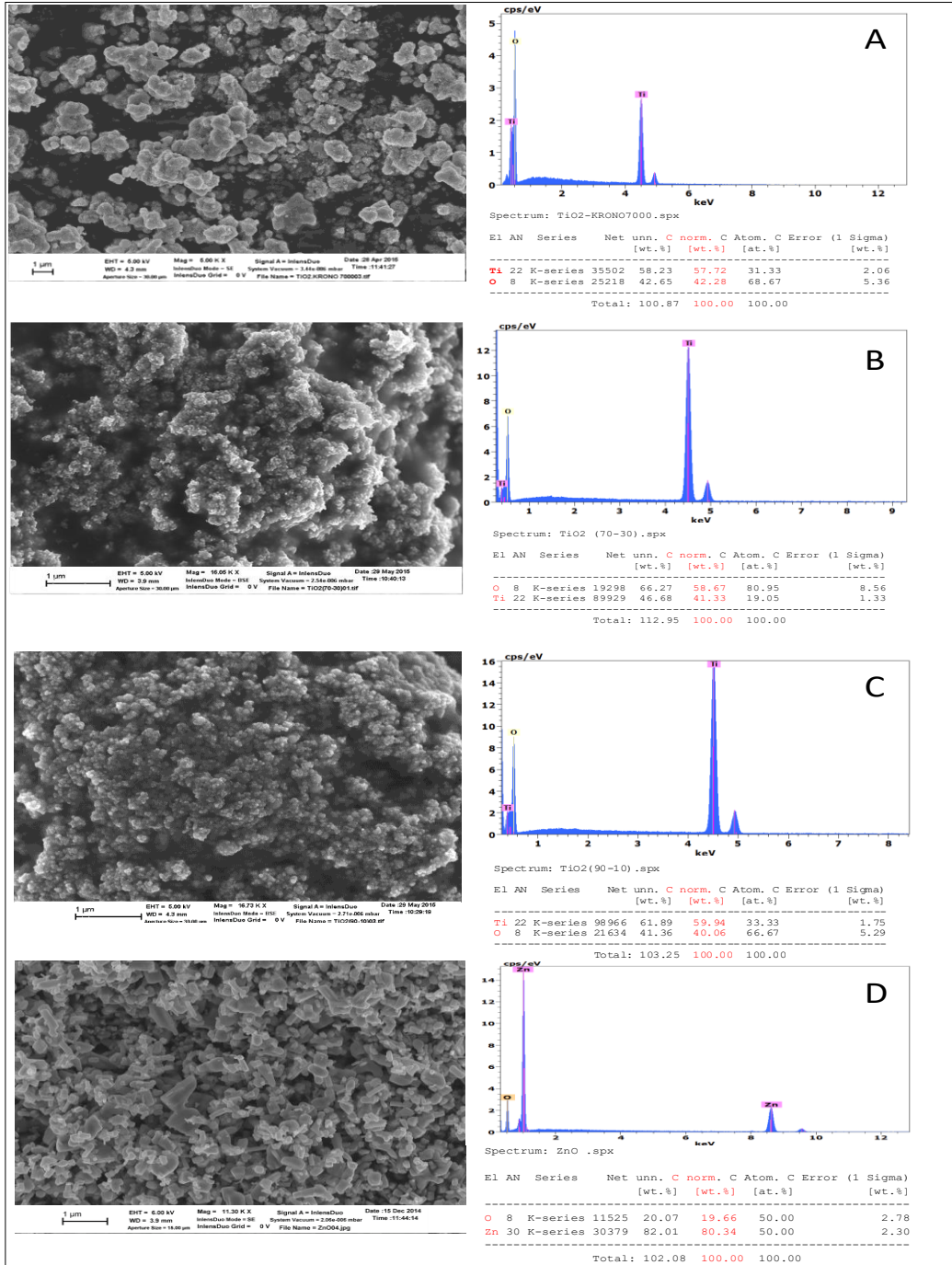


Figure 4.2. SEM image and elemental microanalysis of (A) TiO<sub>2</sub> vlp 7000, (B) TiO<sub>2</sub> P25, TiO<sub>2</sub> Alfa Aesar and (D) ZnO.

According to Brunauer-Emmet Teller (BET) analysis, it was observed ZnO displays smaller surface area ( $7 \text{ m}^2 \text{ g}^{-1}$ ) and bigger particle size ( $<194 \text{ nm}$ ) than TiO<sub>2</sub> Kronos vlp 7000 ( $250 \text{ m}^2 \text{ g}^{-1}$ ,  $<15 \text{ nm}$ ), TiO<sub>2</sub> P25 Degussa ( $55 \text{ m}^2 \text{ g}^{-1}$ ,  $<15 \text{ nm}$ ) and TiO<sub>2</sub> Alfa-Aesar ( $45 \text{ m}^2 \text{ g}^{-1}$ ,  $<32 \text{ nm}$ ). This fact improves the photocatalytic degradation for ZnO because the efficiency of charge carrier's separation what retards effectively the recombination of the photo-generated electrons and holes [Kitsiou et al., 2009].

The optical properties were analysed using UV-DR. The direct band gaps energy was calculated drawing  $[F(R) hv]^{1/2}$  over  $[hv - E_g]$ , where  $F(R) = (1 - R)^2 / (2R)$ ,  $h$  is the Plank constant,  $E_g$  is the band gap energy,  $v$  is the light frequency and  $R$  It is the diffuse reflectance, according to Kubelka-Munk method. The results of the band-gap energy calculated for the used semiconductors show that TiO<sub>2</sub> Kronos vlp 7000 presents a band-gap energy (2.4 eV) lower than the others (3.1, 3.2 and 3.1 eV for TiO<sub>2</sub> P25 Degussa, TiO<sub>2</sub> Alfa-Aesar and ZnO, respectively), making it suitable for use in the visible range. The results suit with the band gaps data determined by other authors [Valenzuela et al., 2002; Sakthivel et al., 2003; Jain et al., 2010; Pozan and Kambur, 2010; Ali et al., 2013].

#### 4.3. OPTIMIZATION OF HETEROGENEOUS PHOTOCATALYSIS PROCESSES IN LABORATORY CONDITIONS

In order to know the optimal operating conditions to develop solar photocatalysis, previous assays were undertaken to adjust the pollutant loading ( $0.3 \text{ mg L}^{-1}$  each one), to select the catalyst (TiO<sub>2</sub> vlp 7000, TiO<sub>2</sub> P25, TiO<sub>2</sub> Alfa Aesar and ZnO), to find out the optimal catalyst concentration (100, 200 and 300  $\text{mg L}^{-1}$ ), to settle the best oxidant loading ( $\text{Na}_2\text{S}_2\text{O}_8$  at 100, 250 and 400  $\text{mg L}^{-1}$ ) and the most favorable pH (5.5, 7.0 and 8.5). The experiments were carried out in a photoreactor under artificial light UVA (maximum 366 nm). Similarly, photolysis assays were performed in spiked water, under UV light but in absence of catalyst and oxidant to study the photolytic process. The remaining percentage of each EDs was calculated in order to know the influence of the photocatalytic process on their elimination.

The plasticizers and preservatives, bisphenol A (BA), bisphenol B (BB), butyl benzylphthalate (BP), diamyl phthalate (DP), ethyl 4-hydroxybenzoate (EP)

and methyl p-hydroxybenzoate (MP), were assessed in an assay and pesticides, malathion (MT), fenitrothion (FT), quinalphos (QP), vinclozoline (VZ), dimethoate (DT), and fenarimol (FR), in another one. The operating conditions are described in Section 3.6 Photocatalytic experiments at Lab Scale.

#### 4.3.1. Photocatalytic experiments with ZnO at lab scale

The optimization of the photocatalytic process methodology for ZnO at laboratory scale was developed by [Vela et al., 2018a, 2019]. The photooxidation of EDs in the absence/presence of ZnO and the effect of the catalyst concentration (100, 200 and 300 mg L<sup>-1</sup>) is shown in Figure 4.3, for tests performed with plasticizers and preservatives, and in Figure 4.4, for experiments performed with pesticides.

It is clear, the photodegradation of EDs without catalyst under UVA irradiation is significantly slow. At the end of photolytic assays (90 min), the remaining percentages varied from 36.7% (BP) to 58.6 % (EP) for the plasticizers and preservatives and from 63.1% (VZ) to 74.3% (QP) for the pesticides.

The experiments have demonstrated the ZnO loading affect the efficiency process as well. There is a photodegradation increase ( $p < 0.05$ ) when catalyst concentration varied from 100 to 200 mg L<sup>-1</sup> but, the degradation is quite similar under 200 and 300 mg L<sup>-1</sup> catalyst concentrations. The remaining percentages for plasticizers and preservatives were from 0.3% (BA) to 2.5% (BB) using 200 mg L<sup>-1</sup> of ZnO and from 0.1% (BB) to 0.7% (MP) for loadings of 300 mg L<sup>-1</sup>. The pesticides obtained results were from 0.0% (DT) to 4.3% (VZ) with a 200 mg L<sup>-1</sup> of ZnO and from 0.0% (DT, FT & MT) to 3.8% (VZ) at 300 mg L<sup>-1</sup> of ZnO. As a result, it is possible to conclude the optimal catalyst loading is 200 mg L<sup>-1</sup>, as increase the HO<sup>•</sup> y O<sub>2</sub><sup>•-</sup> amount what makes the reaction faster. However, the highest catalyst concentration, 300 mg L<sup>-1</sup>, does not produce an increase in the reaction because it causes turbidity and the particles became agglomerated [Fenoll et al., 2015]. High concentration levels could cause a decrease in the degradation rate because the light distribution is not uniform creating a scattered effect. [Ahmed et al., 2011]. For this reason, 200 mg L<sup>-1</sup> were chosen to develop solar photocatalysis experiments.

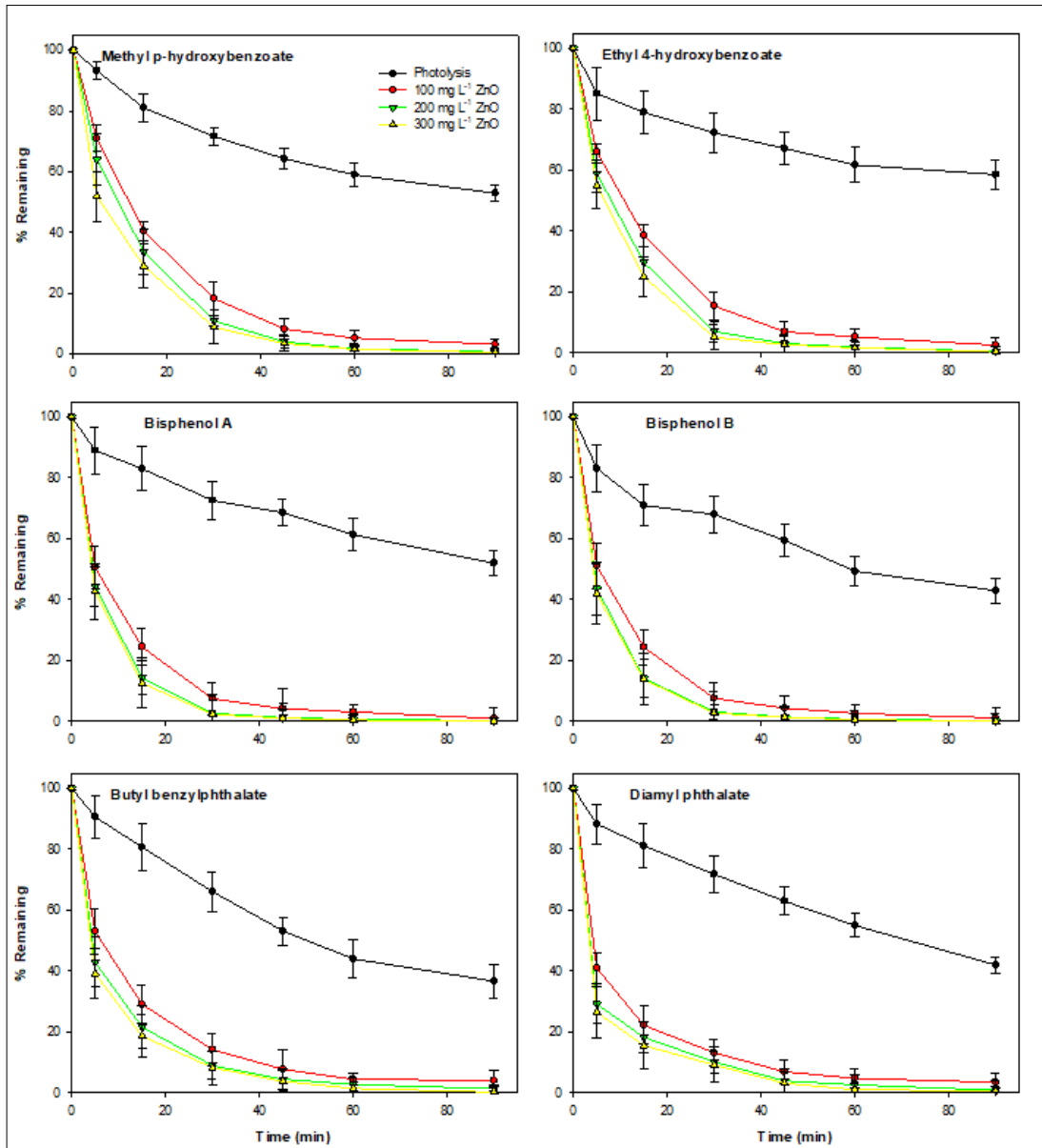


Figure 4.3. Effect of Zn concentration on the photodegradation of the plasticizers and preservatives under laboratory conditions.

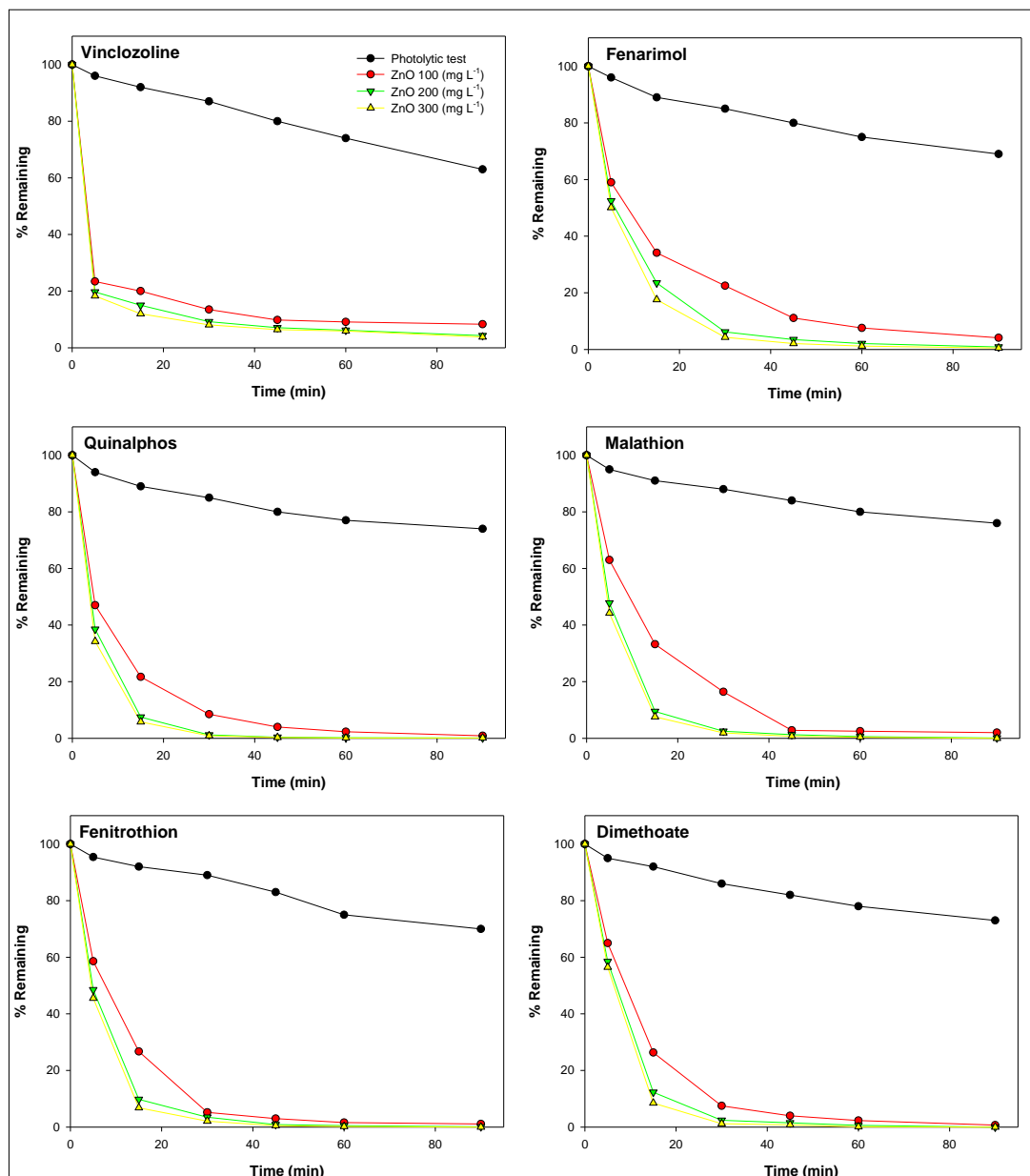
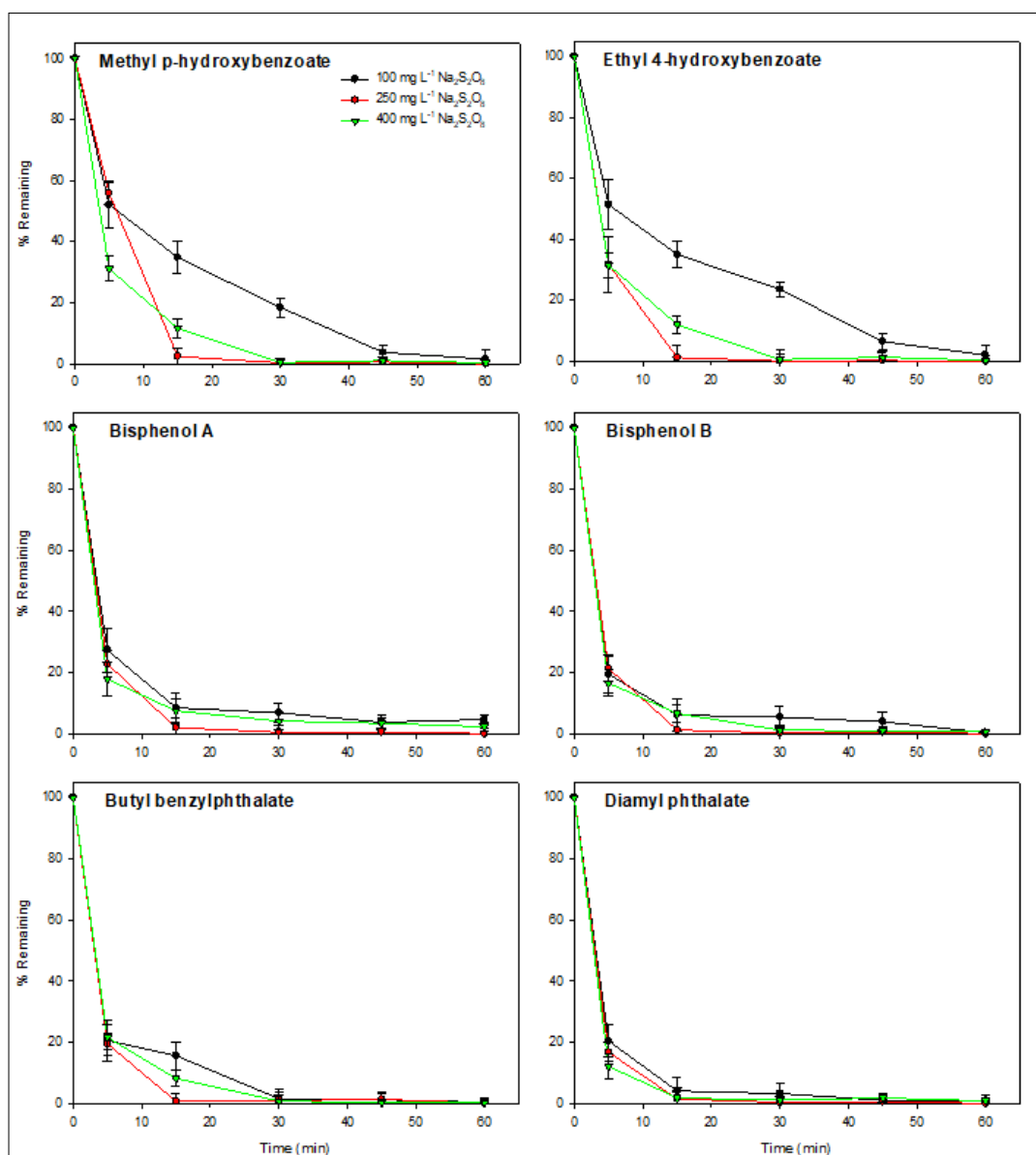


Figure 4.4. Effect of Zn concentration on the photodegradation of the pesticides under laboratory conditions.

On the other hand, to investigate the oxidant effect on the EDs degradation rate, new assays were carried out fixing ZnO concentration (200 mg L<sup>-1</sup>) but

changing the oxidant  $\text{Na}_2\text{S}_2\text{O}_8$  loading. The results are shown in Figure 4.5 for the plasticizers and preservatives and in Figure 4.6 for the pesticides.



**Figure 4.5.** Effect of electron acceptor on the photodegradation of the plasticizers and preservatives using different concentrations of  $\text{Na}_2\text{S}_2\text{O}_8$  at fixed  $\text{ZnO}$  loading ( $200 \text{ mg L}^{-1}$ ) under laboratory conditions.

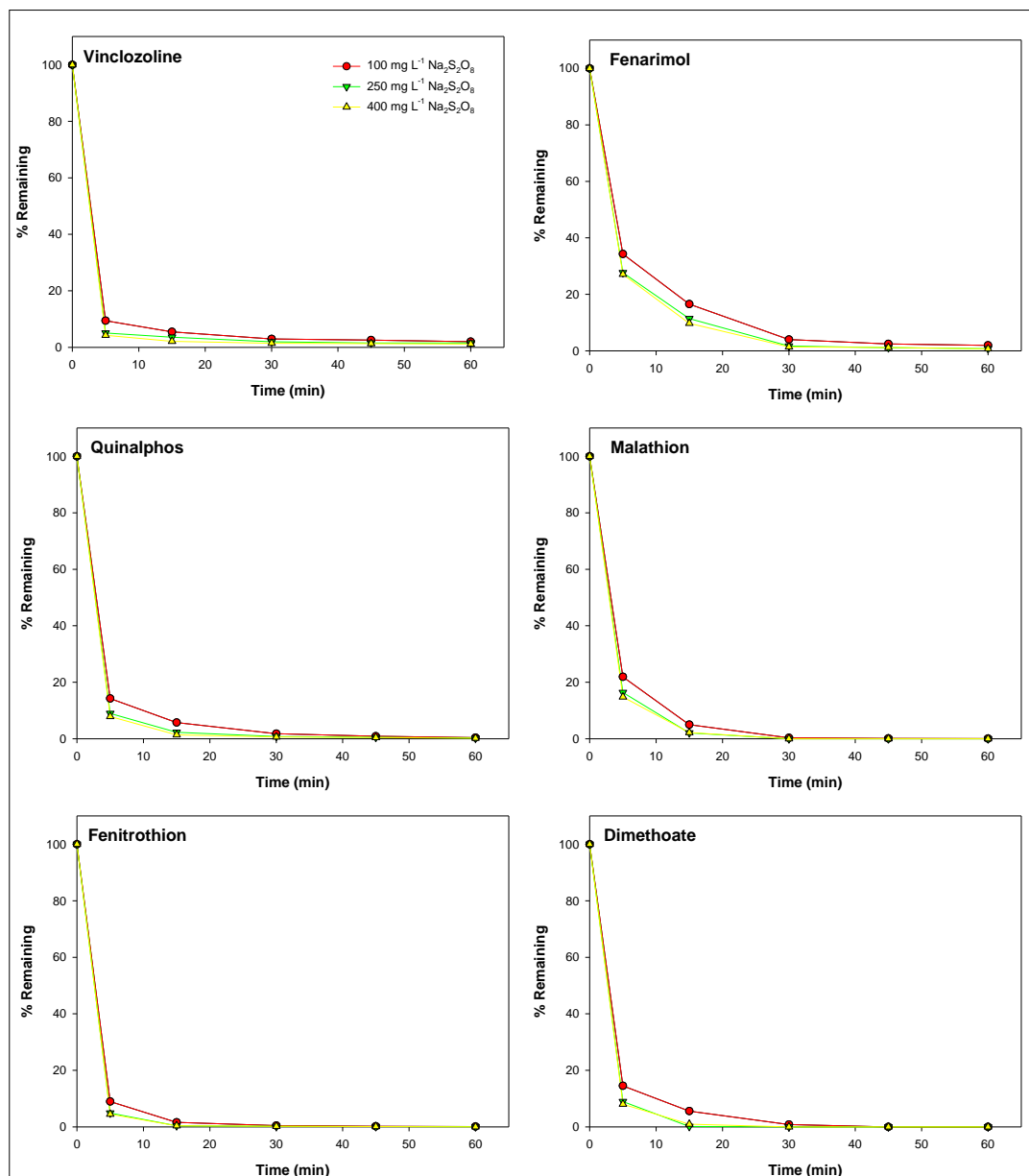


Figure 4.6. Effect of electron acceptor on the photodegradation of the pesticides using different concentrations of  $\text{Na}_2\text{S}_2\text{O}_8$  at fixed  $\text{ZnO}$  loading ( $200 \text{ mg L}^{-1}$ ) under laboratory conditions.

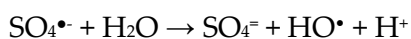
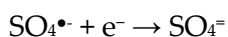
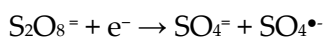
The best results obtained for plasticizers and pesticides turn out  $250 \text{ mg L}^{-1}$  of oxidant with remaining percentages for all compounds ( $< 0.2\%$  remaining).

Concentration levels of 100 mg L<sup>-1</sup> shown remaining percentages from 0.4% (BP) to 4.7% (BA) and with 400 mg L<sup>-1</sup> varied from 0.2% (BP) to 2.3% (BA).

In the pesticides case, the remaining percentage presented a similar behavior although not as many differences between 100 and 400 mg L<sup>-1</sup> ( $p < 0.05$ ). The remaining percentages oscillated from 0.0% (DT) to 2.0% (VZ), from 0.0% (DT, MT) to 1.6% (VZ) and from 0,0% (DT, MT) to 1.2% (VZ) for 100, 250 and 400 mg L<sup>-1</sup>, respectively. For this reason, 250 mg L<sup>-1</sup> was considered the optimum concentration for conducting solar photocatalysis experiments.

As it has been widely mentioned in scientific literature, the heterogeneous photocatalysis efficiency relies on several factors including charge carrier transfer dynamics [Ohtani 2013]. In order to avoid the recombination drawback, the Na<sub>2</sub>S<sub>2</sub>O<sub>8</sub> addition, enhance the reaction as involves the generation of oxidizing species that can compete with the charge carrier recombination. The Na<sub>2</sub>S<sub>2</sub>O<sub>8</sub> use induces the formation of high oxidizing species, SO<sub>4</sub><sup>•-</sup> ( $E^0 = 2.6$  V), and enhances the generation of HO<sup>•</sup> ( $E^0 = 2.8$  V), reducing the pair recombination and accelerate the process [Ahmed et al., 2011].

In our case, the beneficial effect of the persulphate ion can be attributed not only to the decrease in the recombination of e<sup>-</sup>/h<sup>+</sup>, very possibly, also to the generation of SO<sub>4</sub><sup>•-</sup>, a very strong species, and to the formation of HO<sup>•</sup> according to the following reactions:



Sulfate radicals SO<sub>4</sub><sup>•-</sup> have another advantage as their half-life ( $t_{1/2} = 30-40$  μs) last more than HO<sup>•</sup> ( $t_{1/2} < 1$  μs), which permits more stability and better contact with pollutants [Olmez-Hanci and Arslan -Alaton 2013]. The capacity of the persulphate ion is not only attributed to the promotion of charge separation ( $S_2O_8^{2-} + e^- \rightarrow SO_4^{2-} + SO_4^{\bullet-}$ ). Persulphate ion can be activated by heat, transition metals and UV light. The persulphate ion forms two SO<sub>4</sub><sup>•-</sup> through the cleavage of the O - O bond (long bonding distance = 1.497 Å and low bonding energy = 33.5 kcal mol<sup>-1</sup>) [Wallacem et al., 2002] as a result of the absorption of heat energy and/or UV light and more HO<sup>•</sup> [Matzek and Carter 2016]. Nowadays, there is a study that reports the full-scale tertiary treatment implementation based on



sulphate radicals in a WWTP [Rodríguez-Chueca et al., 2018], with excellent results due to the effectiveness reducing the  $e^-/h^+$  recombination, main drawback in heterogeneous photocatalysis using semiconductor materials.

The following step was to study the pH effect on the photocatalytic process based on ZnO at laboratory scale. The Figure 4.7 show the results for plasticizers and preservatives and Figure 4.8 for pesticides. The assays were performed placing  $200 \text{ mg L}^{-1}$  of catalyst loading and  $250 \text{ mg L}^{-1}$  of oxidant.

After the 60 minutes of the photoperiod, the plasticizers and pesticides average of the remaining percentages ( $n = 6$ ) were  $0.94 \pm 1.11\%$ ,  $0.06 \pm 0.01\%$ , y  $0.49 \pm 0.57\%$ , at pH = 5.5, 7.0 and 8.5, respectively. The best results were obtained during the first 20 minutes for pH = 7 and the degradation rate was kept with a negligible decrease during the rest of the experiment.

Pesticides displayed a similar behavior but after 30-40 minutes of exposure were required to obtain the higher degradation rates. The remaining percentages ( $n = 6$ ) were  $2.77 \pm 3.99\%$ ,  $0.88 \pm 1.81\%$  and  $0.0 \pm 0.0 \%$  at pH de 5.5, 7.0 and 8,5, respectively.

The low initial reaction is due to ZnO can react with acidic or alkaline compounds resulting the formation of  $[\text{Zn}(\text{OH})_4]^{2-}$  due to its amphoteric property [Evgenidou et al., 2005]. As the best pH value results were obtained at pH = 7, it was not adjusted in the experiments with the treated wastewater (pH = 7.2) (Table 3.2) in solar photocatalysis.

In heterogeneous photocatalysis the pH study is important as plays a critical role in many stages of the reaction, affecting the catalyst surface charge and the reactive species formed [Chong et al., 2010; Ahmed et al., 2011]. The point zero charge (PZC) has been used in the study of pH and it is the pH in which the catalyst surface charge is zero. In the ZnO case the PZC is near pH = 9.0 and in an acidic solution the positive charge at the surface of the ZnO increases as pH decreases but at pH > PZC the negative charge increases with pH increases [Kosmulski 2016]. Besides, the predominant oxidative species are  $h^+$  at a low pH while at neutral or high pH the predominant oxidative species are  $\text{HO}^\bullet$  and it is expected they increase the number as at high pH the of  $\text{OH}^-$  is available [Lee et al., 2016].

Besides, some authors have studied the pH effect on the particle agglomeration and dissolution of nanoparticles of ZnO in order to investigate the

toxicity in environment [Domingos et al., 2013]. The study reported at pH, near the PZC of ZnO, the particles were strongly agglomerated, reason for which it was decided not to modify the wastewater treated in the solar photocatalysis experiments.

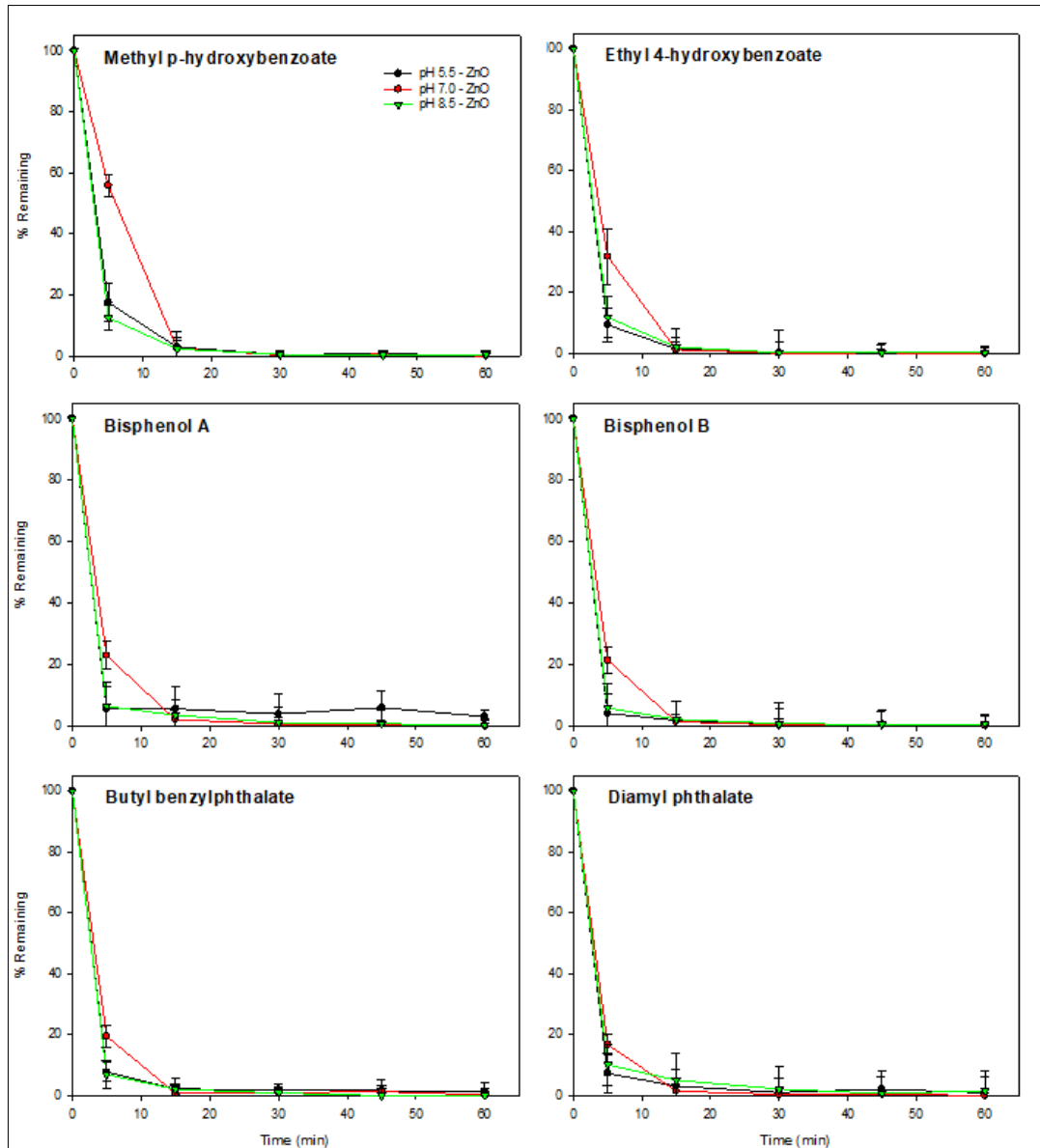


**Figure 4.7.** pH effect on the plasticizers and preservatives photodegradation at fixed ZnO ( $200 \text{ mg L}^{-1}$ ) and  $\text{Na}_2\text{S}_2\text{O}_8$  ( $250 \text{ mg L}^{-1}$ ) concentrations under laboratory conditions.

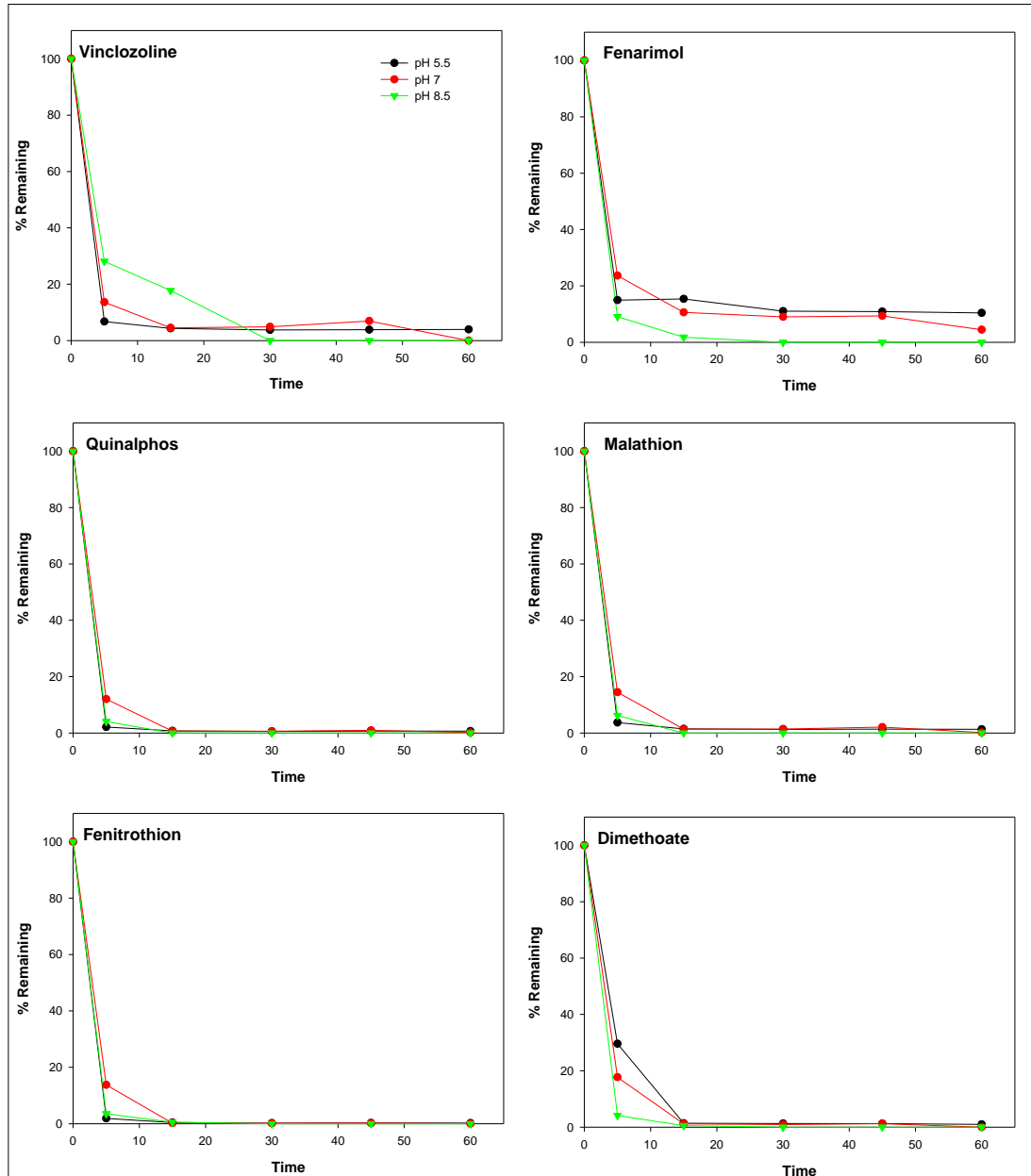


Figure 4.8. pH effect on the pesticides photodegradation at fixed ZnO ( $200 \text{ mg L}^{-1}$ ) and  $\text{Na}_2\text{S}_2\text{O}_8$  ( $250 \text{ mg L}^{-1}$ ) concentrations under laboratory conditions.

#### 4.3.2. Photocatalytic experiments with TiO<sub>2</sub> at lab scale

The photocatalytic assays based on TiO<sub>2</sub> at laboratory scale were designed and performed to investigate the optimal parameters and work with them in the solar photocatalysis [Vela et al., 2018b, 2018c]. The photocatalysis results, the EDs degradation rates with TiO<sub>2</sub> (TiO<sub>2</sub> P25, TiO<sub>2</sub> vlp 7000 y TiO<sub>2</sub> Alfa Aesar), the effect on the type of catalyst and their loading (100, 200 and 300 mg L<sup>-1</sup>) are shown in Figure 4.8 for plasticizers and preservatives and in Figure 4.9 for pesticides.

The remaining percentages of the photolytic process, in absence of TiO<sub>2</sub>, varied from 36.7% to 58.6% in the case of BP y EP, respectively, for the plasticizers and preservatives (Figure 4.8) and from 63.0% to 76.0% for VZ and MT, respectively, for the pesticide (Figure 4.9). The degradation rates were, in all the cases, significantly lower in the photolytic experiments ( $p < 0,05$ ) than using catalysts.

With the aim of comparing the efficiency of the three catalysts (TiO<sub>2</sub> P25, TiO<sub>2</sub> vlp 7000 y TiO<sub>2</sub> Alfa Aesar), different experiments were performed with the plasticizers and preservatives in the photoreactor testing the effect of the catalyst loading (100, 200 y 300 mg L<sup>-1</sup>) (Figure 4.9). The process efficiency was in the following order: TiO<sub>2</sub> P25 >>TiO<sub>2</sub> vlp 7000 > TiO<sub>2</sub> Alfa Aesar, for all the tested pollutants. The average for the remaining rates for the six chemicals and the three loadings were  $24.8 \pm 1.4$  %,  $1.7 \pm 0.3$  % y  $32.0 \pm 2.5$  %, for TiO<sub>2</sub> vlp 7000, TiO<sub>2</sub> P25 y TiO<sub>2</sub> Alfa Aesar, respectively.

The optimal catalyst loading was of 200 mg L<sup>-1</sup> for the three different TiO<sub>2</sub> and their average rates ( $n = 6$ ) were of  $22.4 \pm 12.9$  %,  $1.0 \pm 0.7$  %,  $37.6 \pm 8.2$  % for TiO<sub>2</sub> vlp 7000, TiO<sub>2</sub> P25 and TiO<sub>2</sub> Alfa Aesar, respectively. In some cases, the increase in the catalyst loading (300 mg L<sup>-1</sup>) decreased the degradation rates significantly ( $p < 0,05$ ) probably, due to the reversible reactions (sorption/interaction) between the catalyst and EDs. The optical absorption coefficient, light scattering and radiation level are relevant factors in the system. [Satuf et al., 2005]. The decrease in the degradation level can be attributed to the agglomeration particle tendency as reduce the catalyst active sites [Vela et al., 2017]. As a result, the catalyst loading chosen for the pilot plant experiments was 200 mg L<sup>-1</sup> and TiO<sub>2</sub> Alfa Aesar was dismissed owing to the low efficiency for the further experiments.

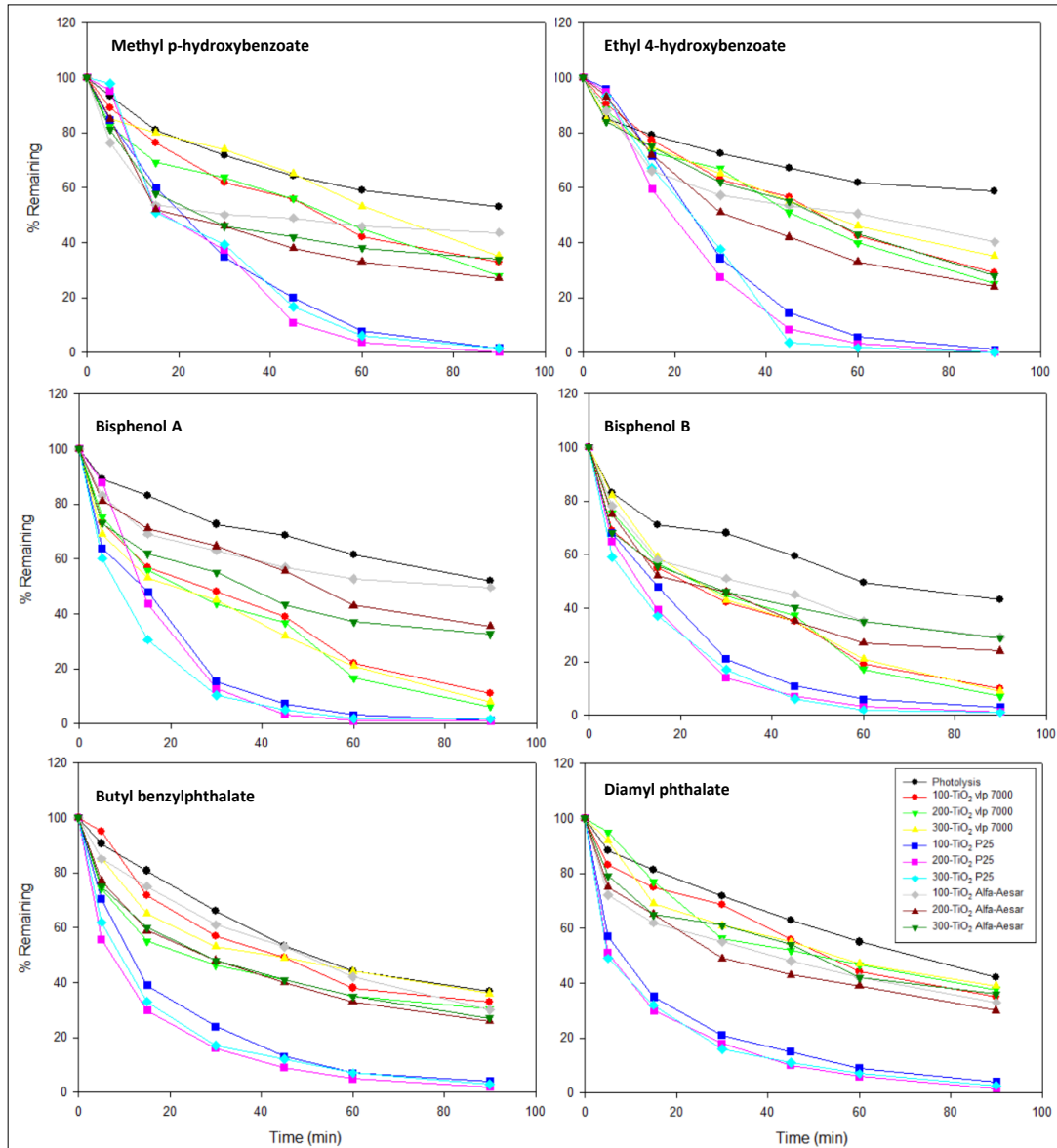


Figure 4.9. Effect of TiO<sub>2</sub> concentration on the photodegradation of the plasticizers and the preservatives under laboratory conditions.

The preliminary assays with the pesticides also demonstrated that the catalyst loading affects the process and the concentration level increases the degradation rate up to the optimum level (200 mg L<sup>-1</sup>) for the two TiO<sub>2</sub> (TiO<sub>2</sub> vlp 7000 y TiO<sub>2</sub> P25), as is shown in Figure 4.10.

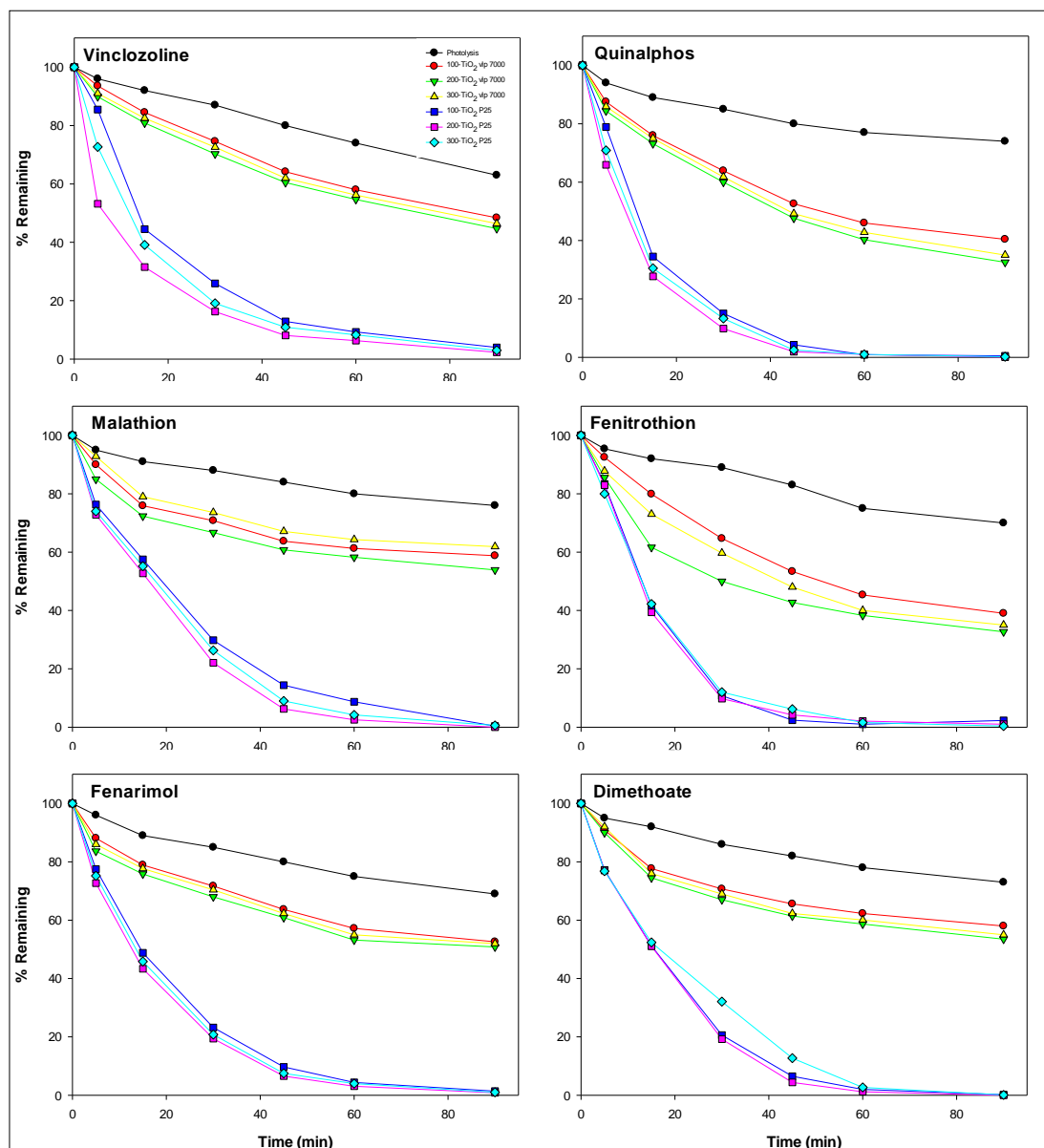


Figure 4.10. Effect of TiO<sub>2</sub> concentration on the photodegradation of the pesticides under laboratory conditions.

In addition, in order to study the oxidant effect on the degradation rate, experiments were carried out at three different  $\text{Na}_2\text{S}_2\text{O}_8$  loadings (100, 250 y 400  $\text{mg L}^{-1}$ ) but the  $\text{TiO}_2$  concentration was fixed in 200  $\text{mg L}^{-1}$ . The results are shown in Figure 4.11 for the plasticizers and the preservatives and in Figure 4.12 for the pesticides studied.

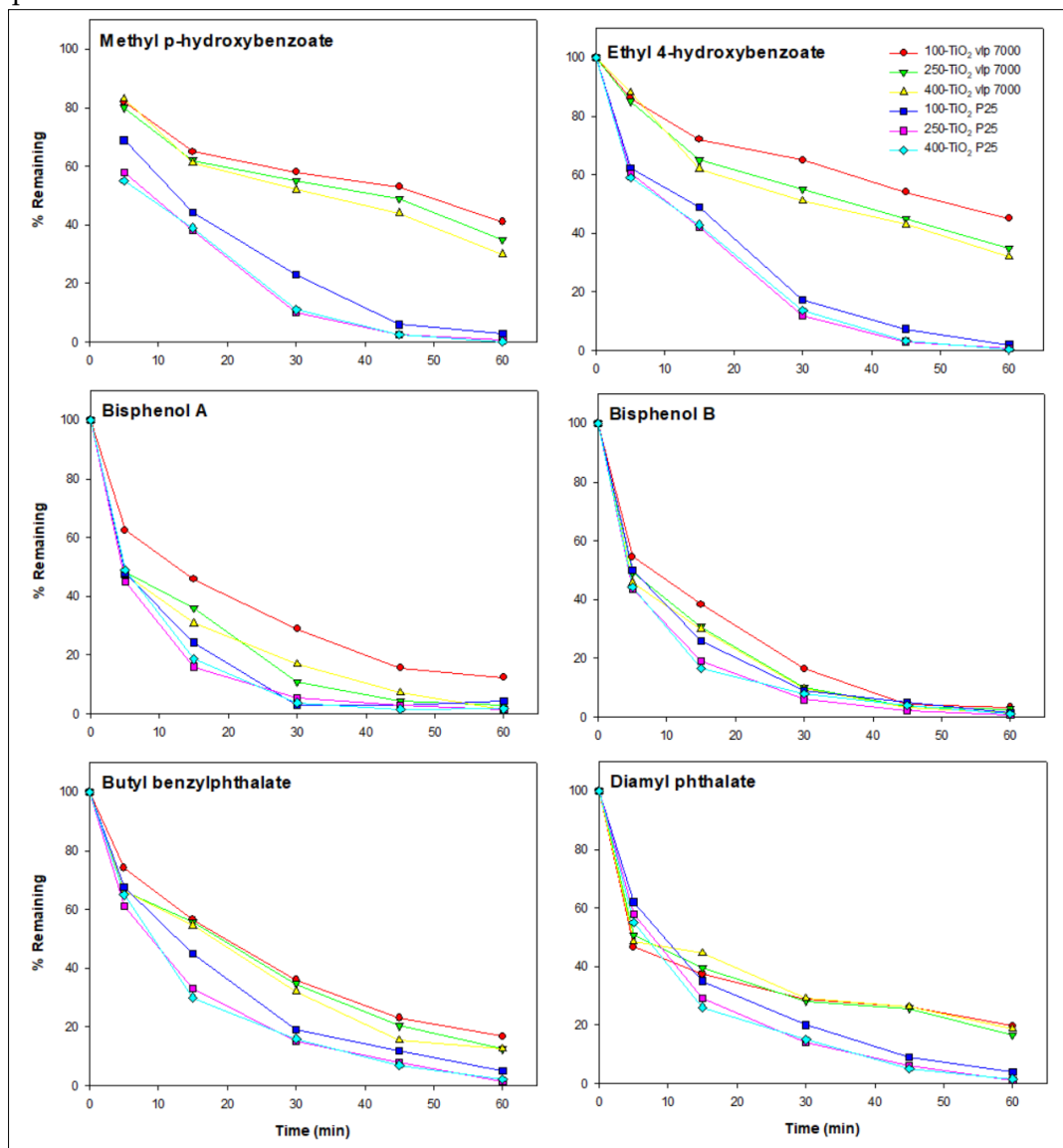


Figure 4.11. Effect of electron acceptor on the photodegradation of plasticizers and preservatives using different concentrations of  $\text{Na}_2\text{S}_2\text{O}_8$  at fixed  $\text{TiO}_2$  loading (200  $\text{mg L}^{-1}$ ) under laboratory conditions.

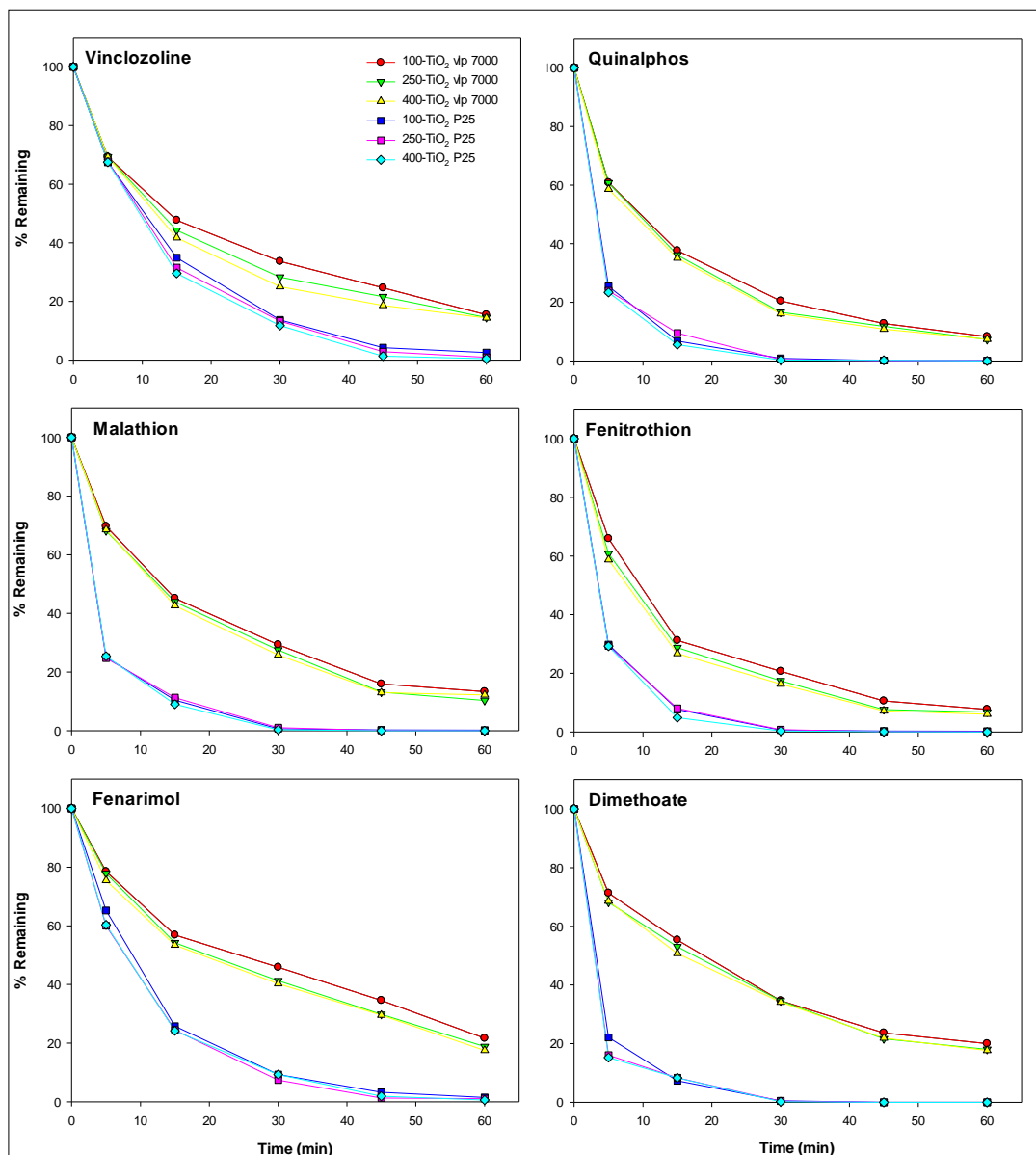


Figure 4.12. Effect of electron acceptor on the photodegradation of pesticides using different concentrations of  $\text{Na}_2\text{S}_2\text{O}_8$  at fixed  $\text{TiO}_2$  loading ( $200 \text{ mg L}^{-1}$ ) under laboratory conditions.

According to the obtained results for the plasticizers and preservatives, it was observed no significant differences ( $p < 0.05$ ) as the  $\text{Na}_2\text{S}_2\text{O}_8$  loading was increased from 100 to 400  $\text{mg L}^{-1}$  in both cases ( $\text{TiO}_2$  P25 and  $\text{TiO}_2$  vlp 7000). The



average of the remaining percentages ( $n = 6$ ) obtained were  $3.3 \pm 1.4 \%$ ,  $1.0 \pm 0.4 \%$  and  $1.2 \pm 0.8 \%$  with  $\text{TiO}_2$  P25 at 100, 250 and 400  $\text{mg L}^{-1}$ , respectively, and  $23.0 \pm 16.5 \%$ ,  $17.5 \pm 14.6 \%$  and  $16.0 \pm 13.4 \%$  using  $\text{TiO}_2$  vlp 7000 at 100, 250 y 400  $\text{mg L}^{-1}$ , respectively.

No considerable differences were observed in the experiments with the pesticides ( $p < 0.05$ ) as the  $\text{Na}_2\text{S}_2\text{O}_8$  was increased from 100 to 400  $\text{mg L}^{-1}$ , in the  $\text{TiO}_2$  P25 case ( $0.8 \pm 1.0 \%$ ,  $0.2 \pm 0.4 \%$  and  $0.2 \pm 0.3 \%$  for 100, 250 y 400  $\text{mg L}^{-1}$ , respectively). However, for  $\text{TiO}_2$  vlp 7000, the higher degradation rates were obtained at 250 and 400  $\text{mg L}^{-1}$  ( $14.4 \pm 5.8 \%$ ,  $12.6 \pm 5.3 \%$  and  $10.9 \pm 4.6 \%$  for 100, 250 y 400  $\text{mg L}^{-1}$ , respectively). For this reason, the loading 250  $\text{mg L}^{-1}$  was considered the optimal concentration level for the following assays at pilot plant scale.

As it was mention previously, persulphate addition enhances the process not only because it reduces the recombination between  $e^+/h^+$  [Ohtani 2013] but also because the oxidant species production as  $\text{SO}_4^\bullet$  y  $\text{HO}^\bullet$  is favorable [Ahmed et al., 2011].

On the other hand, the following step was to study the pH effect in the process using the two selected  $\text{TiO}_2$  ( $\text{TiO}_2$  vlp 7000 y  $\text{TiO}_2$  P25) under laboratory conditions. The experiments were developed at the optimal catalyst and oxidant concentration, 200  $\text{mg L}^{-1}$  and 250  $\text{mg L}^{-1}$ , respectively. The obtained results are shown in Figures 4.13 for the plasticizers and preservatives and in Figure 4.14 for the pesticides.

The degradation rates change along the 60 minutes that the assay lasted. The average of the remaining rates ( $n = 6$ ) for the plasticizers and preservatives using  $\text{TiO}_2$  vlp 7000 were  $35.0 \pm 20.8\%$ ,  $13.8 \pm 9.6\%$ , and  $40.3 \pm 23.0\%$  during the assays at pH 5.5, 7.0 and 8.5, respectively. The remaining rates were lower in the case of  $\text{TiO}_2$  P25,  $3.7 \pm 3.2\%$ ,  $1.3 \pm 0.4\%$ , and  $8.7 \pm 6.0\%$  at pH 5.5, 7.0 and 8.5, respectively. Even though these differences in their rates, the behavior under changes in the pH of the solution were similar:  $7.0 > 5.5 > 8.5$  for both catalysts.

The results demonstrate the high degradation rate was, in all the cases, at neutral pH, which implies the predominant species during the mineralization process were cations. As it was explained previously, the pKa of the EDs and PZC of the catalysts play a primary role in the photocatalysis process. In the case of  $\text{TiO}_2$ , the PZC is quite variable depending on the crystallography (anatase versus

rutile) and the used method, therefore it can present values that vary from 4.7 to 7. According to Kosmulski (2016), the PZC for TiO<sub>2</sub> P25 is approximately 6.3, which means at pH > 6.3 the catalyst surface is negatively charged and positively charged under this value.

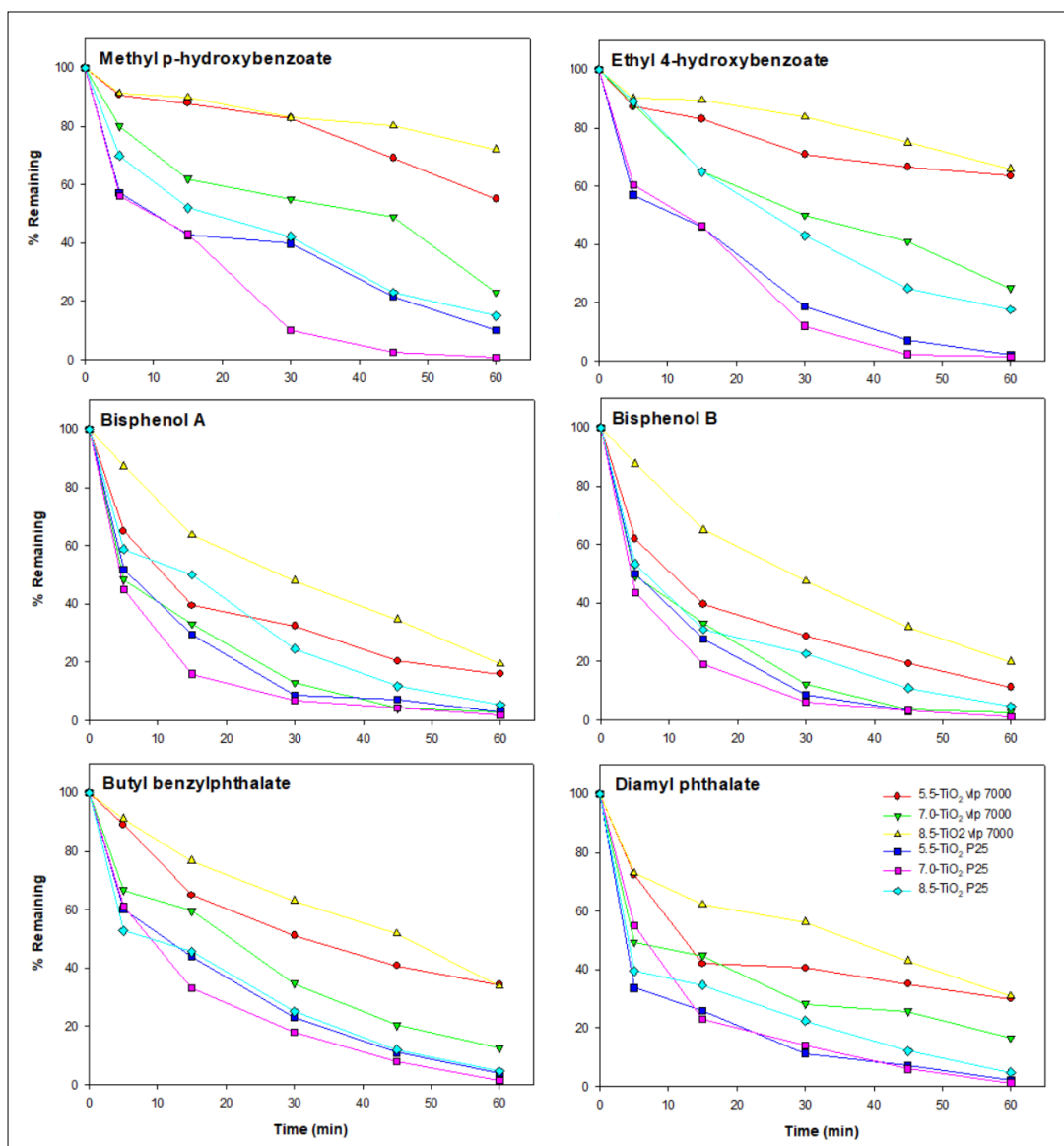


**Figure 4.13.** Effect of pH on the photodegradation of plasticizers and preservatives at fixed TiO<sub>2</sub> (200 mg L<sup>-1</sup>) and Na<sub>2</sub>S<sub>2</sub>O<sub>8</sub> (250 mg L<sup>-1</sup>) concentrations under laboratory conditions.

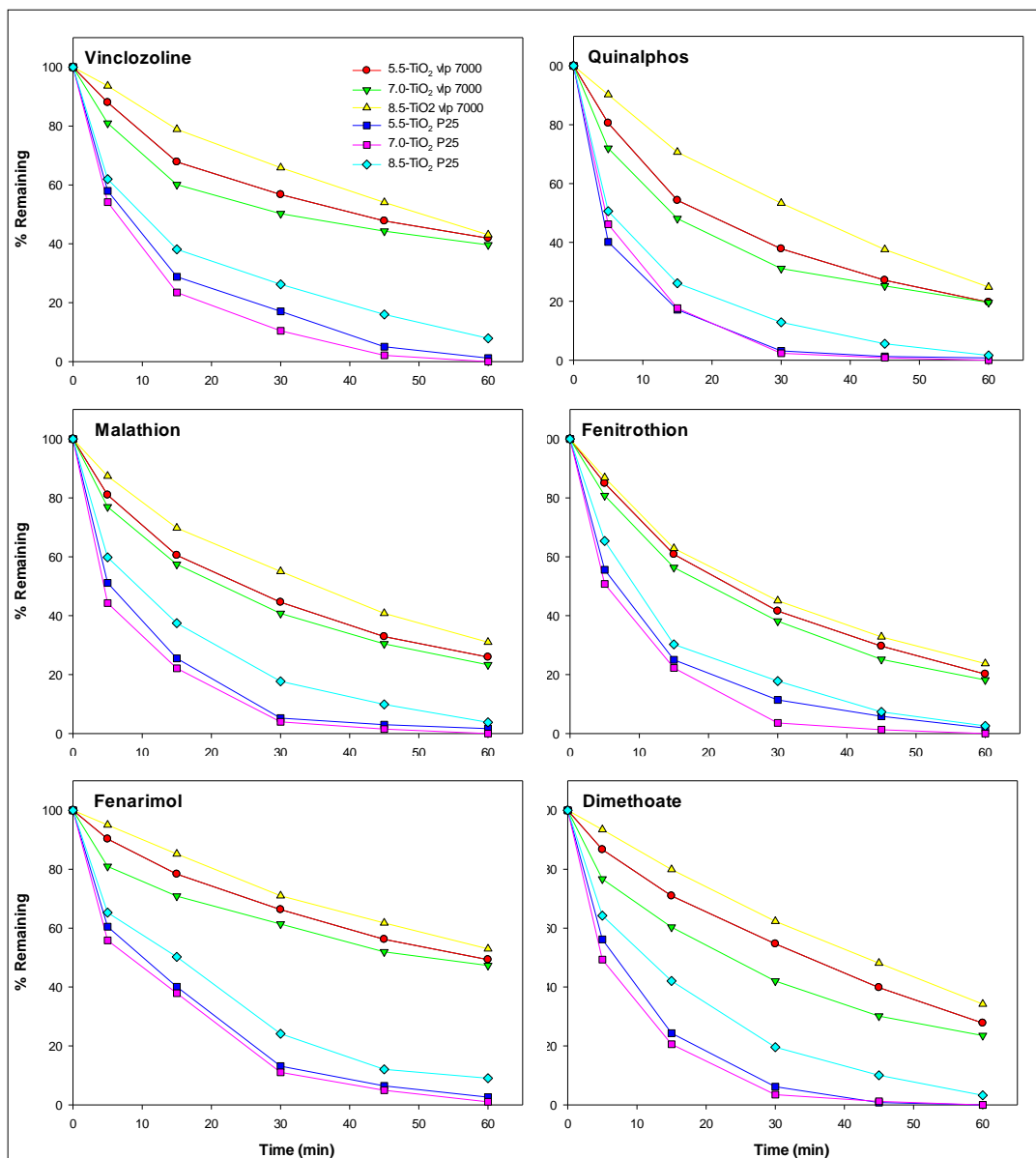


**Figure 4.14.** Effect of pH on the photodegradation of pesticides at fixed  $\text{TiO}_2$  ( $200 \text{ mg L}^{-1}$ ) and  $\text{Na}_2\text{S}_2\text{O}_8$  ( $250 \text{ mg L}^{-1}$ ) concentrations under laboratory conditions

In accordance with Malato et al., (2009), when the pH varies from 3 to 10, the predominant specie is  $-\text{TiOH}$  (80%), while  $-\text{TiO}^- \geq 20\%$  when  $\text{pH} > 10$  and  $-\text{TiOH}_2^+ \geq 20\%$  at  $\text{pH} < 3$ . In the case of  $\text{pH} < \text{pKa}$ , organic compounds are neutral but for  $\text{pH} > \text{pKa}$ , organic compounds are negatively charged, which can

influence significantly in the photocatalysts degradation. When pH = 8.5, the catalyst surface is negatively charged and the EDs as well due to their pKa (8.5 - 10.1), for which repulsion is favorable. However, at pH < 8.5 the organic compounds are electrostatically neutral therefore, pH = 7 was consider optimal to develop the experiments at pilot plant scale.

The pesticides displayed similar performance in terms of pH, despite the TiO<sub>2</sub> P25 efficiency was higher than TiO<sub>2</sub> vlp 7000. The remaining degradation rates after 60 minutes of irradiation were essentially the same (n = 6), 30.8 ± 12.1%, 28.6 ± 12.0% and 31.3 ± 12.5% at pH 5.5, 7.0 and 8.5, respectively, for TiO<sub>2</sub> vlp 7000. These percentages decreased drastically with the use of TiO<sub>2</sub> P25, 1.3 ± 0.9%, 0.3 ± 0.7%, and 4.7 ± 3.1% at pH 5.5, 7.0 and 8.5, respectively. Hence, it is possible to conclude, the photocatalytic oxidation for these compounds was: 7.0 > 5.5 > 8.5 for both catalysts.

These results are in concordance with their pKa and PZC (point zero charge). The PZC for TiO<sub>2</sub> is near 6.3 [Kosmulski, 2016]. Consequently, the surface catalyst is positively charged at pH < 6.3 and negatively charged at pH > 6.3. Therefore, pH neutral was selected to performance the assay at pilot plant scale, as it was done with the plasticizers and preservatives, and the wastewater pH (7.2) was not required to be adjusted (Table 3.2).

#### **4.4. PHOTOCATALYSIS EXPERIMENTS IN A PILOT PLANT UNDER SOLAR RADIATION**

##### **4.4.1. Solar photocatalytic experiments with ZnO**

The photocatalytic process efficiency under solar irradiation was study after evaluating the EDs degradation rate in presence of ZnO and under UV irradiation at laboratory scale [Vela et al., 2018a, 2019]. The operating conditions are presented in the Section 3.7 Experimental Setup of Solar Photocatalytic Trial. The EDs photodegradation rates in tandem ZnO (200 mg L<sup>-1</sup>)/Na<sub>2</sub>S<sub>2</sub>O<sub>8</sub> (250 mg L<sup>-1</sup>) for the plasticizers and preservatives are shown in Figure 4.15.

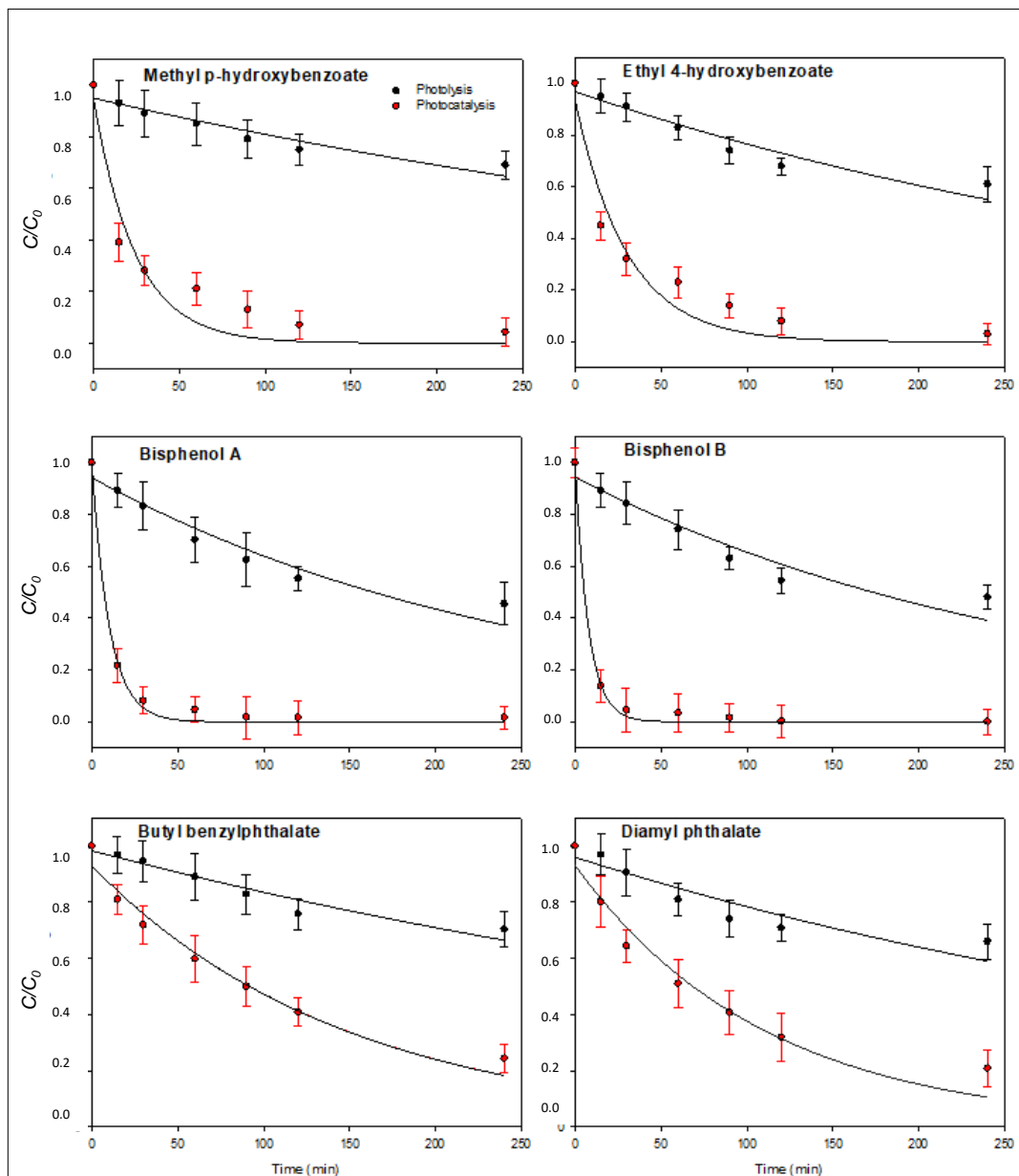


**Figure 4.15.** Evolution of the plasticizer and preservative residues as a function of natural sunlight irradiation time using the tandem ZnO ( $200 \text{ mg L}^{-1}$ )/ $\text{Na}_2\text{S}_2\text{O}_8$  ( $250 \text{ mg L}^{-1}$ ) at pilot plant scale. Error bars denote standard deviation ( $n=3$ ).

The results clearly show that the photodegradation in presence of ZnO is significantly higher than the photolysis ( $p < 0.05$ ), in absence of catalyst. The

average remaining rates ( $n = 3$ ), after 240 minutes of solar irradiation, for the plasticizers and preservatives were  $45.5 \pm 8.2\%$  (BA) and  $70.3 \pm 6.2\%$  (BP) in the photolytic test and in presence of ZnO/Na<sub>2</sub>S<sub>2</sub>O<sub>8</sub>, the rates varied from  $24.3 \pm 5.2\%$  (BP) and  $0.0\% \pm 4.8\%$  (< LQ BB).

Analyzing the results, different behaviors were observed ( $p < 0.05$ ) within the bisphenols, phthalates and parabens groups. The degradation was almost achieved for BA ( $1.6 \pm 4.3\%$  remaining) and for BB the degradation rate was even lower than LQ ( $0.12 \mu\text{g L}^{-1}$ ). In the case of phthalates, the obtained remaining were  $20.8 \pm 6.5\%$  and  $24.3 \pm 5.3\%$  for DP and BP, respectively. Finally, the results for parabens were quite close to bisphenols  $3.0 \pm 4.1\%$  (EP) and  $4.2 \pm 5.3\%$  (MP).

The high degradation rates for BA are in concordance with previous reports. Bechambi et al. (2015) found that after 24 h of UV irradiation, 4% C-doped ZnO reached 100% BA degradation and 70% BA mineralization. Kuo et al. (2010) conclude, BA was degraded within 2.1 a 2.9 h<sup>-1</sup> in presence of TiO<sub>2</sub>, under VIS irradiation and in tandem with different dosages of polietilenglicol. Besides, Zúñiga-Benítez and Peñuela (2017) demonstrate the simultaneous use of TiO<sub>2</sub>/H<sub>2</sub>O<sub>2</sub>/UV reached the 90% of the degradation for MP after 30 minutes of irradiation, being HO• the oxidizing specie in charge of the degradation. Diverse phthalates and BA were degraded in wastewater applying foto-Fenton method and photocatalysis in presence of TiO<sub>2</sub> [Balabanič et al., 2012].

In the study of plasticizers and preservatives, the remaining rates at pilot plant scale were significantly lower ( $p < 0.05$ ) than the results at lab scale  $0.06 \pm 0.01\%$ , ( $n = 6$ ) with TiO<sub>2</sub> (200 mg L<sup>-1</sup>) and Na<sub>2</sub>S<sub>2</sub>O<sub>8</sub> (250 mg L<sup>-1</sup>) concentrations at pH 7.0. This fact, could be attributed to the cations and anions dissolved organic materia (DOM) present in the treated wastewater used, as they can be adsorpted by the catalyst surface [Ahmed et al., 2011; Vela et al., 2015]. Zacharakis et al. (2013) demonstrated the BA degradation using wastewater in presence of TiO<sub>2</sub> or ZnO immobilized in crystal plates was 5 times lower than in pure water, which means the importance of the compounds present in wastewater. According to several authors, the presence of DOM in wastewaters affect the BA photodegradation efficiency [Zhang et al., 2012], phthalate and di-ethyl [Song et al., 2016] using TiO<sub>2</sub> and under UV irradiation.

Different studies have demonstrated that the use of ZnO, as catalyst, achieve higher degradation rates due to its wide conduction band gap ( $E_g = 3.3$

eV), large exciton binding energy (60 meV) and piezoelectric properties. According to Kudo and Miseki (2009), the main consequence in the use of ZnO is the corrosion, mainly under acidic conditions, due to  $Zn^{2+}$  is released as a result of the interaction with the holes ( $ZnO + 2 h^+ \rightarrow Zn^{2+} + \frac{1}{2}O_2$ ). In this study, as can be seen in Figure 4.16, an increase of  $Zn^{2+}$  concentration level was detected after 30 minutes of irradiation ( $137 \pm 11$  to  $186 \pm 8 \mu g L^{-1}$ ) changing into  $103 \pm 11 \mu g L^{-1}$  at the end of the photoperiod (240 min). The highest level of  $Zn^{2+}$  found in water was slightly higher than EC50 using *Vibrio fischeri*, *Daphnia magna* y *Thamnocephalus platyurus* [Heinlaan et al., 2008]. However, our  $Zn^{2+}$  levels are below the WHO's established limit of  $5 mg L^{-1}$  [WHO, 2011].

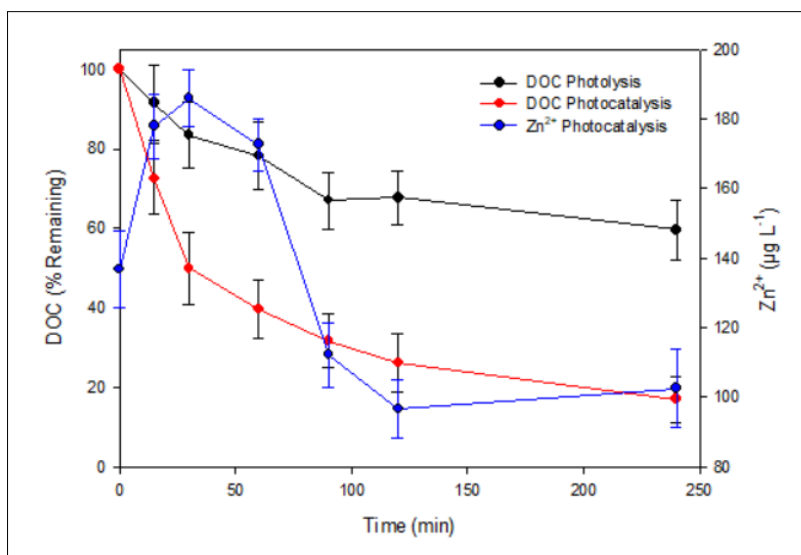


**Figure 4.16.** Evolution of dissolved organic carbon (DOC) during the photolytic and photocatalytic experiments with ZnO and the plasticizer and preservative under natural sunlight irradiation. Error bars denote standard deviation.

In this sense, the inhibition of *Vibrio fischeri* was studied in the experiments at pilot plant scale (Figure 4.17). The toxicity level decreased 70% from the initial value at the end of the photoperiod (240 min),  $11 \pm 5\%$  using ZnO/ $Na_2S_2O_8$  and  $45 \pm 8\%$  in the case of photolysis assay. In both cases, it was observed a lightly increase in the toxicity level near the minute 30, probably because of the

intermediate species formation. However, the level of toxicity was reduced near the 85% at the end of the treatment with ZnO/ Na<sub>2</sub>S<sub>2</sub>O<sub>8</sub>.

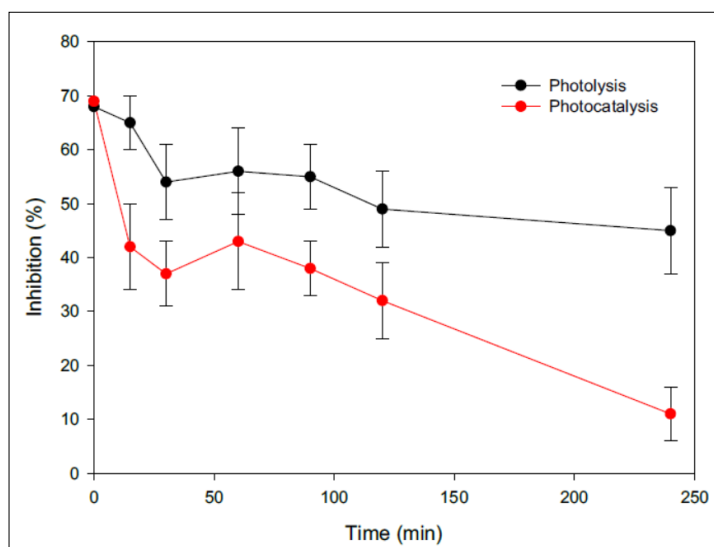


**Figure 4.17.** Evolution of toxicity to *Vibrio fischeri* during the photolytic and photocatalytic experiments with ZnO and plasticizer and preservative under solar irradiation. Error bars denote standard deviation.

A decrease in the DOC was observed during photolytic and photocatalytic assays under solar irradiation Figure 4.17. During the photolytic process, the DOC concentration decreased 60% at the end of the photoperiod (240 min), from  $17.3 \pm 6.5 \text{ mg L}^{-1}$  to  $10.3 \pm 7.5 \text{ mg L}^{-1}$ . Furthermore, in the photocatalytic process, the initial DOC level and after the EDs addition was  $16.4 \pm 6.2 \text{ mg L}^{-1}$  decreasing up to  $2.8 \pm 6.3 \text{ mg L}^{-1}$  at the end of the essay. The required time to decrease the 90% of DOC (DT90) was estimated in 184 minutes ( $R > 0,91$ ) (DT50 = 55 min). Despite a decrease was observed during the photoperiod,  $17.1 \pm 5.8\%$  remaining was still present after 240 minutes of irradiation. This percentage could be because of the different reactions (hydroxylation, dehydration and ring openings) that take place during photocatalysis process with the non-degradable organic compounds' generation and the remaining levels of some EDs, for instance phthalates. This lower mineralization level for phthalates is likely because their hydrophobicity and low level of solubility, mainly.



In the same way, the degradation rates of pesticides using ZnO (200 mg L<sup>-1</sup>)/Na<sub>2</sub>S<sub>2</sub>O<sub>8</sub> (250 mg L<sup>-1</sup>) were investigated. The results are shown in Figure 4.18.

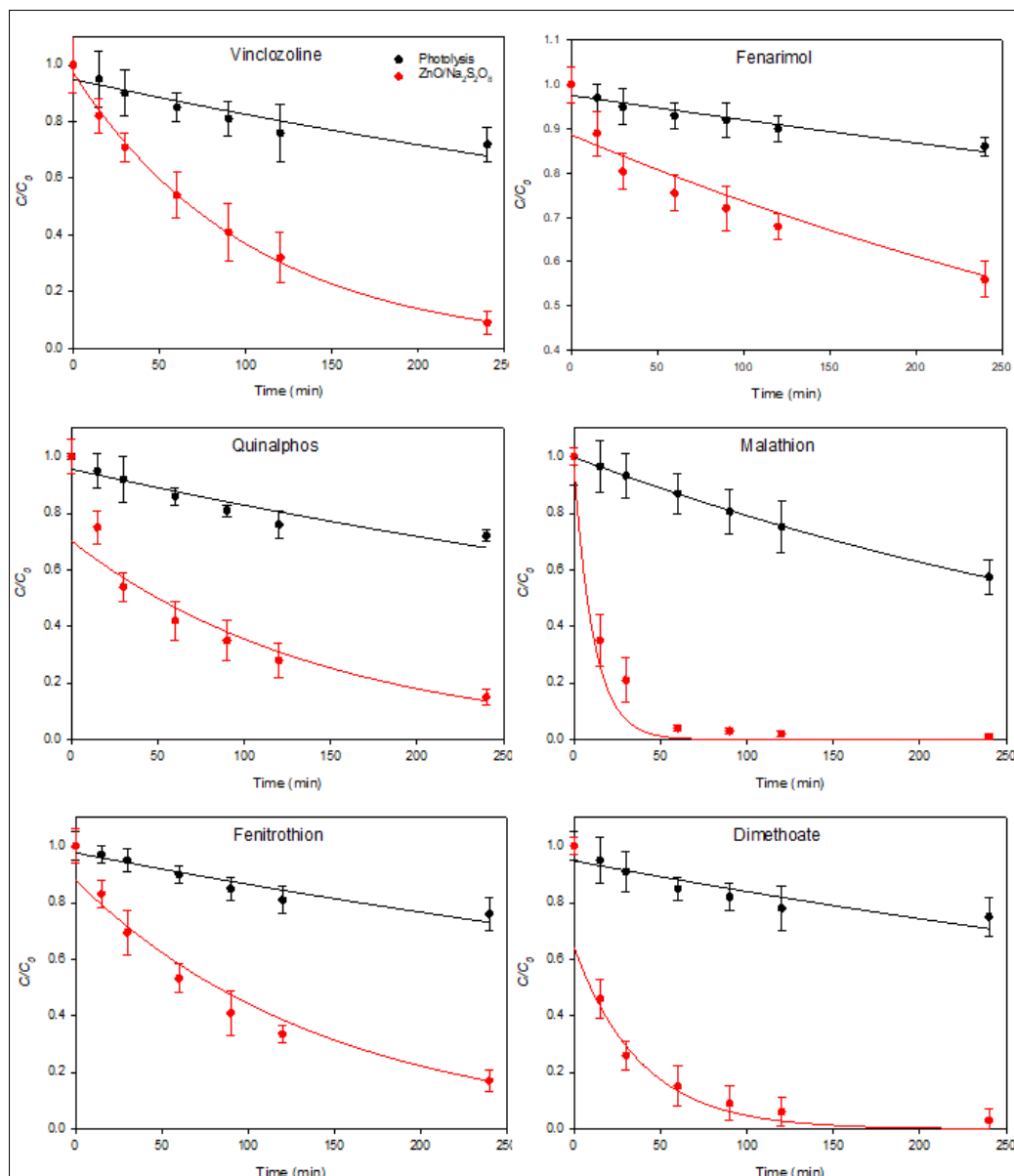


**Figure 4.18.** Evolution of the pesticide residues as a function of sunlight irradiation using the tandem ZnO (200 mg L<sup>-1</sup>)/Na<sub>2</sub>S<sub>2</sub>O<sub>8</sub> (250 mg L<sup>-1</sup>) at pilot plant scale. Error bars denote standard deviation (n=3).

As with plasticizers and preservatives, pesticide degradation rates at 240 min of sun exposure in photolytic tests were significantly lower than those obtained using ZnO/Na<sub>2</sub>S<sub>2</sub>O<sub>8</sub>. The remaining percentages for the pesticides in the photolytic experiment after 240 minutes varied from 57.5 ± 2.0% (MT) and 86.1 ± 6.1% (FR), significantly lower than using ZnO/Na<sub>2</sub>S<sub>2</sub>O<sub>8</sub>. The results for photocatalysis were 7% lower than the initial concentration, except for QP (15.1 ± 3.2%) and FR (56.2 ± 4.1%).

The DOC development in the experiments with pesticides were investigated as well. As it can be seen in Figure 4.19, at the end of the photoperiod, the DOC remaining percentages were 59.6 ± 8.0% and 8.3 ± 7.0% for the photolytic and photocatalytic processes, respectively. In contrast, the electric conductivity (EC) was increased until values of 4.4 dS m<sup>-1</sup>, due to the mineralization and the development of some inorganic ions, mainly SO<sub>4</sub><sup>2-</sup> as S<sub>2</sub>O<sub>8</sub><sup>2-</sup> is transformed into 2 SO<sub>4</sub><sup>2-</sup> during the photocatalytic process.

As in the experiments with the plasticizers and preservatives, the Zn<sup>+2</sup> levels in the water spiked with pesticides, was increased up to 0.28 ± 0.06 mg L<sup>-1</sup> due to the reaction with the holes ( $\text{ZnO} + 2 \text{h}^+ \rightarrow \text{Zn}^{2+} + \frac{1}{2}\text{O}_2$ ) and the break of the Zn-O bonds.

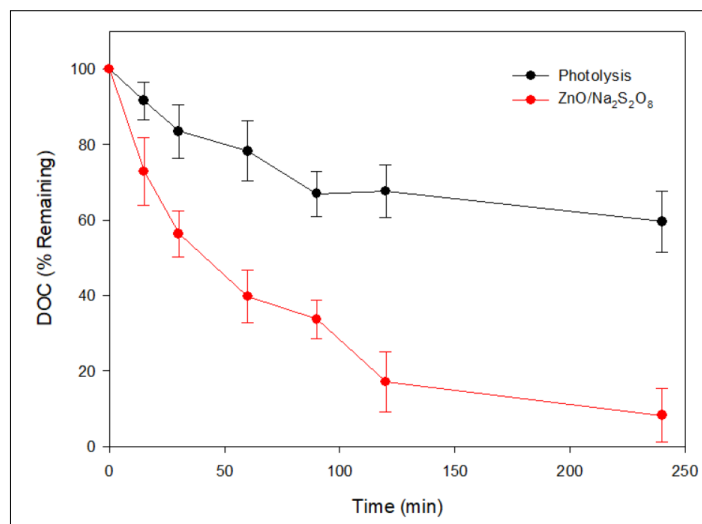


**Figure 4.19.** Evolution of dissolved organic carbon (DOC) during the photolytic and photocatalytic experiments with ZnO and pesticides under natural sunlight irradiation. Error bars denote standard deviation.

The inhibition development of *Vibrio fischeri* during the assays at pilot plant with pesticides were investigated. As it shown in Figure 4.20, the toxicity decreased from the value  $65.7 \pm 8.0\%$  up to a reasonable value of  $12.1 \pm 6.1\%$  at the end of the treatment with  $\text{ZnO}/\text{Na}_2\text{S}_2\text{O}_8$  and of  $68.1 \pm 2.2\%$  to  $48.1 \pm 8.1\%$  in the case of the photolytic experiment.

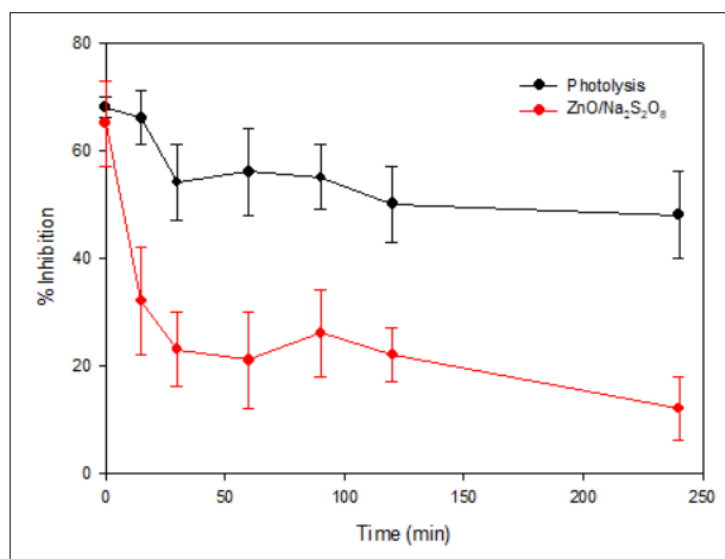


**Figure 4.20.** Evolution of toxicity to *Vibrio fischeri* during the photolytic and photocatalytic experiments with ZnO and pesticides under solar irradiation. Error bars denote standard deviation.

With the aim of studying the degradation kinetic in the photolysis and photocatalytic processes at pilot plant scale, the mathematic calculations were applied, and they are described in Section 3.8 Photocatalytic kinetics. The calculations according Landmuir-Hinchelwood (L-H) in every single one experiment and for each EDs, were conclude with the following kinetic parameters:  $R$ ,  $C/C_0$ ,  $K$  y  $S_{y/x}$ . Besides, the required time to reduce the 50% and the 90% of each compound from water as a consequence of the photodegradation ( $DT_{50}$  y  $DT_{90}$ ) were calculated. To compare the obtained results with different photocatalytic experiments and considering the possible differences among the photocatalytic devices and the irradiation fluctuations  $t_{30W}$  (illumination time normalize) was calculated.

The photolytic and photocatalytic kinetic results using in tandem ZnO/Na<sub>2</sub>S<sub>2</sub>O<sub>8</sub> for plasticizers and preservatives are shown in Tables 4.3 and 4.4, respectively. The Tables 4.5 and 4.6 show the kinetic results for the pesticides under the same conditions, photolysis and ZnO/Na<sub>2</sub>S<sub>2</sub>O<sub>8</sub>.

In the photolytic experiments with the plasticizers (Table 4.3), in all the cases, the kinetics followed apparent first-order curve, with values of R that varied from 0.8222 and 0.9414 in the case of DP y BP, respectively, with a standard estimation error <0.71, in the most unfavourable case. The required time to reduce 50% (DT50) the initial spiked concentration varied from 193 to 462 min ( $t_{30W}$  = 15 - 37 min) for BB y MP, respectively. The DT90 varied from 640 to 1535 min ( $t_{30W}$  = 51 - 123 min), for the same compounds.

**Table 4.3.** First order kinetic parameters (n=3) and normalized illumination time for 50% and 90% degradation calculated for the photolytic degradation of the plasticizers and preservatives under natural sunlight irradiation without photocatalyzer/oxidant.

Plasticizers and preservatives	Photolysis					
	R	C/C <sub>0</sub>	K (min <sup>-1</sup> )	S <sub>y/x</sub> <sup>a</sup>	DT <sub>50</sub> (min) <sup>b</sup>	DT <sub>90</sub> (min) <sup>b</sup>
Methyl p-hydroxybenzoate	0.8987**	0.95***	0.0015**	0.04	462 (37)	1535 (123)
Ethyl 4-hydroxybenzoate	0.9185**	0.96***	0.0023**	0.51	301 (25)	1001 (83)
Bisphenol A	0.9238**	0.92***	0.0036**	0.71	193 (15)	640 (51)
Bisphenol B	0.9030**	0.93***	0.0034**	0.08	204 (16)	677 (54)
Butyl benzylphthalate	0.9414***	0.98***	0.0016***	0.03	433 (36)	1439 (118)
Diamyl phphatalate	0.8222**	0.95***	0.0018**	0.64	385 (33)	1279 (109)

<sup>a</sup> S<sub>y/x</sub>: Standard error of estimate; \*\* ( $p < 0.05$ ); \*\*\* ( $p < 0.001$ ).

<sup>b</sup> In parentheses are the time required for 50% and 90% degradation referred to  $t_{30W}$ .

Similarly, the photocatalytic experiments with ZnO for all the plasticizers and preservatives (Table 4.4) revealed the disappearance kinetics followed an apparent first-order curve, in which R varied from 0.8440 and 0.9731 for DP and BP, respectively, and (S<sub>y/x</sub>) < 0.19 in the most unfavourable case. The required time

to reduce the 50% (DT50) of the initial contamination levels varied from 6 and 112 min ( $t_{30W} = 0 - 27$  min) for BB y BP, respectively, and the DT90 varied from 19 and 371 min ( $t_{30W} = 1 - 27$  min) for the same compounds. The rate constants presented the following order  $BB \approx BA > MP \approx EP > DP > BP$ .

**Table 4.4.** First order kinetic parameters (n=3) and normalized illumination time for 50% and 90% degradation calculated for the photocatalytic degradation of the plasticizers and preservatives under natural sunlight irradiation using ZnO/Na<sub>2</sub>S<sub>2</sub>O<sub>8</sub>.

Plasticizers and preservatives	ZnO					
	R	C/C <sub>0</sub>	K (min <sup>-1</sup> )	S <sub>y/x</sub> <sup>a</sup>	DT <sub>50</sub> (min) <sup>b</sup>	DT <sub>90</sub> (min) <sup>b</sup>
Methyl p-hydroxybenzoate	0.8440**	0.71***	0.0219***	0.19	32 (2)	105 (6)
Ethyl 4-hydroxybenzoate	0.9087**	0.75***	0.0207***	0.16	33 (2)	111 (6)
Bisphenol A	0.9182***	0.97***	0.0896***	0.14	8 (0)	26 (1)
Bisphenol B	0.9346***	0.99***	0.1210***	0.13	6 (0)	19 (1)
Butyl benzylphthalate	0.9731***	0.90***	0.0062***	0.06	112 (8)	371 (27)
Diamyl phphatalate	0.9387***	0.88***	0.0077***	0.10	90 (6)	299 (20)

<sup>a</sup> S<sub>y/x</sub>: Standard error of estimate; \*\* ( $p < 0.05$ ); \*\*\* ( $p < 0.001$ ).

<sup>b</sup> In parentheses are the time required for 50% and 90% degradation referred to  $t_{30W}$ .

The Table 4.5 shows the pesticides photolytic kinetics parameters. The disappearance kinetics follow, as well, an apparent first-order curve, with R that varies from 0.8312 and 0.9996 for DT y MT, respectively, and an estimated standard error (S<sub>y/x</sub>) < 0.04, in the most unfavourable case. The required time to reduce the 50% (DT50) of the initial concentrations oscillated from 301 and 1155 min ( $t_{30W} = 22 - 95$  min) for MT y FR, respectively, while the DT90 varied from 1001 and 3838 min ( $t_{30W} = 74 - 315$  min) for the same compounds.

**Table 4.5.** First order kinetic parameters (n=3) and normalized illumination time for 50% and 90% degradation calculated for the photolytic degradation of the pesticides under natural sunlight irradiation without photocatalyzer/oxidant.

Pesticides	Photolysis					
	R	C/C <sub>0</sub>	K (min <sup>-1</sup> )	S <sub>y/x</sub> <sup>a</sup>	DT <sub>50</sub> (min) <sup>b</sup>	DT <sub>90</sub> (min) <sup>b</sup>
Vinclozoline	0.8688***	0.95***	0.0014**	0.04	495 (39)	1645 (130)
Fenarimol	0.9172***	0.98***	0.0006***	0.01	455 (95)	3838 (315)
Quinalphos	0.8822***	0.96***	0.0014**	0.04	495 (38)	1645 (127)
Malathion	0.9996***	0.91***	0.0023***	0.01	301 (22)	1001 (74)
Fenitrothion	0.9221***	0.98***	0.0012***	0.03	578 (45)	1919 (150)
Dimethoate	0.8312***	0.95***	0.0012**	0.04	578 (46)	1919 (151)

<sup>a</sup> S<sub>y/x</sub>: Standard error of estimate; \*\* (p<0.05); \*\*\* (p<0.001).

<sup>b</sup> In parentheses are the time required for 50% and 90% degradation referred to t<sub>30W</sub>.

In the case of pesticides, the disappearance kinetics followed an apparent first-order curve in the photocatalytic experiments (Table 4.6). The R oscillated from 0.8312 and 0.9996 for DT and MT, respectively, and an estimated standard error (S<sub>y/x</sub>) < 0.04. The required time to reduce the 50% (DT50) of the initial concentrations varied from 8 and 301 min (t<sub>30W</sub> = 1 – 23 min) for MT y FR, respectively, while the DT90 varied from 26 and 1001 (t<sub>30W</sub> = 2 - 75 min) for the same compounds. The order of constant rates were: MT > DT > VZ ≈ QP > FT > FR.

**Table 4.6.** First order kinetic parameters (n=3) and normalized illumination time for 50% and 90% degradation calculated for the photocatalytic degradation of the pesticides under natural sunlight irradiation using ZnO/Na<sub>2</sub>S<sub>2</sub>O<sub>8</sub>.

Pesticides	ZnO					
	R	C/C <sub>0</sub>	K (min <sup>-1</sup> )	S <sub>y/x</sub> <sup>a</sup>	DT <sub>50</sub> (min) <sup>b</sup>	DT <sub>90</sub> (min) <sup>b</sup>
Vinclozoline	0.9981**	0.97***	0.0097***	0.02	71 (4)	237 (14)
Fenarimol	0.9030***	0.91***	0.0023**	0.06	301 (23)	1001 (75)
Quinalphos	0.9242***	0.83***	0.0092**	0.12	75 (3)	250 (11)
Malathion	0.9063***	0.96**	0.0872**	0.15	8 (1)	26 (2)
Fenitrothion	0.9791***	0.93***	0.0082***	0.07	85 (4)	28 (15)
Dimethoate	0.9086***	0.83**	0.0297**	0.16	23 (1)	78 (3)

<sup>a</sup> S<sub>y/x</sub>: Standard error of estimate; \*\* (p<0.05); \*\*\* (p<0.001).

<sup>b</sup> In parentheses are the time required for 50% and 90% degradation referred to t<sub>30W</sub>.

#### 4.4.2. Solar photocatalytic experiments with TiO<sub>2</sub>

Once the optimal operating parameters were determined at laboratory scale during the different experiments performed with TiO<sub>2</sub>, the photodegradation essays were carried out at pilot plant scale, under solar irradiation and in presence of TiO<sub>2</sub> vlp 7000 y TiO<sub>2</sub> P25 [Vela et al., 2018b, 2018c]. The operating conditions are described in Section 3.7 Experimental Setup of Solar Photocatalytic Trial. The EDs photodegradation for plasticizers and preservatives, as a function of time, using in tandem TiO<sub>2</sub> (200 mg L<sup>-1</sup>)/Na<sub>2</sub>S<sub>2</sub>O<sub>8</sub> (250 mg L<sup>-1</sup>) are shown in Figure 4.21.

For the plasticizers and preservatives assays, the initial concentrations at the beginning of the experiment varied from 0.27 to 0.33 mg L<sup>-1</sup> for BP and MP, respectively. Under solar irradiation, the EDs were degraded slowly in the photolytic test in comparison with the results obtain using TiO<sub>2</sub>.

As it can be seen in Figure 4.21, el TiO<sub>2</sub> P25 developed higher degradation rate than TiO<sub>2</sub> vlp 7000 for all the studied compounds. At the end of the photolytic process (240 min), the remaining percentage (media ± RSD) varied from 48.1 ± 5.1% (BB) to 70.3 ± 6.2% (BP). However, the remaining percentages in the photocatalytic processes were significantly ( $p < 0,05$ ) lower, 58.4 ± 6.4% and 0.334 ± 0.003% for BP and BB, respectively, in the case of TiO<sub>2</sub> vlp 7000 ,and 34.1 ± 5.2 and 0.191 ± 0.002% for the same compounds using TiO<sub>2</sub> P25. In both tests the behavior of the three groups were very similar: bisphenols > parabens > phthalates.

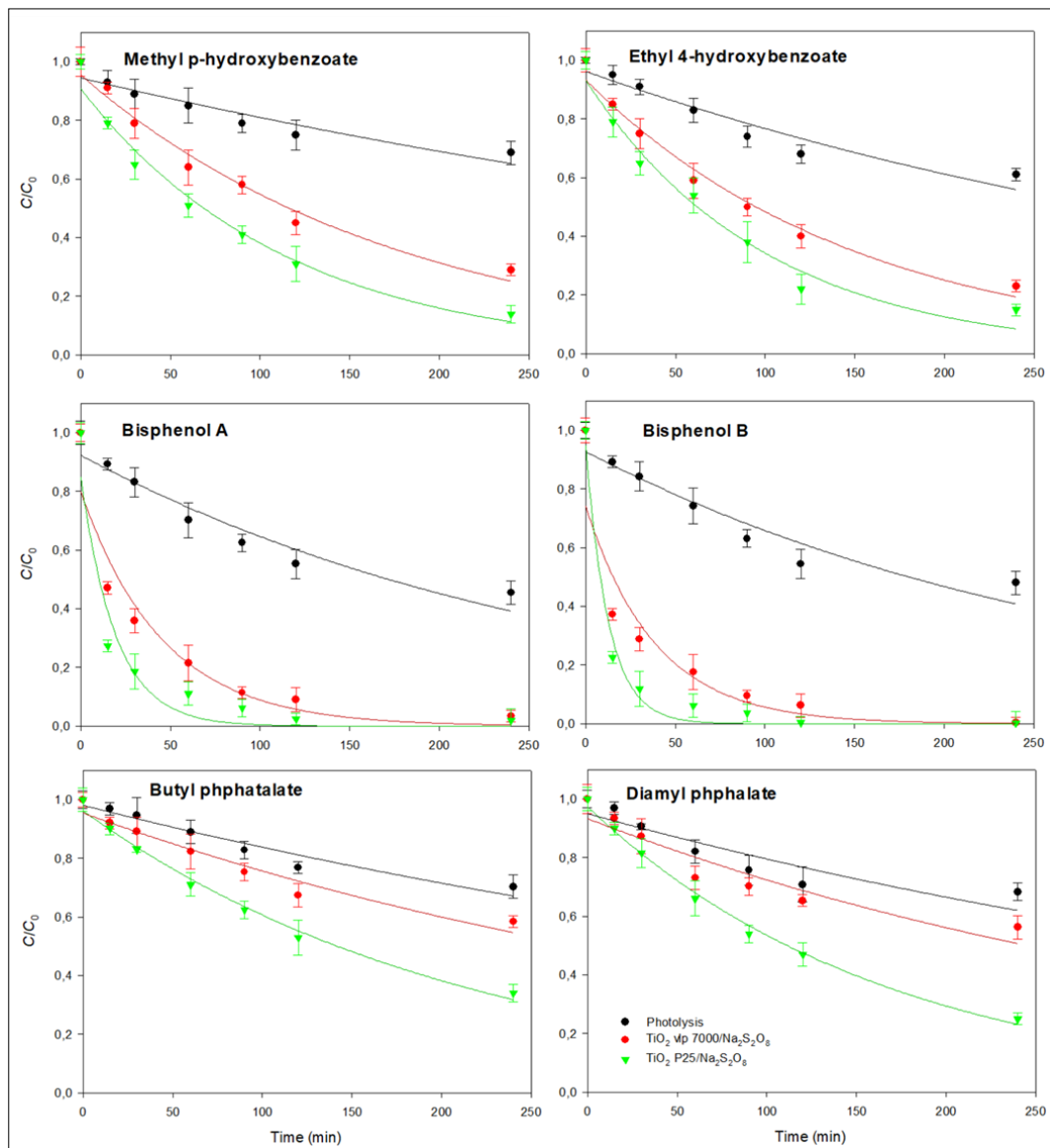


**Figure 4.21.** Evolution of plasticizer and preservative residues as a function of natural sunlight irradiation time using the tandem  $TiO_2$  (200 mg L<sup>-1</sup>)/ $Na_2S_2O_8$  (250 mg L<sup>-1</sup>) at pilot plant scale. Error bars denote standard deviation (n=3).

The DOC development during the experiments with the plasticizers and preservatives was investigated as well. As is shown in Figure 4.22, after the EDs addition, the initial values were  $17.3 \pm 4.5$  mg L<sup>-1</sup>,  $19.6 \pm 3.8$  mg L<sup>-1</sup> and  $18.4 \pm 4.3$



mg L<sup>-1</sup>, for the photolysis, TiO<sub>2</sub> vlp 7000 and TiO<sub>2</sub> P25, respectively. At the end of the photoperiod (240 min), the levels were 10.3 ± 7.5 (59.6%), 7.1 ± 6.1 (36.2%) and 3.2 ± 8.1 (17.4%) mg L<sup>-1</sup> for the photolysis, TiO<sub>2</sub> vlp 7000 and TiO<sub>2</sub> P25, respectively. The required time to reduce 50% the initial DOC was 147 and 82 min for TiO<sub>2</sub> vlp 7000 and el TiO<sub>2</sub> P25, respectively.

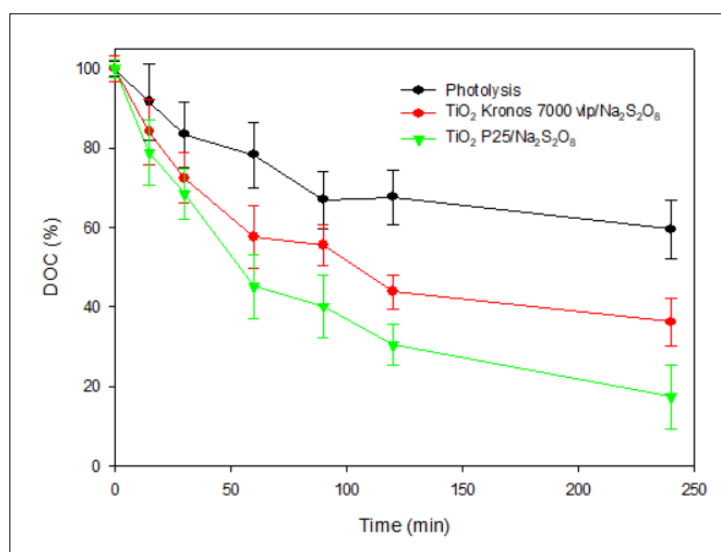


Figure 4.22. Evolution of dissolved organic carbon (DOC) during the photolytic and photocatalytic experiments with TiO<sub>2</sub> and plasticizer and preservative under natural sunlight irradiation. Error bars denote standard deviation.

The results show the mineralization was not completed after the 240 min of irradiation, probably, due to the generation of hydroxylates, alkylate intermediates and residual concentrations of parabens (MP and EP) and phthalates (BP and DP).

On the other hand, as the photodegradation was in progress, it was observed a slight pH decrease (0.4 units), probably in connection with the H<sup>+</sup> production generated because of the presence of S<sub>2</sub>O<sub>8</sub><sup>=</sup> in water (S<sub>2</sub>O<sub>8</sub><sup>=</sup> + H<sub>2</sub>O → OH<sup>•</sup> + H<sup>+</sup>). Parallely to the observed DOC, the EC increased slightly up to 4.4 dS m<sup>-1</sup>, possibly due to the mineralization of some inorganic ions, for instance the S<sub>2</sub>O<sub>8</sub><sup>=</sup>.

It is important to remark, the inorganic ions and DOC play a crucial role in the photocatalytic efficiency. In this study, the water effluent presented high levels of ions such as  $\text{Cl}^-$  ( $464 \text{ mg L}^{-1}$ ),  $\text{SO}_4^{2-}$  ( $485 \text{ mg L}^{-1}$ ),  $\text{NO}_3^-$  ( $9 \text{ mg L}^{-1}$ ),  $\text{Ca}^{2+}$  ( $263 \text{ mg L}^{-1}$ ),  $\text{Mg}^{2+}$  ( $106 \text{ mg L}^{-1}$ ) and  $\text{Na}^+$  ( $694 \text{ mg L}^{-1}$ ) and DOC ( $11 \text{ mg L}^{-1}$ ) (Table 3.2). Depending on the pH of the solution, some dissolved ions can affect the photodegradation rate of several contaminants due to their high superficial adsorption and the tendency of trapping  $\text{h}^+/\text{OH}^\bullet$  [Ahmed et al., 2011]. However, it was observed a weak impact from the ions during the EDs elimination from the water effluent as the DOC presence, mainly macromolecules whose molecular weight were  $> 4,5 \text{ kDa}$ , play more important role than the ions in the inhibition process [Zhang et al., 2012]. The  $\text{Ti}^{4+}$  concentration level dissolved after 240 min of irradiation varied from  $1.2 \pm 0.5 \text{ mg L}^{-1}$  and  $5.4 \pm 1.9 \text{ mg L}^{-1}$  for  $\text{TiO}_2$  P25 and  $\text{TiO}_2$  vlp 7000, respectively. These values were within tolerance levels for *Vibrio fischeri* [Heinlaan et al., 2008].

The inhibition of *Vibrio fischeri* during the photolytic and photocatalytic experiments for the plasticizers and pesticides using  $\text{TiO}_2$  are shown in Figure 4.23.

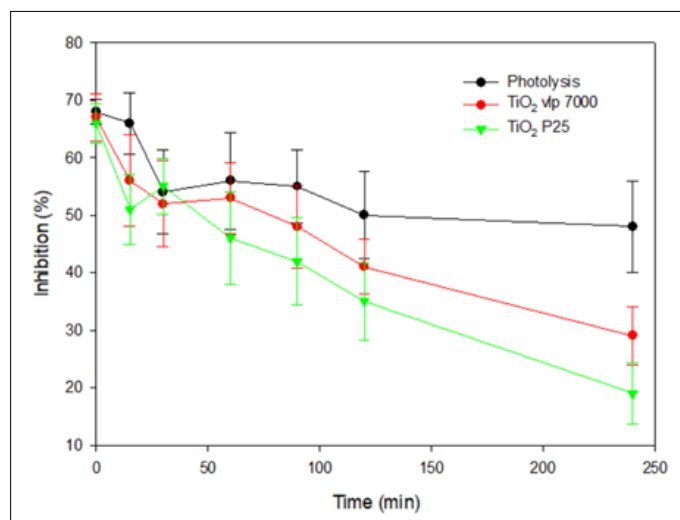


Figure 4.23. Evolution of toxicity to *Vibrio fischeri* during the photolytic and photocatalytic experiments with  $\text{TiO}_2$  and plasticizer and preservative under solar irradiation. Error bars denote standard deviation.

The toxicity decreased from  $67.0 \pm 7.3\%$  (initial value) to  $48.4 \pm 8.3\%$  in photolysis test, and to  $29.3 \pm 5.1\%$  ( $\text{TiO}_2$  vlp 7000) and  $19.2 \pm 5.3\%$  ( $\text{TiO}_2$  P25) at the end of the photoperiod with semiconductors. A light increased was observed after 30 min in the case of  $\text{TiO}_2$  P25, this event could be in connection with intermediates even more toxic than the original compounds. At the end of the treatments, the toxicity decreased up to acceptable values using  $\text{TiO}_2$  P25.

On the other hand, the pesticides photodegradation as a function of solar irradiation, using in tandem  $\text{TiO}_2$  ( $200 \text{ mg L}^{-1}$ )/ $\text{Na}_2\text{S}_2\text{O}_8$  ( $250 \text{ mg L}^{-1}$ ) are shown in Figure 4.24.

The initial concentrations levels varied from  $0.26 \text{ mg L}^{-1}$  (VZ) to  $0.35 \text{ mg L}^{-1}$  (MT). Under solar irradiation and in the photolytic test, the pesticides degradation rates were slower than the results obtained in the photocatalytic process, as it was.  $\text{TiO}_2$  vlp 7000 showed lower degradation rates than  $\text{TiO}_2$  P25 for all the studied compounds. At the end of the photolytic experiment (240 min), only near the 25% of the initial concentration level was reduced ( $73.2 \pm 9.1\%$ ). However, during the photocatalysis the remaining were significantly lower ( $33.2 \pm 25.3\%$  and  $25.1 \pm 24.5\%$  for  $\text{TiO}_2$  vlp 7000 and  $\text{TiO}_2$  P25, respectively).

The results show three different behaviors. MT was the compound with the highest degradation rate as it was degraded completely in presence of  $\text{TiO}_2$  P25 and the remaining percentage rate was  $7.9 \pm 3.2\%$  for  $\text{TiO}_2$  vlp 7000, while the percentages for FR were  $67 \pm 5.2\%$  and  $55 \pm 7.6\%$   $\text{TiO}_2$  vlp 7000 and  $\text{TiO}_2$  P25, respectively. For the rest of the pesticides the remaining percentages (average values) were  $29.2 \pm 10.2\%$  and  $20 \pm 8.4\%$  for  $\text{TiO}_2$  vlp 7000 and  $\text{TiO}_2$  P25, respectively.

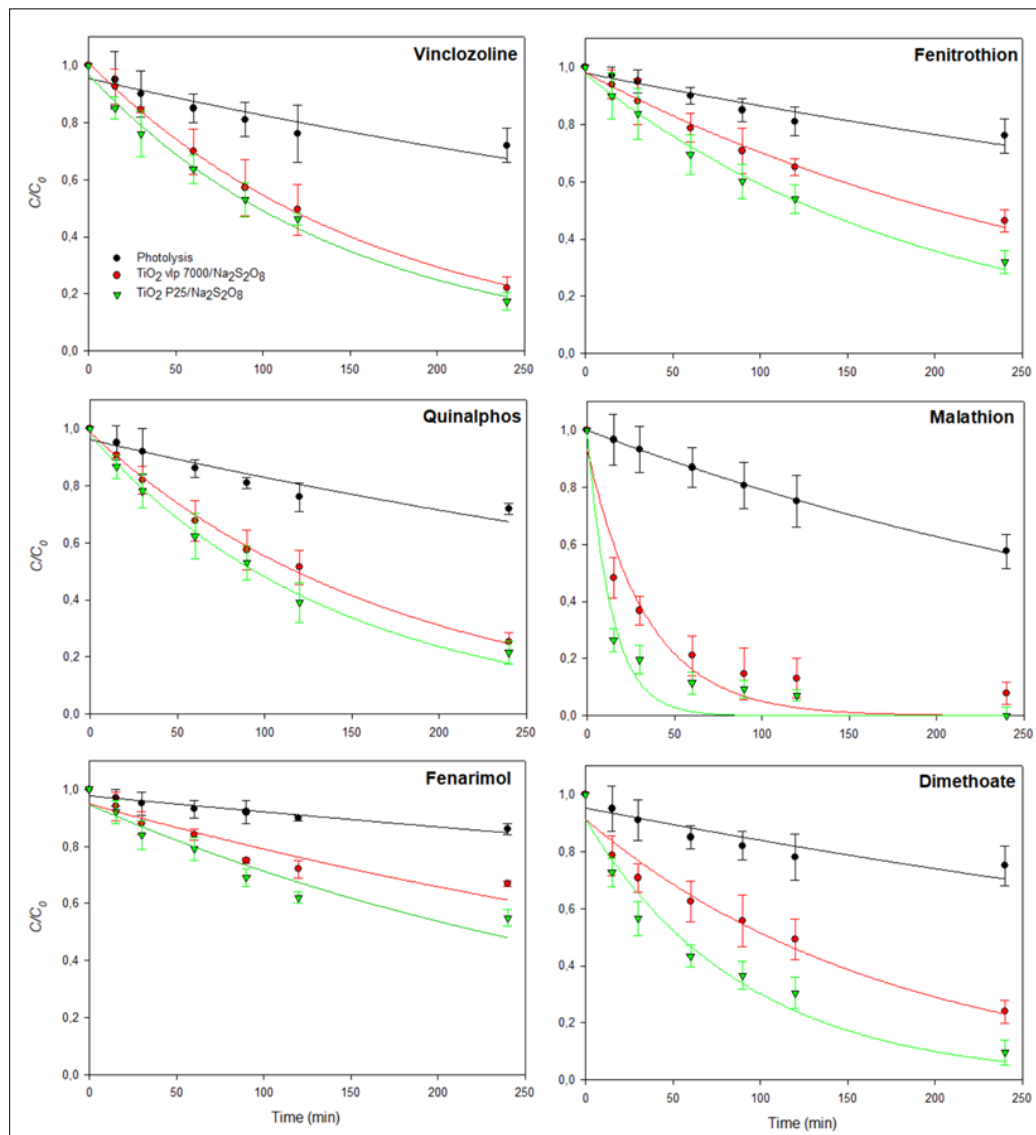


**Figure 4.24.** Evolution of pesticides residues as a function of natural sunlight irradiation time using the tandem  $\text{TiO}_2$  (200 mg  $\text{L}^{-1}$ )/ $\text{Na}_2\text{S}_2\text{O}_8$  (250 mg  $\text{L}^{-1}$ ) at pilot plant scale. Error bars denote standard deviation ( $n=3$ ).

The Figure 4.25 shows dissolved organic carbon (DOC) development during the photolytic and photocatalytic processes in presence of  $\text{TiO}_2$ . The concentration range after the addition of the pesticides was  $16.5 \pm 0.7$  mg  $\text{L}^{-1}$ . At the end of the photoperiod the concentration levels were  $10.3 \pm 2.1$  mg  $\text{L}^{-1}$  (60%),  $4.0 \pm 1.1$  mg  $\text{L}^{-1}$

(24%) and  $2.5 \pm 0.7 \text{ mg L}^{-1}$  (16%) , for the photolysis,  $\text{TiO}_2$  vlp 7000 and  $\text{TiO}_2$  P25, respectively. As can be observed, the mineralization was not completed after the 240 min of irradiation, possibly due to recalcitrant intermediates formed during the experiment.

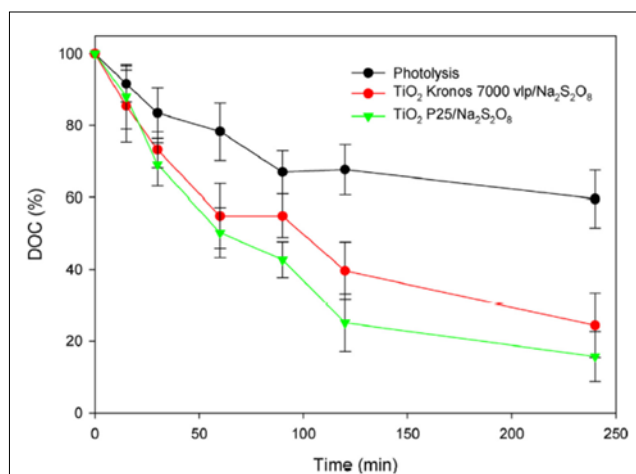


**Figure 4.25.** Evolution of dissolved organic carbon (DOC) during the photolytic and photocatalytic experiments with  $\text{TiO}_2$  and pesticides under natural sunlight irradiation. Error bars denote standard deviation.

As it was observed in the treatments using  $\text{ZnO}$ , as the photodegradation developed there was a pH light decrease ( $< 0.6$  units), mainly in connection with the generated  $\text{H}^+$  due to the presence of  $\text{S}_2\text{O}_8^=$  in water ( $\text{S}_2\text{O}_8^= + \text{H}_2\text{O} \rightarrow \text{OH}^\bullet + \text{H}^+$ ). Parallely to the DOC decrease, the EC increased up to  $4.2 \text{ dS m}^{-1}$ , because of the mineralization and the development of some inorganic ions, for example  $\text{SO}_4^=$ . On the other hand, the obtained oxidation-reduction potential (ORP) increased constantly from 210 mV (initial test) to 315 mV at the end of the experiment which means, the oxidation level was increased during the treatment using  $\text{TiO}_2$  P25. The  $\text{O}_2$  dissolved level was maintained in the average  $6 - 10 \text{ mg L}^{-1}$ .

Furthermore, a slight increase in the levels of  $\text{Cl}^-$  ( $679$  to  $714 \text{ mg L}^{-1}$  and  $699$  to  $796 \text{ mg L}^{-1}$ , for  $\text{TiO}_2$  vlp 7000 and  $\text{TiO}_2$  P25, respectively) and  $\text{NO}_3^-$  ( $9$  to  $19$  and  $9$  to  $20 \text{ mg L}^{-1}$ ,  $\text{TiO}_2$  vlp 7000 and  $\text{TiO}_2$  P25, respectively) were detected after 240 minutes of irradiation, mainly due to the mineralization process, as the dissolved

ions and the organic compounds could have affected the pesticide degradation rates because of their adsorption on the catalyst surface [Ahmed et al., 2011].

The  $\text{SO}_4^-$  levels were increased as well from 648 to 711  $\text{mg L}^{-1}$  ( $\text{TiO}_2$  vlp 7000) and 696 to 785  $\text{mg L}^{-1}$  ( $\text{TiO}_2$  P25) due to the  $\text{S}_2\text{O}_8^-$  transformation into 2  $\text{SO}_4^-$  during the process. Some authors suggested an inhibition effect ( $\text{SO}_4^- < \text{NO}_3^- < \text{Cl}^-$ ) during the photodegradation of some pesticides. This effect could be explained because of the competition of these ions for the active sites on the  $\text{TiO}_2$  catalyst surface, reducing, this way the reaction [Mahmoodih et al., 2007].

In terms of  $\text{PO}_4^{3-}$ , no significant differences were detected in their levels (about 5.2  $\text{mg L}^{-1}$ ) during the photocatalytic experiments.

Similarly, the concentration levels for  $\text{Na}^+$  ( $726 \pm 21 \text{ mg L}^{-1}$ ),  $\text{K}^+$  ( $44 \pm 1 \text{ mg L}^{-1}$ ),  $\text{Ca}^{2+}$  ( $248 \pm 6 \text{ mg L}^{-1}$ ) and  $\text{Mg}^{2+}$  ( $103 \pm 1 \text{ mg L}^{-1}$ ) did not show significant differences during the process.

On the other hand, the dissolved concentration level for  $\text{Ti}^{4+}$  at the end of the assays (240 min) was lower than  $6.1 \pm 1.3 \text{ } \mu\text{g L}^{-1}$  for both photocatalytic assays. However, according to Heilaan et al. (2008),  $\text{TiO}_2$  bulk nanoparticles colloidal suspensions are no-toxic for *Vibrio fischeri* even at 20  $\text{g L}^{-1}$ .

Figure 4.26 show inhibition development for *Vibrio fischeri* for the two  $\text{TiO}_2$  used in this study.

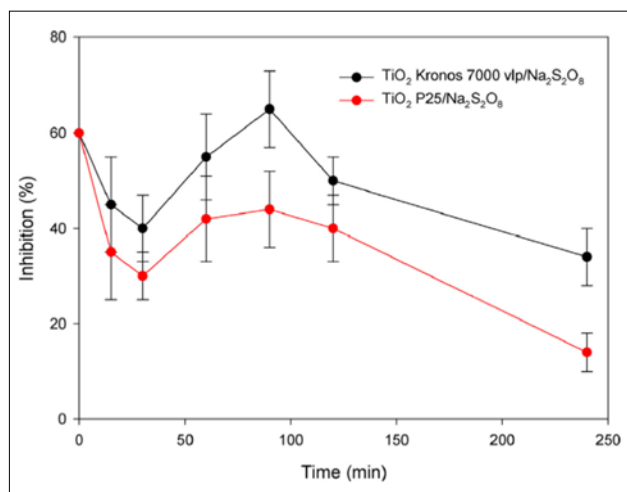


**Figure 4.26.** Evolution of toxicity to *Vibrio fischeri* during the photolytic and photocatalytic experiments with  $\text{TiO}_2$  and pesticides under solar irradiation. Error bars denote standard deviation.

As can be seen, the toxicity decreased from 60% (initial value) to  $15.3 \pm 4.4\%$  and  $27.1 \pm 6.3\%$  at the end of the treatments with TiO<sub>2</sub> P25 and TiO<sub>2</sub> vlp 7000, respectively. In both cases, it was observed an increased even until 90 minutes. Probably, due to the stable intermediates generated during the early stages of the process. At the end of the process the toxicity decreased until acceptable values for TiO<sub>2</sub> P25.

On the other hand, with the aim of studying the photolytic and photocatalytic degradation rates at pilot plant scale using TiO<sub>2</sub> the suitable kinetics models were applied according the procedures described in Section 3.8 Photocatalytic kinetics. The Landmuir-Hinchelwood (L-H) model for the assays developed were used for each EDs and the following kinetic parameters were calculated: R, C/C<sub>0</sub>, K y S<sub>y/x</sub>.

Besides, the required time to reduce the 50% and the 90% of each contaminant from water due to the photodegradation was calculated (DT<sub>50</sub> y DT<sub>90</sub>). As in previous cases, to compare the obtained results in the different assays with other photocatalytic experiments and because of the differences among the devices and irradiation fluctuations  $t_{30W}$  was calculated.

The Tables 4.7 and 4.8 show the kinetic parameters for the assays with plasticizers and preservatives in presence of TiO<sub>2</sub> vlp 7000 and TiO<sub>2</sub> P25, respectively. The Tables 4.9 and 4.10 show the results for the samples with pesticides using TiO<sub>2</sub> vlp 7000 and TiO<sub>2</sub> P25, respectively. The Tables 4.3 and 4.5, included in the previous section, show the adjustments undertaken in the photolytic experiments.

In the case of the plasticizers and preservatives, all the compounds follow a pseudo-first order degradation rate, with values of R that vary from 0.8382 (BA using TiO<sub>2</sub> P25) to 0.9947 (DP using TiO<sub>2</sub> P25). The estimated standard error (S<sub>y/x</sub>) was < 0.20 in the most unfavorable case (BA with TiO<sub>2</sub> P25). The lower degradation rate was observed for all the compounds in the photolytic process, the results are shown in Table 4.3.

According to the rate constants calculated (min<sup>-1</sup>) there were significant differences ( $p < 0,05$ ) in the photocatalytic efficiency. The highest degradation rate was observed, in all the cases, with TiO<sub>2</sub> P25. The rate constant (as the average for all EDs constants) for TiO<sub>2</sub> P25 was near 3 values higher than for TiO<sub>2</sub> vlp 7000 ( $K_{P25} \approx 2.7 \times K_{vlp\ 7000}$ ). The average rate constant was ( $n = 6$ )  $0.0108 \pm 0.0103$  min<sup>-1</sup> and

$0.0267 \pm 0.0312 \text{ min}^{-1}$  in all the experiments with  $\text{TiO}_2$  vlp 7000 and  $\text{TiO}_2$  P25, respectively.

**Table 4.7.** First order kinetic parameters (n=3) and normalized illumination time for 50% and 90% degradation calculated for the photocatalytic degradation of the plasticizers and preservatives under natural sunlight irradiation using  $\text{TiO}_2$  vlp 7000.

Plasticizers and preservatives	$\text{TiO}_2$ vlp 7000					
	R	$C/C_0$	$K$ ( $\text{min}^{-1}$ )	$S_{y/x}$ <sup>a</sup>	DT <sub>50</sub> (min) <sup>b</sup>	DT <sub>90</sub> (min) <sup>b</sup>
Methyl p-hydroxybenzoate	0.9777***	0.95***	0.0056***	0.06	124 (9)	411 (30)
Ethyl 4-hydroxybenzoate	0.9814***	0.93***	0.0066***	0.06	105 (8)	349 (25)
Bisphenol A	0.9242***	0.80***	0.0220**	0.15	32 (2)	105 (6)
Bisphenol B	0.9220***	0.74**	0.0257*	0.17	27 (1)	90 (5)
Butyl benzylphthalate	0.9497***	0.95***	0.0023***	0.04	301 (24)	1001 (79)
Diamyl phphatalate	0.8867***	0.93***	0.0025**	0.07	277 (22)	921 (74)

<sup>a</sup>  $S_{y/x}$ : Standard error of estimate; \* ( $p < 0.01$ ); \*\* ( $p < 0.05$ ); \*\*\* ( $p < 0.001$ ).

<sup>b</sup> In parentheses are the time required for 50% and 90% degradation referred to  $t_{30W}$ .

The degradation rates, in all the cases, were  $\text{BB} \approx \text{BA} > \text{MP} \approx \text{EP} > \text{DP} > \text{BP}$ , as in ZnO experiments. The average rate constants for the parabens (MP and EP), bisphenols (BA and BB) and phthalates (BP y DP), in the tandem  $\text{TiO}_2$  vlp 7000/ $\text{Na}_2\text{S}_2\text{O}_8$  were  $0.0061 \pm 0,0007 \text{ min}^{-1}$  (parabens),  $0,0239 \pm 0,0026 \text{ min}^{-1}$  (bisphenols) and  $0,0024 \pm 0,0001 \text{ min}^{-1}$  (phthalates), while for  $\text{TiO}_2$  P25/ $\text{Na}_2\text{S}_2\text{O}_8$  were  $0,0094 \pm 0,0009 \text{ min}^{-1}$  (parabens),  $0,0654 \pm 0,0193 \text{ min}^{-1}$  (bisphenols) y  $0,0053 \pm 0,0010 \text{ min}^{-1}$  (phthalates).

In the experiments with  $\text{TiO}_2$  vlp 7000/ $\text{Na}_2\text{S}_2\text{O}_8$ , the required time to reduce 50% (DT50) the initial concentration levels oscillated between 27 and 301 min ( $t_{30W} = 1 - 24$  min) for BB and BP, respectively, while the DT90 varied between 90 and 1001 minutes ( $t_{30W} = 5 - 79$  min) for the same compounds. The results in the experiments with  $\text{TiO}_2$  P25/ $\text{Na}_2\text{S}_2\text{O}_8$  were lower, DT50 between 9 and 151 minutes ( $t_{30W} = 0 - 11$  min), for BB and BP, respectively, while DT90 varied between 29 and 501 minutes ( $t_{30W} = 1 - 37$ ) for the same compounds.



**Table 4.8.** First order kinetic parameters (n=3) and normalized illumination time for 90% degradation calculated for the photocatalytic degradation of the plasticizers and preservatives under natural sunlight irradiation using TiO<sub>2</sub> P25.

Plasticizers and preservatives	TiO <sub>2</sub> P25					
	R	C/C <sub>0</sub>	K (min <sup>-1</sup> )	S <sub>y/x</sub> <sup>a</sup>	DT <sub>50</sub> (min) <sup>b</sup>	DT <sub>90</sub> (min) <sup>b</sup>
Methyl p-hydroxybenzoate	0.9832***	0.91***	0.0087***	0.06	80 (5)	265 (17)
Ethyl 4-hydroxybenzoate	0.9555***	0.93***	0.0100***	0.10	69 (4)	230 (13)
Bisphenol A	0.8382***	0.85**	0.0517*	0.20	13 (1)	45 (2)
Bisphenol B	0.9165***	0.95**	0.0790**	0.15	9 (0)	29 (1)
Butyl benzylphthalate	0.9913***	0.96***	0.0046***	0.03	151 (11)	501 (37)
Diamyl phphatalate	0.9947***	0.97***	0.0060***	0.03	116 (8)	384 (28)

<sup>a</sup> S<sub>y/x</sub>: Standard error of estimate; \* ( $p < 0.01$ ); \*\* ( $p < 0.05$ ); \*\*\* ( $p < 0.001$ ).

<sup>b</sup> In parentheses are the time required for 50% and 90% degradation referred to  $t_{30W}$ .

The Tables 4.9 and 4.10 show the photocatalytic kinetic parameters obtained from pesticides with TiO<sub>2</sub> vlp 7000 and TiO<sub>2</sub> P25, respectively.

**Table 4.9.** First order kinetic parameters (n=3) and normalized illumination time for 50% and 90% degradation calculated for the photocatalytic degradation of the pesticides under natural sunlight irradiation using TiO<sub>2</sub> vlp 7000.

Pesticides	TiO <sub>2</sub> vlp 7000					
	R	C/C <sub>0</sub>	K (min <sup>-1</sup> )	S <sub>y/x</sub> <sup>a</sup>	DT <sub>50</sub> (min) <sup>b</sup>	DT <sub>90</sub> (min) <sup>b</sup>
Vinclozoline	0.9989***	1.01***	0.0062***	0.01	112 (8)	371 (26)
Fenarimol	0.9062**	0.95***	0.0018***	0.04	385 (32)	1270 (108)
Quinalphos	0.9966***	0.99***	0.0058***	0.02	120 (9)	397 (29)
Malathion	0.9286***	0.93***	0.0292**	0.09	24 (2)	79 (6)
Fenitrothion	0.9921***	0.98***	0.0033***	0.02	210 (16)	698 (53)
Dimethoate	0.9540***	0.91***	0.0057***	0.06	122 (9)	404 (30)

<sup>a</sup> S<sub>y/x</sub>: Standard error of estimate; \*\* ( $p < 0.05$ ); \*\*\* ( $p < 0.001$ ).

<sup>b</sup> In parentheses are the time required for 50% and 90% degradation referred to  $t_{30W}$ .

**Table 4.10.** First order kinetic parameters (n=3) and normalized illumination time for 50% and 90% degradation calculated for the photocatalytic degradation of the pesticides under natural sunlight irradiation using TiO<sub>2</sub> P25.

Pesticides	TiO <sub>2</sub> P25					
	R	C/C <sub>0</sub>	K (min <sup>-1</sup> )	S <sub>y/x</sub> <sup>a</sup>	DT <sub>50</sub> (min) <sup>b</sup>	DT <sub>90</sub> (min) <sup>b</sup>
Vinclozoline	0.9915***	0.97***	0.0068***	0.03	102 (10)	339 (23)
Fenarimol	0.9133***	0.95***	0.0028**	0.05	247 (21)	817 (69)
Quinalphos	0.9828***	0.98***	0.0071***	0.03	98 (7)	324 (23)
Malathion	0.9495***	0.99***	0.0711**	0.08	10 (1)	32 (3)
Fenitrothion	0.9926***	0.97***	0.0050***	0.02	139 (10)	461 (35)
Dimethoate	0.9357***	0.91***	0.0111***	0.07	62 (5)	207 (15)

<sup>a</sup> S<sub>y/x</sub>: Standard error of estimate; \*\* ( $p < 0.05$ ); \*\*\* ( $p < 0.001$ ).

<sup>b</sup> In parentheses are the time required for 50% and 90% degradation referred to  $t_{30W}$ .

The degradation rate followed an apparent first-order curve, where R oscillated from 0.9062 and 0.9989 for FR and VZ, respectively (TiO<sub>2</sub> vlp 7000) and 0.9133 and 0.9926 for FR and FT respectively (TiO<sub>2</sub> P25), and the standard error of estimate (S<sub>y/x</sub>) was <0.09, in the most unfavourable case.

The lower degradation rates for all the compounds were observed during the photolytic assay, results are shown in Table 4.5.

The results revealed MT is the compound with the highest rate constant (0.0292 and 0.0711 min<sup>-1</sup> for TiO<sub>2</sub> vlp 7000 and TiO<sub>2</sub> P25, respectively), while FR showed the lowest rate constant (0.0018 and 0.0028 min<sup>-1</sup> for TiO<sub>2</sub> vlp 7000 and TiO<sub>2</sub> P25, respectively). The rate constant (as an average for all the pesticides) for TiO<sub>2</sub> P25 was 2 values higher than TiO<sub>2</sub> vlp 7000 ( $K_{P25} \approx 2 K_{vlp7000}$ ). The rate constants were MT > VZ > DT  $\approx$  QP > FT > FR with TiO<sub>2</sub> vlp 7000 and MT > DT > QP  $\approx$  VZ > FT > FR with TiO<sub>2</sub> P25.

The required time to reduce 50% (DT<sub>50</sub>) the contamination level in the initial samples were between 24 and 385 min ( $t_{30W} = 2 - 32$  min) for MT and FR, respectively, while DT<sub>90</sub> varied between 79 and 1270 ( $t_{30W} = 6 - 108$  min) for the same compounds and with TiO<sub>2</sub> vlp 7000. In the assay with TiO<sub>2</sub> P25, DT<sub>50</sub> varied between 10 and 247 min ( $t_{30W} = 1 - 21$  min) for MT and FR, respectively, and DT<sub>90</sub> oscillated 32 and 817 min ( $t_{30W} = 3 - 69$  min), for the same compounds.

#### 4.4.3. Comparative analysis between the solar photocatalytic assays with ZnO y TiO<sub>2</sub>

With the purpose of comparing the efficiency of the semiconductors used in the different photodegradation treatments under solar irradiation and at pilot plant scale, the rate constants (K) were calculated for each EDs according to the equation of Langmuir-Hinshelwood (L-H) considering the normalized illuminated ( $t_{30w}$ ). In the Table 4.11 are shown the rate constants for each EDs studied.

**Table 4.11.** EDs rate constants obtained in the photocatalytic treatment under solar irradiation.

Compounds	Photocatalyzers		
	ZnO/Na <sub>2</sub> S <sub>2</sub> O <sub>8</sub> Kt <sub>30w</sub> (min <sup>-1</sup> )	TiO <sub>2</sub> vlp 7000/ Na <sub>2</sub> S <sub>2</sub> O <sub>8</sub> Kt <sub>30w</sub> (min <sup>-1</sup> )	TiO <sub>2</sub> P25/Na <sub>2</sub> S <sub>2</sub> O <sub>8</sub> Kt <sub>30w</sub> (min <sup>-1</sup> )
Vinclozoline	0.1674	0.0893	0.0989
Fenarimol	0.0307	0.0214	0.0336
Quinalphos	0.2064	0.0798	0.0994
Malathion	1.1702	0.3629	0.7512
Fenitrothion	0.1578	0.0433	0.0664
Dimethaote	0.8411	0.0764	0.1507
Methyl p- hydroxybenzoate	0.3953	0.0758	0.1320
Ethyl 4- hydroxybenzoate	0.3747	0.0924	0.1720
Bisphenol A	1.7495	0.4011	1.1408
Bisphenol B	2.2683	0.4676	1.5528
Butyl benzylphthalate	0.0851	0.0291	0.0615
Diamyl phphatalate	0.1168	0.0312	0.0828

The average rate constant calculated from the 12 compounds demonstrated the tandem ZnO/Na<sub>2</sub>S<sub>2</sub>O<sub>8</sub> presents the highest photocatalysis efficiency. The average rate constants (n = 12) were  $0.6303 \pm 0.7342$ ,  $0.3618 \pm 0.5055$  and  $0.1475 \pm 0.1620$  min<sup>-1</sup> for ZnO, TiO<sub>2</sub> P25 and TiO<sub>2</sub> vlp 7000, respectively. Which means, the rate constant (as an average for all the EDs) for ZnO was approximately between 1.7 and 4.3 value higher than for the systems TiO<sub>2</sub> P25 and TiO<sub>2</sub> vlp 7000, respectively. As a result, the highest degradation EDs in wastewater treated were: ZnO > TiO<sub>2</sub> P25 > TiO<sub>2</sub> vlp 7000.

The structural and superficial properties characteristic in each semiconductor can be responsible for the different photocatalytic activity for ZnO comparing to TiO<sub>2</sub> [Salah et al., 2004].

TiO<sub>2</sub> has been the photocatalyst commercially available due to its properties (low toxicity, excellent activity, high photochemical stability and reasonable band gap) for which it has been widely study for scientific community [Ohtani et al., 2010; Herrmann, 2012; Vela et al., 2017]. However, the effect of ZnO is less documented and the differences between these two oxides is a present research.

TiO<sub>2</sub> P25 is cheap, photostable in solution and non-toxic but the principal drawback is the impossibility to absorb visible light [Gupta and Tripathi, 2011]. It is important to remark, that on average only the 2.5% of the radiation during the essays belongs to UV (2,33% UVA, 0,15% UVB y 0,02% UVC) and the (97,5%) is VIS and NIR radiation. In order to tackle this disadvantage, different strategies have been developed using visible light to activate TiO<sub>2</sub>, mainly with environmental purposes [Peláez et al., 2012; Fagan et al., 2016]. Dopping TiO<sub>2</sub> has been widely used to reduce the band gap, increasing the light absorption. TiO<sub>2</sub> band gap can be reduced dopping titanium with carbon. The use of this methodology, as in the case of Kronos vlp 7000, allows TiO<sub>2</sub> to use not only UV radiation but also visible light with wavelengths > 400 nm because the low band gap energy 2.4 eV ( $\lambda < 535$  nm). The oxygen substitution for atoms of carbon is responsible of the visible absorption [Goldstein et al., 2008; Gupta and Tripathi, 2011].

However, the results of this study indicated TiO<sub>2</sub> P25 efficiency is higher than TiO<sub>2</sub> vlp 7000. The presence of rutile in TiO<sub>2</sub> P25 Degussa (A: 69.4%; R: 30.6%) can explain the better photocatalytic activity in comparison with TiO<sub>2</sub> vlp 7000 (A: 99.4%; R: 0.6%) and TiO<sub>2</sub> Alfa-Aesar (A: 87.7%; R: 12.3%). As Hurun et al. (2003) mention, rutile absorbs photons and generates the pair electron-hole because electrons are transferred into the anatase phase. Consequently, the recombination effect is reduced, and the holes can be mobilized along the particle surface.

In the same way, ZnO is a really interesting semiconductor due to its direct band gap ( $E_g = 3.3$  eV), high activation energy (60 meV) and piezoelectrical properties. Different facts could justify the high activity level for ZnO, for instance the absorption of more photons. Despite both semiconductors materials present

similar band gap energy, the lower activity for TiO<sub>2</sub> can be explained due to the shorter wavelength needed to activate the catalyst, 380 nm for TiO<sub>2</sub> and 440 nm for ZnO. As a result, the apparent extra rate for ZnO could be because neither ZnO nor TiO<sub>2</sub> absorb all the light received but in the case of ZnO it is absorb even more.

As for the surface area of the semiconductors, ZnO presents a superficial area ( $7 \text{ m}^2 \text{ g}^{-1}$ ) lower and a particle size ( $< 194 \text{ nm}$ ) larger than TiO<sub>2</sub> Kronos vlp 7000 ( $250 \text{ m}^2 \text{ g}^{-1}$ ,  $< 15 \text{ nm}$ ), TiO<sub>2</sub> P25 Degussa ( $55 \text{ m}^2 \text{ g}^{-1}$ ,  $< 15 \text{ nm}$ ) and TiO<sub>2</sub> Alfa-Aesar ( $45 \text{ m}^2 \text{ g}^{-1}$ ,  $< 32 \text{ nm}$ ) (Table 4.2). Nevertheless, presents higher levels of electronic mobility, which implies less charge recombination [Kitsiou et al., 2009].

The reflectance diffuse spectrophotometry UV-DR values, showed the capacity for ZnO to absorb light in the visible region is higher than TiO<sub>2</sub>. Furthermore, the observed differences between ZnO and el TiO<sub>2</sub> are connected with the structure and diameter of the particles and their optical properties. ZnO presents a specific surface ( $7 \text{ m}^2 \text{ g}^{-1}$ ) lower than TiO<sub>2</sub> P25 ( $55 \text{ m}^2 \text{ g}^{-1}$ ). Nevertheless, ZnO shows higher electronic conductivity than TiO<sub>2</sub> [Baxter y Aydil 2006]. Furthermore, stoichiometry drives ZnO mobility at least 2 values higher than TiO<sub>2</sub> achieving recombination rates lower than TiO<sub>2</sub> [Kitsiou et al., 2009].

On the other hand, and in relation to the different EDs degradation rates, the results are consistent with previous reports, for instance the studies with the pesticides triclopyr and daminozid [Qamar et al., 2006], dimetoate, carbaryl, methidathion and oxydemeton-methyl [Vicente et al., 2014] and the pesticides derivated from the spirocyclic acid [Ohtani, 2013] in presence of different titanium TiO<sub>2</sub> P25 and others.

A revision of the bibliography showed BA as one of the most studied EDs due to the high exposure in humans because is used in many industrial processes, for instance the epoxy resins. For this reason, TiO<sub>2</sub> was study to test the efficiency at removing these chemicals from aquatic systems [Reddy et al., 2018].

However, the bibliography for plasticizers and preservatives are scarcely. Velegraki et al., (2015) with the aim of eliminate MP from water, obtained similar results using different commercial nanoparticles of TiO<sub>2</sub> (Aeroxide P-25, Kronos Vlp 7000 and Kronos Vlp 7001) in a photoreactor with a xenon lamp. The study concluded, the Aeroxide of TiO<sub>2</sub> P25 was the optimal catalytic material to photodegrade MP, even in the case of low catalyst dosage. Song et al., (2016)

demonstrated the higher efficiency of diethyl phthalate using UV/H<sub>2</sub>O<sub>2</sub> than UV/TiO<sub>2</sub>. Some noble metals as Ag and el Pd in combination with TiO<sub>2</sub>, showed a decrease superior than 50% of the initial concentration for parabens (methyl-, ethyl-, propil- buthyl- y bencilparaben), after 180 minutos of the reaction [Gomes et al., 2017]. Similarly, the use of dopped TiO<sub>2</sub> with N has demonstrated the efficiency at eliminating EP under solar irradiation [Petala et al., 2015]. In the same line of these results, other studies have indicated the ZnO efficiency at removing BA under UV is higher thanTiO<sub>2</sub> [An et al., 2018] y EP [Frontistis et al., 2017].

#### 4.4.5. Economic assessment for water treatment

Besides the experimental research and the model design, it is convenient to develop economic studies, as they can show an innovative technology in a competitive prize. It is possible to use the different methodologies to estimate the cost in the water treatments, including the final prize (installations, project contingencies, the engineering expenses and future substitutions) as well as the operating expenses (personnel, maintenance, electricity operations and different services), which makes possible to assess the treatment annual economic impact [Gimenez et al., 2015].

On these conditions, a comparison among the treatments using TiO<sub>2</sub> (P25 and vlp 7000) and ZnO, under experimental scale are shown in Table 4.12. Considering Murcia Region (SE of Spain) receives near 3,000 h of solar light per year on average and the useful time (UT) for the pilot plant was estimated 480 min day<sup>-1</sup>, the treatment capacity (TC) in our system was calculated following the equation:

$$TC = UT \times V \times 365 / DT90 \text{ m}^3 \text{ year}^{-1}$$

where V is treated water volume (100 L) and DT90 is the required time (min) to reduce 90% the initial concentration.

**Table 4.12:** Economic assessment for water photocatalytic treatment with ZnO and TiO<sub>2</sub> (P25 and vlp 7000).

	Costs <sup>a</sup>	Photocatalytic Treatment			
		ZnO	TiO <sub>2</sub> P25	TiO <sub>2</sub> vlp 7000	
<b>I</b>	<b>Facility + Project Contingency (€/year)<sup>b</sup></b>	32,694.21	3,269.42	3,269.42	3,269.42
<b>II</b>	<b>Engineering project (€/year)</b>	(10% I)	326.94	326.94	326.94
<b>III</b>	<b>Operation and maintenance (€/year)</b>	(2.5% I + II)	89.91	89.91	89.91
<b>IV</b>	<b>Consumables (€/year)</b>	Unit price			
	Na <sub>2</sub> S <sub>2</sub> O <sub>8</sub>	10 €	584.00	634.78	43.76
	ZnO	30 €	1401.60		
	TiO <sub>2</sub> P25	38 €		1929.74	
	TiO <sub>2</sub> vlp 7000	40 €			1297.78
	Total reagents		1985.60	2564.52	1703.33
<b>V</b>	<b>Service (€/year)</b>	Unit price			
	Rinse water (€/L)	0.0025	292.00	317.39	202.78
	Electricity (€/kW h <sup>-1</sup> )	0.12	648.24	648.24	648.24
	Total service		940.24	965.63	851.02
	Total I+II+III+IV+V		6612.11	7216.42	6240.62
<b>VI</b>	<b>Overheads (€/year)</b>	(10% I+II+III+IV+V)	661.21	721.64	624.06
	Total (I+II+III+IV+V+VI)		7273.32	7938.07	4,994.18
	DT <sub>90</sub> (min)		75	69	108
	TC (m <sup>3</sup> /year)		233.60	253.91	162.22
	Treatment cost (€/m <sup>3</sup> ) <sup>c</sup>		31.14	31.26	42.32
			(40.18)	(39.58)	(55.34)

<sup>a</sup> Personnel cost are not included.

<sup>b</sup> The facility cost (building and civil works, solar collector, deposits, measurement equipment, industrial benefit, etc.) has been calculated on the basis of a 10 years period.

<sup>c</sup> In parentheses is the treatment cost considering only a period of work 240 of days per year.

The results shown Table 4.12 has been calculated for FR, one of the most recalcitrant EDs, using DT<sub>90</sub> and the normalized illumination time obtained during the three solar photodegradative treatments (108, 69 and 75 min for TiO<sub>2</sub> vlp 7000, TiO<sub>2</sub> P25 and ZnO, respectively). As DT<sub>90</sub> values were used, the results can be transfer to other studies.

Considering a work period of 365 days per year, the treatment cost was estimated in 31.14, 31.26 y 42.32 € m<sup>-3</sup> for the photocatalytic process in presence of ZnO, TiO<sub>2</sub> P25 and TiO<sub>2</sub> vlp 7000, respectively. Yet, if only 240 days are considered because of the inclement weather, the cost are incremented in (40.18, 39.59 y 55.34 € m<sup>-3</sup>).

Significant differences were found among the costs of the treatments because the required time to reduce 90% the contaminant loading varied for each contaminant. For instance, the cost estimated to treat one of the most persistent plasticize BP were 18.07, 22.55 and 34.32, € m<sup>-3</sup> in the case of treatments with ZnO, TiO<sub>2</sub> P25 and TiO<sub>2</sub> vlp 7000, respectively. The treatment costs should be compared with other wastewater treatments (physical and chemical treatment, electrochemical processes, or foto-Fenton) to obtain more precise conclusions.



## **V - CONCLUSIONS**



## V - CONCLUSIONS

1. The methodology developed for the determination of residual ED concentrations in wastewater treatment effluents by LL extraction and analysis through GC-MS has been validated and can be considered suitable for detecting residual concentrations of the compounds under study.

2. The characterisation of the treatment plant effluents used in the solar photocatalysis experiments has shown that the main physical-chemical parameters analysed comply with the requirements of current legislation.

3. The characterisation of the semiconductors used in this study has revealed that the content of the anatase (A) and rutile (R) phases in Degussa P25 TiO<sub>2</sub> powder is 69.4A:30.6R, in Alpha Aesar TiO<sub>2</sub> is 87.7A:12.3R, while 7000 vlp TiO<sub>2</sub> crystallises mainly in the anatase phase (99.4A:0.6R). The ZnO has a hexagonal wurtzite structure. ZnO nanoparticles are predominantly smaller than 200 nm in diameter with a hexagonal structure, while TiO<sub>2</sub> vlp 7000, TiO<sub>2</sub> P25 Degussa and TiO<sub>2</sub> Alpha Aesar are much smaller. In relation to BET, ZnO has a lower surface area and a larger particle size than TiO<sub>2</sub> Kronos vlp 7000, TiO<sub>2</sub> P25 Degussa and TiO<sub>2</sub> Alpha-Aesar. The band-gap energy values calculated for the various semiconductors show that Kronos vlp 7000 TiO<sub>2</sub> has a lower band-gap energy than the other semiconductors studied.

4. Photocatalysis experiments under laboratory conditions carried out in the photoreactor, for a load for each pollutant of 300 µg L<sup>-1</sup>, have shown that the optimum operational conditions for carrying out the various heterogeneous photocatalysis experiments under natural conditions under solar irradiation were 200 µg L<sup>-1</sup> of catalyst, 250 µg L<sup>-1</sup> of oxidant at a neutral pH. In all cases, degradation rates have been significantly lower in photolysis than in experiments using photocatalysts. The amount of catalyst has affected the process, increasing the degradation of the compounds as the load increases to the optimum

concentration (200 mg L<sup>-1</sup>). The efficiency of the process has been of the order: ZnO > TiO<sub>2</sub> P25 >>TiO<sub>2</sub> vlp 7000 > TiO<sub>2</sub> Alfa Aesar, for all the compounds studied. The addition of persulphate has improved the performance of the process, not only because it decreases the recombination of e<sup>-</sup>/h<sup>+</sup> but also because highly oxidising intermediate species have been produced such as SO<sub>4</sub><sup>•-</sup> y HO<sup>•</sup>. The highest rate of degradation has occurred in all cases at neutral pH values, which indicates that the process has been favoured by the predominance of cationic or neutral species generated in the mineralisation.

5. Photodegradation tests at pilot plant level under solar irradiation and under optimal conditions confirm that the elimination of compounds in the presence of a catalyst is significantly higher than in its absence (direct photolysis). The rate of degradation of the EDs in the treated wastewater has been of the order of magnitude: ZnO > TiO<sub>2</sub> P25 > TiO<sub>2</sub> vlp 7000. Photolysis has only marginally contributed to the degradation process, which implies that degradation is due to catalyst/oxidant and photon interactions. Carbon-doped TiO<sub>2</sub> (Kronos vlp 7000) can use part of the visible light spectrum due to a lower band gap energy, however, the photocatalytic efficiency of P25 TiO<sub>2</sub> has been higher, probably due to its higher rutile content. In this context, the use of semiconductors (mainly ZnO and P25 TiO<sub>2</sub>) in tandem with Na<sub>2</sub>S<sub>2</sub>O<sub>8</sub> to prevent e<sup>-</sup>/h<sup>+</sup> pairs recombination under sunlight radiation can be proposed as an attractive tool to eliminate or at least considerably reduce the initial amounts of EDs present in wastewater effluents before their release to the environment or reuse for agricultural purposes.

6. The use of heterogeneous solar photocatalysis can be considered as a suitable technology to remove many DEs from wastewater effluents, especially in areas such as south-eastern Spain, where the scarcity of irrigation water is a major problem, and there are more than 3,000 h of sunlight per year. Furthermore, the treatment can be considered economically sustainable although the cost depends largely on the nature of the pollutant in the effluent and the photocatalytic treatment used.

## **VI - REFERENCES**



## VI - REFERENCIAS

- Agriculture & Environment Research Unit (AERU) at the University of Hertfordshire (2018). Pesticide Properties Database. Available <https://sitem.herts.ac.uk/aeru/footprint/es/> [Accessed: 2018-10-27].
- Ahmed S, Rasul MG, Brown R, Hashib MA (2011). Influence of parameters on the heterogeneous photocatalytic degradation of pesticides and phenolic contaminants in wastewater: a short review. *J Environ Manage* 92(3):311-330.
- Ali Z, Ali S, Ahmad I, Khan I, Rahnamaye Aliabad HA (2013). Structural and optoelectronic properties of the zinc titanate perovskite and spinel by modified Becke–Johnson potential. *Phys. Rev. B Condens. Matter* 420:54–57.
- Amtout A and Leonelli R (1995). Optical properties of rutile near its fundamental band gap. *Physical Review B* 51(11):6842-6851.
- An SN, Choi NC, Choi JW (2018). Photodegradation of bisphenol a with ZnO and TiO<sub>2</sub>: influence of metal ions and fenton process. *Water Air Soil Pollut.* 229. Article 43.
- Archer E, Petrie B, Kasprzyk-Hordern B, Wolfaardt GM (2017). The fate of pharmaceuticals and personal care products (PPCPs), endocrine disrupting contaminants (EDCs), metabolites and illicit drugs in a WWTW and environmental waters. *Chemosphere* 174:437-446.
- Asahi R, Taga Y, Mannstadt W, Freeman AJ (2000). Electronic and Optical Properties of Anatase TiO<sub>2</sub>. *Phys. Rev. B* 61.
- Balabanič D, Hermosilla D, Merayo N, Klemenčič AK, Blanco A (2012). Comparison of different wastewater treatments for removal of selected endocrine-disruptors from paper mill wastewaters. *J Environ Sci Health ATox Hazard Subst Environ Eng* 47:1350–1363.
- Banjac Z, Ginebreda A, Kuzmanovic M, Marce R, Nadal M, Riera JM, Barcelo D. (2015). Emission factor estimation of ca. 160 emerging organic microcontaminants by inverse modeling in a Mediterranean river basin (Llobregat, NE Spain). *Sci Total Environ* 520:241-252.

- Barceló D (2003). Emerging pollutants in water analysis. *Trends in Analytical Chemistry* 22(10): xiv-xvi.
- Batt AL, Furlong ET, Mash HE, Glassmeyer ST, Kolpin DW (2017). The importance of quality control in validating concentrations of contaminants of emerging concern in source and treated drinking water samples. *Sci Total Environ* 579:1618-1628.
- Baxter JB, Aydil, ES (2006). Dye-sensitized solar cells based on semiconductor morphologies with ZnO nanowires. *Sol Energy Mater Sol Cells*, 90:607–622.
- Bechambi O, Sayadi S, Najjar W (2015). Photocatalytic degradation of bisphenol A in the presence of C-doped ZnO: effect of operational parameters and photodegradation mechanism. *J Ind Eng Chem* 32:201–210
- Berger E, Potouridis T, Haeger A, Puttmann W, Wagner M (2015). Effect-directed identification of endocrine disruptors in plastic baby teethers. *J Appl Toxicol* 35(11):1254-1261.
- Booij K, Robinson CD, Burgess RM, Mayer P, Roberts CA, Ahrens L, Allan I, Brant J, Jones L, Kraus UR, Larsen MM, Lepom P, Petersen J, Profrock D, Roose P, Schafer S, Smedes F, Tixier C, Vorkamp K, Whitehouse P (2016). Passive Sampling in Regulatory Chemical Monitoring of Nonpolar Organic Compounds in the Aquatic Environment. *Environ Sci Technol* 50(1):3-17.
- Carson, R., L. Darling, L. Darling, C. Houghton Mifflin and P. Riverside (1962). *Silent spring*.
- Chong MN, Jin B, Chow CWK, Saint C (2010) Recent developments in photocatalytic water treatment technology: a review. *Water Res* 44:2997–3027
- Colborn T, vom Saal FS, Soto AM (1993). Developmental effects of endocrine-disrupting chemicals in wildlife and human. *Environ Health Perspect* 101(5):378-384.
- Colburn T. (1997). *Our Stolen Future*. London, New English Library.
- Commission of the European Communities (1999). COM (1999) 706. Community Strategy for Endocrine Disruptors a range of substances suspected of interfering with the hormone systems of humans and wildlife. Brussels, 17.12.1999. Available at: <https://eur-lex.europa.eu/LexUriServ/LexUriServ.do?uri=COM:1999:0706:FIN:EN:PDF> [Accessed 20 June 2020].



- Commission of the European Communities (2001). COM (2001) 262. Communication from the Commission to the Council and the European Parliament on the implementation of the Community Strategy for Endocrine Disrupters – a range of substances suspected of interfering with the hormone systems of humans and wildlife (COM(1999) 706). Brussels, 14.06.2001. Available at: <https://eur-lex.europa.eu/LexUriServ/LexUriServ.do?uri=COM:2001:0262:FIN:EN:PDF> [Accessed 20 June 2020].
- Commission of the European Communities (2004). SEC (2004) 1372. Commission Staff Working Document on the implementation of the Community Strategy for Endocrine Disrupters – a range of substances suspected of interfering with the hormone systems of humans and wildlife (COM(1999) 706). Brussels, 28.10.2004. Available at: [https://ec.europa.eu/environment/chemicals/endocrine/pdf/sec\\_2004\\_1372.pdf](https://ec.europa.eu/environment/chemicals/endocrine/pdf/sec_2004_1372.pdf) [Accessed 20 June 2020].
- Commission of the European Communities (2007). SEC (2007) 1635. Commission Staff Working Document on the implementation of the "Community Strategy for Endocrine Disrupters" - a range of substances suspected of interfering with the hormone systems of humans and wildlife (COM (1999) 706), (COM (2001) 262) and (SEC (2004) 1372). Brussels, 30.11.2007. Available at: [https://ec.europa.eu/environment/chemicals/endocrine/pdf/sec\\_2007\\_1635.pdf](https://ec.europa.eu/environment/chemicals/endocrine/pdf/sec_2007_1635.pdf) [Accessed 20 June 2020].
- Daughton CG (2004). Non-regulated water contaminants: emerging research. *Environ Impact Assess Rev* 24(7-8):711-732.
- Deb P, Bhan A, Hussain I, Ansari KI, Bobzean SA, Pandita TK, Perrotti LI, Mandal SS (2016). Endocrine disrupting chemical, bisphenol-A, induces breast cancer associated gene HOXB9 expression in vitro and in vivo. *Gene* 590(2):234-243.
- Desbiolles F, Malleret L, Tiliacos C, Wong-Wah-Chung P, Laffont-Schwob I (2018). Occurrence and ecotoxicological assessment of pharmaceuticals: Is there a risk for the Mediterranean aquatic environment? *Sci Total Environ* 639:1334-1348.

- Diamanti-Kandarakis E, Bourguignon JP, Giudice LC, Hauser R, Prins GS, Soto AM, Zoeller RT, Gore AC (2009). Endocrine-disrupting chemicals: an Endocrine Society scientific statement. *Endocr Rev* 30(4):293-342.
- Djurišić A, Leung Y, Ng AMC (2014). Strategies for improving the efficiency of semiconductor metal oxide photocatalysis. *Materials Horizons* 1:400.
- Dodge LE, Kelley KE, Williams PL, Williams MA, Hernandez-Diaz S, Missmer SA, Hauser R (2015). Medications as a source of paraben exposure. *Reprod Toxicol* 52:93-100.
- Domènech X, Jardim W, Litter M (2004). Procesos avanzados de oxidación para la eliminación de contaminantes. En: *Eliminación de Contaminantes por Fotocatálisis Heterogénea*. Editor: Miguel Blesa, Red CYTED VIII-G, 3-26.
- Domingos RF, Rafiei Z, Monteiro CE, Khan MAK, Wilkinson KJ (2013). Agglomeration and dissolution of zinc oxide nanoparticles: Role of pH, ionic strength and fulvic acid. *Environ Chem* 10:306–312.
- Edwards TM, Myers JP (2008). Environmental exposures and gene regulation in disease etiology. *Cien Saude Colet* 13(1):269-281.
- European Commission (2000). Directive 2000/60/EC of the European Parliament and of the Council of 23 October 2000 establishing a framework for Community action in the field of water policy. Available at: [http://eur-lex.europa.eu/resource.html?uri=cellar:5c835afb-2ec6-4577-bdf8-756d3d694eeb.0004.02/DOC\\_1&format=PDF](http://eur-lex.europa.eu/resource.html?uri=cellar:5c835afb-2ec6-4577-bdf8-756d3d694eeb.0004.02/DOC_1&format=PDF) [Accessed 25 June 2020].
- European Commission (2001). Decision No 2455/2001/EC of the European Parliament and of the council of 20 November 2001 establishing the list of priority substances in the field of water policy and amending Directive 2000/60/EC. Available at: <http://eur-lex.europa.eu/legal-content/EN/TXT/PDF/?uri=CELEX:32001D2455&from=ES> [Accessed 25 June 2020].
- European Commission (2006). Directive 2006/118/EC of the European Parliament and of the council of 12 December 2006 on the protection of groundwater against pollution and deterioration. Available at: <http://eur-lex.europa.eu/legal-content/EN/TXT/PDF/?uri=CELEX:32006L0118&from=EN> [Accessed 25 June 2020].

- European Commission (2008). Directive 2008/105/EC of the European Parliament and of the council of 16 December 2008 on environmental quality standards in the field of water policy, amending and subsequently repealing Council Directives 82/176/EEC, 83/513/EEC, 84/156/EEC, 84/491/EEC, 86/280/EEC and amending Directive 2000/60/EC of the European Parliament and of the Council. Available at: <http://eur-lex.europa.eu/LexUriServ/LexUriServ.do?uri=OJ:L:2008:348:0084:0097:en:PDF> [Accessed 25 June 2020].
- European Commission (2013). Directive 2013/39/EU of the European Parliament and of the council of 12 August 2013 amending Directives 2000/60/EC and 2008/105/EC as regards priority substances in the field of water policy. Available at: <http://eur-lex.europa.eu/LexUriServ/LexUriServ.do?uri=OJ:L:2013:226:0001:0017:EN:PDF> [Accessed 25 June 2020].
- Evgenidou E, Fytianos K, Poullos I (2005) Photocatalytic oxidation of dimethoate in aqueous solutions. *J Photochem Photobiol A Chem* 175:29–38.
- Fagan R, McCormack DE, Dionysiou DD, Pillai SC, 2016. A review of solar and visible light active TiO<sub>2</sub> photocatalysis for treating bacteria, cyanotoxins and contaminants of emerging concern. *Mater Sci Semicond Process* 42:2-14.
- Fawell J, Ong CN (2012). Emerging Contaminants and the Implications for Drinking Water. *Int J Water Resour D* 28(2):247-263.
- Fenoll J, Garrido I, Hellín P, Flores P, Vela N, Navarro S (2015) Photocatalytic oxidation of pirimicarb in aqueous slurries containing binary and ternary oxides of zinc and titanium. *J Photochem Photobiol A Chem* 298:24–32
- Fenoll J, Sabater P, Navarro G, Perez-Lucas G, Navarro S (2013). Photocatalytic transformation of sixteen substituted phenylurea herbicides in aqueous semiconductor suspensions: intermediates and degradation pathways. *J Hazard Mater* 244-245:370-379.
- Frias Chicharro A, Gonzalez-Alonso S, Montero Rubio JC, Valcarcel Rivera Y (2014). Evaluation of the Efficacy of the Sewage Treatment Plant of Toledo, Spain in the Elimination of Drugs of Abuse and the Estimation of Consumption. *Revista Espanola De Salud Publica* 88(2):289-299.

- Frontistis Z, Antonopoulou M, Venieri D, Dailianis S, Konstantinou I, Mantzavinos D (2017). Solar photocatalytic decomposition of ethyl paraben in zinc oxide suspensions. *Catal Today* 280:139-148.
- Frye CA, Bo E, Calamandrei G, Calza L, Dessi-Fulgheri F, Fernandez M, Fusani L, Kah O, Kajta M, Le Page Y, Patisaul HB, Venerosi A, Wojtowicz AK, Panzica GC (2012). Endocrine disrupters: a review of some sources, effects, and mechanisms of actions on behaviour and neuroendocrine systems. *J Neuroendocrinol* 24(1):144-159.
- Gaya U, Abdullah A. (2008). Heterogeneous Photocatalytic Degradation of Organic Contaminants Over Titanium Dioxide: A Review of Fundamentals, Progress and Problems. *J Photochem Photobiol C* 9:1-12.
- Geissen V, Mol H, Klumpp E, Umlauf G, Nadal, van der Ploeg M, van de Zee S, Ritsema CJ (2015). Emerging pollutants in the environment: A challenge for water resource management. *Int. Soil Water Conserv. Res* 3(1):57-65.
- Gimenez J, Bayarri B, Gonzalez O, Malato S, Peral J, Esplugas S (2015). Advanced oxidation processes at laboratory scale: environmental and economic impacts. *ACS Sustain Chem Eng* 3:3188-3196.
- Glaze WH (1986). Reaction products of ozone: a review. *Environ Health Perspect* 69:151-157.
- Goldstein S, Behar D, Rabani J (2008). Mechanism of visible light photocatalytic oxidation of methanol in aerated aqueous suspensions of carbon-doped TiO<sub>2</sub>. *J Phys Chem C* 112:15134-15139.
- Gomes J, Leal I, Bednarczyk K, Gmurek M, Stelmachowski M, Zaleska-Medynska A, Bastos FC, Quinta-Ferreira ME, Costa R, Quinta-Ferreira RM, Martins RC (2017). Detoxification of parabens using UV-A enhanced by noble metals - TiO<sub>2</sub> supported catalysts. *J Environ Chem Eng* 5:3065-3074.
- Gonzalez S, Lopez-Roldan R, Cortina JL (2012). Presence and biological effects of emerging contaminants in Llobregat River basin: A review. *Environ Pollut* 161:83-92.
- Greenspan LC, Lee MM (2018). Endocrine disrupters and pubertal timing. *Curr Opin Endocrinol Diabetes Obes* 25(1):49-54.
- Gupta SM, Tripathi M (2011). A review of TiO<sub>2</sub> nanoparticles. *Chin Sci Bull* 56:1639-1657.

- Harley KG, Berger KP, Kogut K Parra K, Lustig RH, Greenspan LC, Calafat AM, Ye X, Eskenazi B (2019). Association of phthalates, parabens and phenols found in personal care products with pubertal timing in girls and boys. *Hum Reprod* 34(1):109-117.
- Heindel JJ, Blumberg B, Cave M, Machtinger R, Mantovani A, Mendez MA, Nadal A, Palanza P, Panzica G, Sargis R, Vandenberg LN, vom Saal F (2017). Metabolism disrupting chemicals and metabolic disorders. *Reprod Toxicol* 68:3-33.
- Heinlaan M, Ivask A, Blinova I, Dubourguie HC, Kahru A (2008) Toxicity of nanosized and bulk ZnO, CuO and TiO<sub>2</sub> to bacteria *Vibrio fischeri* and crustaceans *Daphnia magna* and *Thamnocephalus platyurus*. *Chemosphere* 71:1308–1316.
- Herrmann JM (2012). Titania-based true heterogeneous photocatalysis. *Environ Sci Pollut Res* 19:3655–3665.
- Hurun C, Agrios AG, Gray KA, Rajh T, Thurnaur MC (2003). Explaining the enhanced photocatalytic activity of Degussa P25 mixed-phase TiO<sub>2</sub> using EPR. *J Phys Chem B* 107:4545-4549.
- Ibhadon A, Fitzpatrick P (2013). Heterogeneous Photocatalysis: Recent Advances and Applications. *Catalysts* 3(1):189.
- Jain PK, Kumar D, Kumar A, Kaur D (2010). Structural, optical and dielectric properties of ZnTiO<sub>3</sub> ceramics. *Optoelectron Adv Mat* 4:299–304.
- Jurado A, Vazquez-Sune E, Carrera J, Lopez de Alda M, Pujades E, Barcelo D. (2012). Emerging organic contaminants in groundwater in Spain: A review of sources, recent occurrence and fate in a European context. *Sci Tot Environ* 440:82-94.
- Kanakaraju D, Glass B, Oelgemöller M (2014). Titanium dioxide photocatalysis for pharmaceutical wastewater treatment. *Environ Chem Lett* 12:27-47.
- Kitsiou V, Filippidis N, Mantzavinos D, Pouios I (2009). Heterogeneous and homogeneous photocatalytic degradation of the insecticide imidacloprid in aqueous solutions. *Appl Catal B Environ* 86:27–35.
- Kiyama R, Wada-Kiyama Y (2015). Estrogenic endocrine disruptors: Molecular mechanisms of action. *Environ Int* 83:11-40.
- Kmetykó Á, Mogyorósi K, Pusztai P, Radu T, Kónya Z, Dombi A, Hernádi K (2014). Photocatalytic H<sub>2</sub> Evolution Using Different Commercial TiO<sub>2</sub>

- Catalysts Deposited with Finely Size-Tailored Au Nanoparticles: Critical Dependence on Au Particle Size. *Materials* 7(12):7615.
- Kosmulski M (2016) Isoelectric points and points of zero charge of metal (hydr)oxides: 50 years after parks' review. *Adv Coll Inter Sci* 238:1–61.
- Kudo A, Miseki Y (2009) Heterogeneous photocatalyst materials for water splitting. *Chem Soc Rev* 38:253–278.
- Kuo CY, Wu CH, Lin HY (2010). Photocatalytic degradation of bisphenol A in a visible light/TiO<sub>2</sub> system. *Desalination* 256:37–42.
- Kurwadkar S (2017). Groundwater Pollution and Vulnerability Assessment. *Water Environ Res* 89(10):1561-1579.
- Lapworth DJ, Baran N, Stuart ME, Ward RS (2012). Emerging organic contaminants in groundwater: A review of sources, fate and occurrence. *Environ Pollut* 163:287-303.
- Lauretta R, Sansone A, Sansone M, Romanelli F, Appetecchia M (2019). Endocrine Disrupting Chemicals: Effects on Endocrine Glands. *Front Endocrinol* 10:178.
- Lee KM, Lai CW, Ngai KS, Juan JC (2016). Recent developments of zinc oxide based photocatalyst in water treatment technology: A review. *Water Res* 88:428– 448.
- Lei M., Zhang L., Lei J, Zong L, Li J, Wu Z, Wang Z (2015). Overview of Emerging Contaminants and Associated Human Health Effects. *Biomed Res Int* 2015:404796.
- Leusch FDL, Neale P, AArnal C, Aneck-Hahn NH, Balaguer P, Bruchet A, Escher BI, Esperanza M, Grimaldi M, Leroy G, Scheurer M, Schlichting R, Schriks M, Hebert A (2018). Analysis of endocrine activity in drinking water, surface water and treated wastewater from six countries. *Water Res* 139:10-18.
- Liu B, Zhao X, Terashima C, Fujishima A, Nakata K (2014). Thermodynamic and kinetic analysis of heterogeneous photocatalysis for semiconductor systems. *Phys Chem Chem Phys* 16:8751–8760.
- Lopez-Pacheco IY, Silva-Nunez A, Salinas-Salazar C, Arevalo-Gallegos A, Lizarazo-Holguin LA, Barcelo D, Iqbal HMN, Parra-Saldivar R (2019). Anthropogenic contaminants of high concern: Existence in water resources and their adverse effects. *Sci Total Environ* 690:1068-1088.

- López-Serna R, Postigo C, Blanco J, Pérez S, Ginebreda A, L. de Alda M, Petrović M, Munné A, Barceló D (2012). Assessing the effects of tertiary treated wastewater reuse on the presence emerging contaminants in a Mediterranean river (Llobregat, NE Spain). *Environ Sci Pollut Res Int* 19(4):1000-1012.
- Mahmoodi NM, Armani M, Lymaee NY, Gharanjig K, (2007). Photocatalytic degradation of agricultural N-heterocyclic organic pollutants using immobilized nanoparticles of titania. *J Hazard Mater* 145:65–71.
- Malato S, Fernández-Ibáñez P, Maldonado MI, Blanco J, Gernjak W (2009). Decontamination and disinfection of water by solar photocatalysis: Recent overview and trends. *Catalysis Today* 147(1):1-59.
- Mangalgi KP, He K, Blaney L (2015). Emerging contaminants: a potential human health concern for sensitive populations. *PDA J Pharm Sci Technol* 69(2):215-218.
- Matzek LW, Carter, KE (2016). Activated persulfate for organic chemical degradation: A review. *Chemosphere* 151:178–188.
- Mnif W, Hassine AI, Bouaziz A, Bartegi A, Thomas O, Roig B (2011). Effect of endocrine disruptor pesticides: a review. *Int J Environ Res Public Health* 8(6):2265-2303.
- Monneret C (2017). What is an endocrine disruptor?. *C R Biol* 340(9-10):403-405.
- Nilsen E, Smalling KL, Ahrens L, Gros M, Miglioranza KSB, Pico Y, Schoenfuss HL (2019). Critical review: Grand challenges in assessing the adverse effects of contaminants of emerging concern on aquatic food webs. *Environ Toxicol Chem* 38(1):46-60.
- Ohtani B (2013). Titania Photocatalysis beyond Recombination: A Critical Review. *Catalysts* 3(4):942.
- Ohtani B, Mahaney OOP, Amano F, Murakam N, Abe R. (2010). What are titania photocatalysts?: An exploratory correlation of photocatalytic activity and physical properties. *J Adv Oxid Technol*, 13:247–261.
- Olea N, Fernandez M (2007). Endocrine disruption. *J Epidemiol Community Health* 61(5):372-373.
- Olmez-Hanc T, Arslan-Alaton I. (2013). Comparison of sulfate and hydroxyl radical based advanced oxidation of phenol. *Chem. Eng. J*, 224:10–16.
-

- Pardeshi SK, Patil AB (2009). Solar photocatalytic degradation of resorcinol a model endocrine disrupter in water using zinc oxide. *J Hazard Mater* 163(1):403-409.
- Pelaez M, Nolan NT, Pillai SC, Seery MK, Falaras P, Kontos AG, Dunlop PSM, Hamilton JWJ, Byrne JA, O'Shea K, Entezari MH, Dionysiou DD (2012). A review on the visible light active titanium dioxide photocatalysts for environmental applications. *Appl Catal B Environ* 125:331-349.
- Petala A, Frontistis Z, Antonopoulou M, Konstantinou I, Kondarides DI, Mantzavinos D. (2015). Kinetics of ethyl paraben degradation by simulated solar radiation in the presence of N-doped TiO<sub>2</sub> catalysts. *Water Res* 81:157-166.
- Petersen G, Rasmussen D, Gustavson K (2007). Study on enhancing the Endocrine Disrupter priority list with a focus on low production volume chemicals, DHI Water & Environment, Horsholm, Denmark, [http://ec.europa.eu/environment/endocrine/documents/final\\_report\\_2007.pdf](http://ec.europa.eu/environment/endocrine/documents/final_report_2007.pdf) [Accessed 20 June 2020].
- Petrie B, Barden R, Kasprzyk-Hordern B (2015). A review on emerging contaminants in wastewaters and the environment: current knowledge, understudied areas and recommendations for future monitoring. *Water Res* 72:3-27.
- Philippat C, Bennett D, Calafat A M, Picciotto IH (2015). Exposure to select phthalates and phenols through use of personal care products among Californian adults and their children. *Environ Res* 140:369-376.
- Postigo C, López de Alda MJ, Barceló D. (2010). Drugs of abuse and their metabolites in the Ebro River basin: occurrence in sewage and surface water, sewage treatment plants removal efficiency, and collective drug usage estimation. *Environ Int* 36(1):75-84.
- Pozan GS, Kambur A (2014). Significant enhancement of photocatalytic activity over bifunctional ZnO-TiO<sub>2</sub> catalysts for 4-chlorophenol degradation, *Chemosphere* 105:152-159.
- Prusinski L, Al-Hendy A, Yang Q (2016). Developmental exposure to endocrine disrupting chemicals alters the epigenome: Identification of reprogrammed targets. *Gynecol Obstet Res* 3(1):1-6.



- Qamar M, Muneer M, Bahnemann D (2006). Heterogeneous photocatalysed degradation of two selected pesticide derivatives: triclopyr and daminozid in aqueous suspensions of titanium dioxide. *J Environ Manag* 80:99–106.
- Rani C, Singaram K (2016). Endocrine disrupting compounds in water and wastewater and their treatment options - A review. *Int J Environ Tech Manag* 19:392-431.
- Reddy P, Kim K-H, Kavitha B, Kumar V, Raza N, Kalagara S (2018). Photocatalytic degradation of bisphenol A in aqueous media: A review. *J Environ manag* 213:189-205.
- Rehman S, Usman Z, AlDraihem M, Rehman N, Rehman I, Ahmad G (2018). Endocrine disrupting chemicals and impact on male reproductive health. *Transl Androl Urol* 7(3):490-503.
- Rodgers KM, Udesky JO, Rudel RA, Brody JG (2018). Environmental chemicals and breast cancer: An updated review of epidemiological literature informed by biological mechanisms. *Environ Res* 160:152-182.
- Rodríguez-Chueca J, Laski E, García-Cañibano C, Martín de Vidales MJ, Encinas A, Kuch B, Marugán J (2018). Micropollutants removal by full-scale UV-C/sulfate radical based advanced oxidation processes. *Sci Tot Environ* 630:1216–1225.
- Sakkiah S, Wang T, Zou W, Wang Y, Pan B, Tong W, Hong H (2017). Endocrine Disrupting Chemicals Mediated through Binding Androgen Receptor Are Associated with Diabetes Mellitus. *Int J Environ Res Public Health* 15(1).
- Sakthivel S, Neppolian B, Shankar MV, Arabindoo B, Palanichamy M, Murugesan V (2003). Solar photocatalytic degradation of azo dye: comparison of photocatalytic efficiency of ZnO and TiO<sub>2</sub>. *Sol Energy Mater Sol Cells* 77:65–82.
- Salah NH, Bouhelassa M, Bekkouche S, Boultif A (2004). Study of photocatalytic degradation of phenol. *Desalination* 166:347–354.
- Salimi MA, Esrafil M, Gholami A, Jonidi Jafari R, Rezaei Kalantary M, Farzadkia M, Kermani M, Sobhi H (2017). Contaminants of emerging concern: a review of new approach in AOP technologies. *Environ Monit Assess* 189.
- Satuf M, Brandi R, Cassano A, Alfano O (2005). Experimental method to evaluate the optical properties of aqueous titanium dioxide suspensions. *Ind Eng. Chem Res* 44:6643-6649.

- Sauve S, Desrosiers M (2014). A review of what is an emerging contaminant. *Chem Cent J* 8(1):15.
- Slama R, Bourguignon JP, Demeneix B, Ivell R, Panzica G, Kortenkamp A, Zoeller RT (2016). Scientific Issues Relevant to Setting Regulatory Criteria to Identify Endocrine-Disrupting Substances in the European Union. *Environ Health Perspect* 124(10):1497-1503.
- Song C, Wang L, Ren J, Lv B, Sun Z, Yan J, Li X, Liu J (2016). Comparative study of diethyl phthalate degradation by UV/H<sub>2</sub>O<sub>2</sub> and UV/TiO<sub>2</sub>: kinetics, mechanism, and effects of operational parameters. *Environ Sci Pollut Res* 23:2640–2650
- Spasiano D, Marotta R, Malato S, Fernandez-Ibañez P, Di Somma I (2015). "Solar photocatalysis: Materials, reactors, some commercial, and pre-industrialized applications. A comprehensive approach." *App Catal B: Environ* 170-171:90-123.
- Stevens A A (1982). Reaction products of chlorine dioxide. *Environ Health Perspect* 46: 101-110.
- Swedenborg E, Ruegg J, Makela S, Pongratz I (2009). Endocrine disruptive chemicals: mechanisms of action and involvement in metabolic disorders. *J Mol Endocrinol* 43(1): 1-10.
- Toxnet, 2017. Toxicology Data Network (TOXNET®). US National Library of Medicine, MD, USA. Available in: <https://toxnet.nlm.nih.gov>. [Accessed 15 March 2018].
- Tran N, Reinhard HM, Gin KY (2018). Occurrence and fate of emerging contaminants in municipal wastewater treatment plants from different geographical regions-a review. *Water Res* 133: 182-207.
- Valenzuela MA, Bosch P, Jiménez-Becerrill J, Quiroz O, Páez AI (2002). Preparation, characterization and photocatalytic activity of ZnO Fe<sub>2</sub>O<sub>3</sub> and ZnFe<sub>2</sub>O<sub>4</sub>. *J Photochem Photobiol A* 148 177–182.
- Vela N, Fenoll J, Garrido I, Navarro G, Gambín M, Navarro S (2015). Photocatalytic mitigation of triazinone herbicide residues using titanium dioxide in slurry photoreactor. *Catal Today* 252: 70–77.
- Vela N, Calín M, Yáñez-Gascón MJ, Garrido I, Pérez-Lucas G, Fenoll J, Navarro S. (2018a) Photocatalytic oxidation of six endocrine disruptor chemicals in

- wastewater using ZnO at pilot plant scale under natural sunlight. *Environ Sci Pollut Res* 25:34995–35007.
- Vela N, Calín M, Yáñez-Gascón MJ, Garrido I, Pérez-Lucas G, Fenoll J, Navarro S (2018b) Photocatalytic oxidation of six pesticides listed as endocrine disruptor chemicals from wastewater using two different TiO<sub>2</sub> samples at pilot plant scale under sunlight irradiation. *J Photochem Photobiol* 353: 271–278
- Vela N, Calín M, Yáñez-Gascón MJ, Garrido I, Pérez-Lucas G, Fenoll J, Navarro S (2018c) Solar reclamation of wastewater effluent polluted with bisphenols, phthalates and parabens by photocatalytic treatment with TiO<sub>2</sub>/ Na<sub>2</sub>S<sub>2</sub>O<sub>8</sub> at pilot plant scale. *Chemosphere* 212 95-104
- Vela N, Calín M, Yáñez-Gascón MJ, Garrido I, Pérez-Lucas G, Fenoll J, Navarro S (2019). Removal of Pesticides with Endocrine Disruptor Activity in Wastewater Effluent by Solar Heterogeneous Photocatalysis Using ZnO/Na<sub>2</sub>S<sub>2</sub>O<sub>8</sub>. *Water Air Soil Pollut* 230:134
- Vela N, Perez-Lucas G, Fenoll J, Navarro S 2017. Recent overview on the abatement of pesticide residues in water by photocatalytic treatment using TiO<sub>2</sub>. In: Janus, M. (Ed.), *Applications of Titanium Dioxide*. Intech, Croatia, pp. 147-177.
- Velegraki T, Hapeshi E, Fatta-Kassinos D, Poulios I. 2015. Solar-induced heterogeneous photocatalytic degradation of methyl-paraben. *Appl Catal B Environ* 178:2-11.
- Vicente R, Soler J, Arques A, Amat AM, Frontistis Z, Xekoukoulotakis N, Mantzavinos D (2014). Comparison of different TiO<sub>2</sub> samples as photocatalyst for the degradation of a mixture of four commercial pesticides. *J Chem Technol Biotechnol* 89:1259–1264.
- Wallace B, Purcell M, Furlong J (2002). Total organic carbon analysis as a precursor to disinfection by-products in potable water: Oxidation technique considerations. *J Environ Monit* 4:35–42.
- Wink DA, Nims RW, Saavedra JE, Utermahlen WE, Ford PC (1994). The Fenton oxidation mechanism: reactivities of biologically relevant substrates with two oxidizing intermediates differ from those predicted for the hydroxyl radical. *Proc Natl Acad Sci U S A* 91(14): 6604-6608.

- World Health Organization (WHO) (2011). Guidelines for drinking-water quality. Fourth Edition. Geneva Switzerland. Available at: <http://www.who.int> [Accessed 18 June 2020].
- Yasmina M, Korichi M, Sidrouhou H, Chaouche K (2014). Treatment heterogeneous photocatalysis; Factors influencing the photocatalytic degradation by TiO<sub>2</sub>. Conference: TMREES14 International Conference Technologies and Materials for Renewable Energy, Environment and SustainabilityAt: Beirut – Lebanon. April 2014.
- Zacharakis A, Chatzisyneon E, Binas V, Frontistis Z, Venieri D, Mantzavinos D (2013). Solar photocatalytic degradation of bisphenol A on immobilized ZnO or TiO<sub>2</sub>. *Int J Photoener*. <https://doi.org/10.1155/2013/570587>
- Zepp RG, Faust BC, Hoigne J (1992). Hydroxyl radical formation in aqueous reactions (pH 3-8) of iron (II) with hydrogen peroxide: the photo-Fenton reaction. *Environ Sci Technol* 26(2):313-319.
- Zhang W, Li Y, Su Y, Mao K, Wang Q (2012). Effect of water composition on TiO<sub>2</sub> photocatalytic removal of endocrine disrupting compounds (EDCs) and estrogenic activity from secondary effluent. *J Hazard Mater* 215-216 252-258.
- Zoeller RT, Bergman A, Becher G, Bjerregaard P, Bornman R, Brandt I, Iguchi T, Jobling S, Kidd KA, Kortenkamp A, Skakkebaek NE, Toppari J, Vandenberg LN (2014). A path forward in the debate over health impacts of endocrine disrupting chemicals. *Environ Health* 13:118.
- Zúñiga-Benítez H, Peñuela GA (2017) Methylparaben removal using heterogeneous photocatalysis: effect of operational parameters and mineralization/biodegradability studies. *Environ Sci Pollut Res Int* 24:6022–6030.

## **VII - APPENDIX**



## VII - APPENDIX

The results of this research have been published in the following scientific papers. The articles published are listed below.

1. Vela N. Calín M. Yáñez-Gascón MJ. Garrido I. Pérez-Lucas G. Fenoll J. Navarro S. Solar reclamation of wastewater effluent polluted with bisphenols, phthalates and parabens by photocatalytic treatment with  $\text{TiO}_2/\text{Na}_2\text{S}_2\text{O}_8$  at pilot plant scale. *Chemosphere*. 212: 95-104. 2018. ISSN: 0045-6535. Citations from WOS core collection (november 2020): 11.

Journal Impact Factor Trend: 5.108. Source: JCR (Science Citation Index, Social Sciences Citation Index, 2018). Position: 29/265 (Q1). Area: Environmental Sciences.

2. Vela N. Calín M. Yáñez-Gascón MJ. Garrido I. Pérez-Lucas G. Fenoll J. Navarro S. Photocatalytic oxidation of six pesticides listed as endocrine disruptor chemicals from wastewater using two different  $\text{TiO}_2$  samples at pilot plant scale under sunlight irradiation. *Journal of Photochemistry and Photobiology A-Chemistry*. 353: 271-278. 2018. ISSN 1010-6030. Citations from WOS core collection (november 2020): 24.

Journal Impact Factor Trend: 3.261. Source: JCR (Science Citation Index, Social Sciences Citation Index, 2018). Position: 60/148 (Q2). Area: Chemistry, Physical.

3. Vela N. Calín M. Yáñez-Gascón MJ. Garrido I. Pérez-Lucas G. Fenoll J. Navarro S. Photocatalytic oxidation of six endocrine disruptor chemicals in wastewater using  $\text{ZnO}$  at pilot plant scale under natural sunlight. *Environmental science and pollution research*. 25: 34995-35007. 2018. ISSN: 0944-1344. Citations from WOS core collection (november 2020): 16.

Journal Impact Factor Trend: 2.914. Source: JCR (Science Citation Index, Social Sciences Citation Index, 2018). Position: 91/251 (Q2). Area: Environmental Sciences.

4. N. Vela, M. Calín, M. J. Yáñez-Gascón, A. el Aatik, I. Garrido, G. Pérez-Lucas, J. Fenoll, S. Navarro. Removal of pesticides with endocrine disruptor activity in wastewater effluent by solar heterogeneous photocatalysis using ZnO/Na<sub>2</sub>S<sub>2</sub>O<sub>8</sub>. *Water, Air & Soil Pollution*. 230: 134. 2019. ISSN: 0049-6979. Citations from WOS core collection (november 2020): 2.

Journal Impact Factor Trend: 1.900; Source: JCR (Science Citation Index, Social Sciences Citation Index, 2019). Position: 64/93 (Q3). Area: Water Resources.

The results of this research have also been presented at various international scientific meetings. The contributions are listed below.

1. 9<sup>th</sup> European Meeting on Solar Chemistry and Photocatalysis: Environmental Applications. 2016. Strasbourg, France. Contributions: 1. Comparison of different TiO<sub>2</sub> samples used as photocatalyst to remove pesticides with endocrine disrupting activity in water. 2. Photocatalytic Degradation of Bisphenol and Phthalate compounds in Water Using ZnO/UV.

2. 5<sup>th</sup> European Conference Environmental Applications of Advanced Oxidation Processes. 2017. Prague, Czech Republic. Contributions: 1. Photooxidation of different endocrine disrupting chemicals in wastewater using zinc oxyde as photocatalyst. 2. Photocatalytic degradation of pesticides with endocrine disrupto activity in wasterwater uding different TiO<sub>2</sub> samples.

3. 6<sup>th</sup> International Conference on Semiconductor Photochemistry. 2017. Oldeburg, Germany. Contribution: Photooxidation of six pesticides in water assisted by ZnO under solar irradiation.

4. 10<sup>th</sup> World Congress of Chemical Engineering. 2017. Barcelone, Spain. Contribution: Photocatalytic degradation of endocrine disrupting chemicals in wastewater using different TiO<sub>2</sub> samples.

The Catholic University of Murcia has funded this research through the Project PMAFI 27/14.



